

AFAPL-TR-78-6
Part II

LEVEL

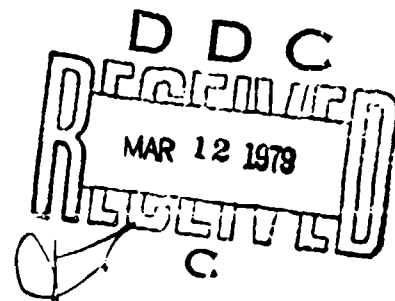
2

AD A0 65554

**ROTOR-BEARING DYNAMICS
TECHNOLOGY DESIGN GUIDE**
Part II Ball Bearings

SHAKER RESEARCH CORP.
BALLSTON LAKE, NEW YORK 12019

FEBRUARY 1978



DDC FILE COPY
000

TECHNICAL REPORT AFAPL-TR-78-6, Part II
Interim Report for Period April 1976 – October 1977

Approved for public release; distribution unlimited.

AIR FORCE AERO PROPULSION LABORATORY
AIR FORCE WRIGHT AERONAUTICAL LABORATORIES
AIR FORCE SYSTEMS COMMAND
WRIGHT-PATTERSON AIR FORCE BASE, OHIO 45433

79 03 08 063

NOTICE

When Government drawings, specifications, or other data are used for any purpose other than in connection with a definitely related Government procurement operation, the United States Government thereby incurs no responsibility nor any obligation whatsoever; and the fact that the Government may have formulated, furnished, or in any way supplied the said drawings, specifications, or other data, is not to be regarded by implication or otherwise as in any manner licensing the holder or any other person or corporation, or conveying any rights or permission to manufacture, use, or sell any patented invention that may in any way be related thereto.

This report has been reviewed by the Information Office (OI) and is releasable to the National Technical Information Service (NTIS). At NTIS, it will be available to the general public, including foreign nations.

This technical report has been reviewed and is approved for publication.

John B. Schrand

JOHN B. SCHRAND
Project Engineer

Howard F. Jones

HOWARD F. JONES
Chief, Lubrication Branch

FOR THE COMMANDER

Blackwell C. Dunnam

BLACKWELL C. DUNNAM
Chief, Fuels and Lubrication Division

"If your address has changed, if you wish to be removed from our mailing list, or if the addressee is no longer employed by your organization please notify AFAPL/SFL, WPAFB, OH 45433 to help us maintain a current mailing list."

Copies of this report should not be returned unless return is required by security considerations, contractual obligations, or notice on a specific document.

Unclassified

SECURITY CLASSIFICATION OF THIS PAGE (When Data Entered)

DD FORM 1 JAN 73 1473 POSITION OF 1 NOV 65 IS OBSOLETE

Unclassified

SECURITY CLASSIFICATION OF THIS PAGE (When Data Entered)

PAGES

ARE
MISSING
IN
ORIGINAL
DOCUMENT

Unclassified

SECURITY CLASSIFICATION OF THIS PAGE(When Data Entered)

The resulting program is reasonably small and easy to use. Lastly, the stiffness data included in the original Part IV have been updated and are included in appendices.



Unclassified

SECURITY CLASSIFICATION OF THIS PAGE(When Data Entered)

FORWARD

This report was prepared by Shaker Research Corporation under USAF Contract No. AF33615-76-C-2038. The contract was initiated under Project 304B, "Fuels, Lubrication, and Fire Protection", Task 304806, "Aerospace Lubrication", Work Unit 30480685, "Rotor-Bearing Dynamics Design".

The work reported herein was performed during the period 15 April 1976 to 15 November 1977, under the direction of John B. Schrand (AFAPL/SFL) and Dr. James F. Dill (AFAPL/SFL), Project Engineers. The report was released by the authors in December 1977.



TABLE OF CONTENTS

<u>Section</u>		<u>Page</u>
I	INTRODUCTION AND SUMMARY	1
II	ANALYSIS	3
	2.1 General Bearing Model and Coordinate System	3
	2.2 General Bearing Support Characteristics	6
	2.3 Ball Bearing Characterization	9
	2.4 Load-Deflection Relationships	13
	2.5 Ball Bearings under Radial Load	13
	2.6 Bearings under Thrust Load	18
	2.7 Ball Bearings under Combined Loading	23
III	APPLICATION OF COMPUTER PROGRAM	36
	3.1 Input Format	36
	3.2 Output Format	38
IV	DESIGN DATA	40
	4.1 Radial Stiffness Versus Radial Load	40
	4.2 Axial Stiffness Versus Thrust Load	43
	4.3 Radial Stiffness Versus Radial Load with Preload	43
APPENDIX A	- Computer Program for Calculating the Stiffness Matrix of a Ball Bearing	47
APPENDIX B	- Bearing Stiffness Design Charts - Pure Radial Load	63
APPENDIX C	- Bearing Stiffness Design Charts - Pure Thrust Load	89
APPENDIX D	- Bearing Stiffness Design Charts - Angular Contact Bearing with Preload - $\beta = 25^\circ$	75
APPENDIX E	- Bearing Stiffness Design Charts - Angular Contact Bearing with Preload - $\beta = 15^\circ$	89
REFERENCES		102

LIST OF ILLUSTRATIONS

<u>Number</u>	<u>Title</u>	<u>Page</u>
1a	Bearing Stiffness Model	4
1b	Bearing Location Coordinate System	4
2	Linearization of Ball Bearing Stiffness	8
3	Ball Bearing Coordinate System	10
4	Ball Bearing Dimensions and Index, q	11
5	Radially Loaded Ball Bearing	14
6	Radial Stiffness Parameter Versus Radial Load	20
7	Angular Contact Ball Bearing Under Thrust Load	21
8	Thrust Stiffness Parameter Versus Thrust Load	24
9	Ball Forces at High Speed Conditions	25
10	Ball Motion Vectors	27
11	Illustration of Race Control Concept	29
12	Spin Torque Vectors	31
13	Race Curvature Center Deflection	32
14	Input Data for Sample Problem	37
15	Output Data for Sample Problem	39
B-1	Radial Stiffness for Deep Groove Ball Bearings, Pure Radial Load	64
B-2	Radial Stiffness for Deep Groove Ball Bearings, Pure Radial Load	65
B-3	Radial Stiffness for Deep Groove Ball Bearings, Pure Radial Load	66
B-4	Radial Stiffness for Deep Groove Ball Bearings, Pure Radial Load	67
C-1	Axial Stiffness Versus Axial Load, No Radial Load	70
C-2	Axial Stiffness Versus Axial Load, No Radial Load	71
C-3	Axial Stiffness Versus Axial Load, No Radial Load	72
C-4	Axial Stiffness Versus Axial Load, No Radial Load	73
D-1	Radial Stiffness for Angular Contact Bearing, Preload -- Selected Light, $\beta = 25^\circ$	74
D-2	Radial Stiffness for Angular Contact Bearing, Preload -- Selected Light, $\beta = 25^\circ$	77

List of Illustrations (continued)

<u>Number</u>	<u>Title</u>	<u>Page</u>
D-3	Radial Stiffness for Angular Contact Bearing, Preload -- Selected Light, $\beta = 25^\circ$	78
D-4	Radial Stiffness for Angular Contact Bearing, Preload -- Selected Light, $\beta = 25^\circ$	79
D-5	Radial Stiffness for Angular Contact Bearing, Preload -- Moderate, $\beta = 25^\circ$	80
D-6	Radial Stiffness for Angular Contact Bearing, Preload -- Moderate, $\beta = 25^\circ$	81
D-7	Radial Stiffness for Angular Contact Bearing, Preload -- Moderate, $\beta = 25^\circ$	82
D-8	Radial Stiffness for Angular Contact Bearing, Preload -- Moderate, $\beta = 25^\circ$	83
D-9	Radial Stiffness for Angular Contact Bearing, Preload -- Preferred Heavy, $\beta = 25^\circ$	84
D-10	Radial Stiffness for Angular Contact Bearing, Preload -- Preferred Heavy, $\beta = 25^\circ$	85
D-11	Radial Stiffness for Angular Contact Bearing, Preload -- Preferred Heavy, $\beta = 25^\circ$	86
D-12	Radial Stiffness for Angular Contact Bearing, Preload -- Preferred Heavy, $\beta = 25^\circ$	87
E-1	Radial Stiffness for Angular Contact Bearing, Preload -- Selected Light, $\beta = 15^\circ$	88
E-2	Radial Stiffness for Angular Contact Bearing, Preload -- Selected Light, $\beta = 15^\circ$	89
E-3	Radial Stiffness for Angular Contact Bearing, Preload -- Selected Light, $\beta = 15^\circ$	90
E-4	Radial Stiffness for Angular Contact Bearing, Preload -- Selected Light, $\beta = 15^\circ$	91
E-5	Radial Stiffness for Angular Contact Bearing, Preload -- Moderate, $\beta = 15^\circ$	92
E-6	Radial Stiffness for Angular Contact Bearing, Preload -- Moderate, $\beta = 15^\circ$	93
E-7	Radial Stiffness for Angular Contact Bearing, Preload -- Moderate, $\beta = 15^\circ$	94
E-8	Radial Stiffness for Angular Contact Bearing, Preload -- Moderate, $\beta = 15^\circ$	95
		96
		97

List of Illustrations (continued)

<u>Number</u>	<u>Title</u>	<u>Page</u>
E-9	Radial Stiffness for Angular Contact Bearing, Preload -- Preferred Heavy, $\beta = 15^\circ$	98
E-10	Radial Stiffness for Angular Contact Bearing, Preload -- Preferred Heavy, $\beta = 15^\circ$	99
E-11	Radial Stiffness for Angular Contact Bearing, Preload -- Preferred Heavy, $\beta = 15^\circ$	100
E-12	Radial Stiffness for Angular Contact Bearing, Preload -- Preferred Heavy, $\beta = 15^\circ$	101

LIST OF TABLES

<u>Number</u>	<u>Description</u>	<u>Page</u>
1	Sample Case Deep Groove Ball Bearing-----	36
2	Deep Groove Bearing-----	41
3	Angular Contact Bearing-----	42
4	Axial Loaded Deep Groove Bearings-----	44

NOMENCLATURE

<u>Symbol</u>	<u>Description</u>	<u>Units</u>
a	Semi-major axis of pressure ellipse	in.
b	Semi-minor axis of pressure ellipse	in.
B	Total curvature = $f_1 + f_2 - 1$	
B_{ij}	Damping component, change of force in i direction due to velocity in j direction; $i = x, y, z$; $j = x, y, z$.	<u>lb-sec</u> in
\underline{B}_N	Damping matrix	
	$\begin{bmatrix} (\underline{B}_N)_{\text{lineal}} & 0 & 0 \\ 0 & 0 & 0 \\ 0 & 0 & (\underline{B}_N)_{\text{angular}} \end{bmatrix}$	
$(\underline{B})_{\text{lineal}}$	Damping matrix due to lateral velocities	<u>lb-sec</u> in
	$\begin{bmatrix} B_{xx} & B_{xy} \\ B_{yx} & B_{yy} \end{bmatrix}_{\text{lineal}}$	
$(\underline{B})_{\text{angular}}$	Damping matrix due to angular velocities	<u>in-lb-sec</u> radian
	$\begin{bmatrix} B_{xx} & B_{xy} \\ B_{yx} & B_{yy} \end{bmatrix}_{\text{angular}}$	
C	Basic dynamic capacity	lb.

<u>Symbol</u>	<u>Description</u>	<u>Units</u>
d	Ball diameter	in.
D	Diameter	in.
E	Pitch diameter	in.
E'	Operating pitch diameter	in.
E_B	Modulus of elasticity for ball	lbs/in ²
E_R	Modulus of elasticity for race	lbs/in ²
$E(\epsilon)$	Complete elliptic integral of the second kind formed with the modulus sine where $\cos\epsilon = b/a$	
i	r/d	
F_i	Applied load in i direction, i = x, y, z	lbs.
F_c	Ball centrifugal load	lbs.
\underline{F}	Force matrix = $\begin{bmatrix} F_x \\ F_y \\ F_z \end{bmatrix}$	lbs.
i	Imaginary number unit vector = $\sqrt{-1}$	
$J_x(\zeta)$	Radial load integral	
K	Ball-race stiffness	lb/in.
K_{ij}	Stiffness component, change of force in i direction due to displacement in j direction. i = x, y, z; j = x, y, z	lb/in.
K_N	Stiffness matrix	
	$\begin{bmatrix} (K_N)_{\text{lineal}} & 0 & 0 \\ 0 & 0 & 0 \\ 0 & 0 & (K_N)_{\text{angular}} \end{bmatrix}$	

<u>Symbol</u>	<u>Description</u>	<u>Units</u>
$(K)_{\text{lineal}}$	Stiffness matrix due to lateral displacements	lb/in.
	$\begin{bmatrix} K_{xx} & K_{xy} \\ K_{yx} & K_{yy} \end{bmatrix}_{\text{lineal}}$	
$(K)_{\text{angular}}$	Stiffness matrix due to angular rotations	<u>in.-lb</u> <u>rad</u>
	$\begin{bmatrix} K_{xx} & K_{xy} \\ K_{yx} & K_{yy} \end{bmatrix}_{\text{angular}}$	
K_z	Axial deflection constant	
$K(\epsilon)$	Complete elliptic integral of first kind	
M	Applied moment	in.-lb
M_g	Gyroscopic moment	in.-lb
n	Number of balls	
P	Ball load	lb.
P_D	Diametral clearance	in.
Q	Spin torque	in.-lb
r	Raceway groove curvature radius	in.
R	Pitch radius	in.
\underline{x}	Column vector =	$\begin{bmatrix} \delta_x \\ \delta_y \\ \delta_z \\ \dot{\delta}_x \\ \dot{\delta}_y \end{bmatrix}$

<u>Symbol</u>	<u>Description</u>	<u>Units</u>
\underline{w}_N	Column vector = $\begin{bmatrix} \delta_x \\ \delta_y \\ \theta_x \\ \theta_y \end{bmatrix}$	
\underline{z}_N	Impedance matrix = $\underline{K}_N + i \underline{\nu B}_N$	

<u>Symbol</u>	<u>Description</u>	<u>Units</u>
α	Angle between ball rotational axis and center line of bearing	radians, $^{\circ}$
β	Contact angle	radians, $^{\circ}$
β'	Free contact angle	radians, $^{\circ}$
γ	$\frac{d \cos\beta}{E}$	
Γ	Residues of Newton-Raphson equation	
δ	Displacement	in.
δ_x	Lateral displacement in x direction	in.
δ_y	Lateral displacement in y direction	in.
δ_z	Axial displacement	in.
Δ	Ball-race deflection or normal approach	in.
ζ	$= \frac{1}{2} \left[1 + \frac{P_D}{2 \delta_{\max}} \right]$	
c_i	Hertzian contact parameter; Eqs. (73,88,91,92)	
η_B	$= \frac{4(1-v_B^2)}{E_B}$	in. 2 / lb
η_R	$= \frac{4(1-v_R^2)}{E_R}$	in. 2 / lbs
θ_x	Angular rotation about x axis	radians, $^{\circ}$
θ_y	Angular rotation about y axis	radians, $^{\circ}$
θ_z	Angular rotation about z axis	radians, $^{\circ}$
μ	Coefficient of sliding friction	
ν	Frequency of vibration	radians/sec
v_B	Poisson's ratio for ball	

<u>Symbol</u>	<u>Description</u>	<u>Units</u>
ν_R	Poisson's ratio for race	radians/sec
ω_B	Rotational velocity of ball	radians/sec
ω_1	Rotational velocity of outer race relative to cage	radians/sec
ω_2	Rotational velocity of inner race relative to cage	radians/sec
ω_s	Ball spin rotational velocity	radians/sec
Ω_E	Absolute orbiting velocity of ball	radians/sec
Ω_1	Absolute rotational velocity of outer race	radians/sec
Ω_2	Absolute rotational velocity of inner race	radians/sec
ϕ	Angular location of ball	radians. ^o

SUBSCRIPTS

<u>Symbol</u>	<u>Description</u>
b	Refers to bearing
B	Refers to ball
c	Refers to centrifugal
i	Refers to outer ($i = 1$) or inner ($i = 2$) race
l	Refers to loaded extent of bearing
max	Refers to maximum condition
p	Refers to pedestal
q	Refers to ball circumferential position
R	Refers to race
x	Refers to x direction
y	Refers to y direction
z	Refers to z direction
1	Refers to outer race
2	Refers to inner race

SECTION I

INTRODUCTION AND SUMMARY

In recent years, the Rotor-Bearing Dynamics Design Technology Series, AFAPL-TR-65-45 (Parts I through X) has been considered by many engineers to be an important part of their basic analytical tool kit. However, since the issuance of the first volume, in May of 1965, the state-of-the-art has significantly advanced. Further, new techniques of data presentation have been developed, computer capabilities have increased and some minor typographical and technical errors were uncovered.

Part IV of AFAPL-TR-65-45 treated design data for typical deep-groove and angular contact bearings. The data was presented in graphical form and consisted of direct radial stiffness, load carrying capacity, and load levels. In addition design guidelines and limitations were discussed. The major deficiencies of this original volume were that centrifugal effects due to high speed were ignored, and axial and angular stiffness information were omitted.

Subsequent to the publication of Part IV, several extensive treatments of ball bearings including elastohydrodynamic, thermal, and cage effects have been published. The computer program of Mauriello, LaGasse, and Jones (3) considers both elastohydrodynamic and cage effects. The more recent computer based design guide prepared by Crecelius and Pirvics (4) treats elastohydrodynamic, thermal, and cage effects for a system of ball and roller bearings.

Thus very sophisticated analytical tools are available for the design and application of ball bearings. Neither of these tools, however, provide the user with the stiffness matrix required for solution of rotor dynamics problems. In addition both computer programs are very large and require an extensive computer facility for use.

The present volume is intended as an update of the original Part IV(1). Those aspects of the original Part IV(1) which treated general design

aspects of ball bearings, load capacity, speed limitations, etc. have been deleted since their coverage is superficial compared to the more sophisticated computer tools now available (3,4). Only those parts directly connected with preparation of input for the rotordynamic response programs (Volume I of the revised series) have been retained. The complete stiffness matrix is calculated including centrifugal effects. Considerations such as elastohydrodynamic and cage effects are not included since they have little influence on the calculation of ball bearing stiffness. The resulting program (Appendix A) is reasonably small and easy to use. Lastly, the stiffness data included in the original Part IV have been updated and are included in Appendices B, C and D.

SECTION II

ANALYSIS

2.1 General Bearing Model and Coordinate System

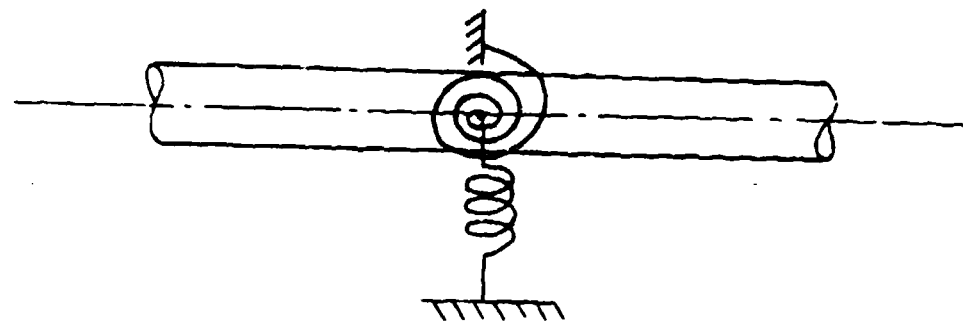
Accurate calculation of the lateral dynamic response of a high-speed rotor depends on realistic characterization of the support bearings. In the most general case, both linear and angular motions are restrained by the support bearings at the attachment location. In the analytical model, the reaction force and the reaction moment of each bearing are felt by the rotor through a single station of the rotor axis. As schematically illustrated in Figure 1a, a coil spring restraining the lateral displacement and a torsion spring which tends to oppose an inclination are attached to the same point of the rotor axis. A complete description of the characteristics of the support bearings, however, involves much more than the specification of the two spring constants. This is because:

- The lateral motion of the rotor axis is concerned with two displacement components and two inclination components.
- The restraining characteristics may include cross coupling among various displacement/inclination coordinates.
- The restraining force/moment may not be temporally in phase with the displacement/inclination.
- The restraining characteristics of the bearing may be dependent on either the rotor speed or the frequency of vibration, or both.
- Bearing pedestal compliance may not be negligible.

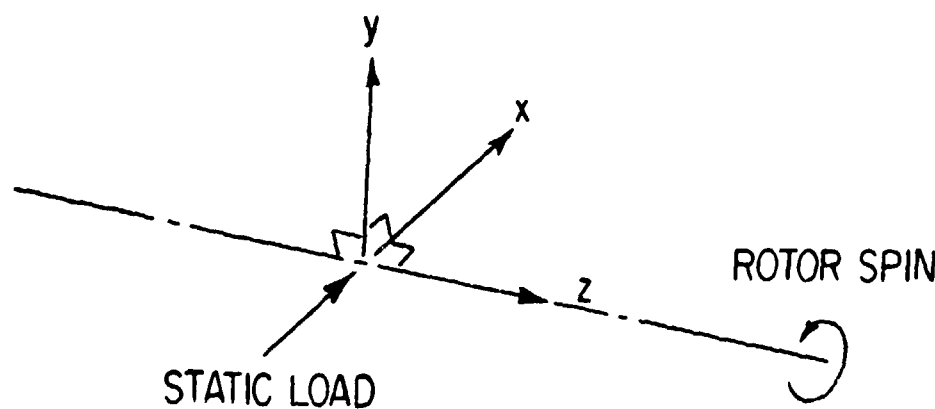
To accommodate the above considerations, the support bearing characteristics are described in Reference 2 by a four-degrees-of-freedom impedance matrix as defined in Equation (1):

$$\underline{R}_N = - \underline{Z}_N \cdot \underline{W}_N \quad (1)$$

where \underline{W}_N is a column vector containing elements which are the two lateral displacements (δ_x , δ_y) and the two lateral inclinations (θ_x , θ_y) of the



(a) Bearing Stiffness Model



(b) Bearing Location
Coordinate System

Figure 1

rotor axis at the bearing station N.

Employing a right handed Cartesian representation in a lateral plane as depicted in Figure 1b, the z-axis is coincident with the spin vector of the rotor. The x-axis is oriented in the direction of the external static load, and the y-axis is perpendicular to both z and x axes forming the right handed triad (x, y, z). (δ_x, δ_y) are respectively lateral lineal displacement components of the rotor axis along the (x, y) directions. (θ_x, θ_y) are lateral inclination components respectively in the (z-x, z-y) planes. Note that θ_x is a rotation about the y-axis, while θ_y is a rotation about the negative x-axis.

$\underline{\underline{Z}}_N$ is a complex (4 x 4 matrix), and in accordance with the common notation for stiffness and damping coefficients, may be expressed as

$$\underline{\underline{Z}}_N = \underline{\underline{K}}_N + i\nu \underline{\underline{B}}_N \quad (2)$$

where $\underline{\underline{K}}_N$ is the stiffness matrix and $\underline{\underline{B}}_N$ is the damping matrix. ν is the frequency of vibration. Most commonly, lateral linear and angular displacements do not interact with each other so that the non-vanishing portions of $\underline{\underline{K}}_N$ and $\underline{\underline{B}}_N$ are separate 2 x 2 matrices. That is

$$\underline{\underline{K}}_N = \begin{bmatrix} (\underline{\underline{K}}_N)_{\text{lineal}} & 0 & 0 \\ 0 & 0 & (\underline{\underline{K}}_N)_{\text{angular}} \\ 0 & 0 & 0 \end{bmatrix} \quad (3)$$

$$\underline{\underline{B}}_N = \begin{bmatrix} (\underline{\underline{B}}_N)_{\text{lineal}} & 0 & 0 \\ 0 & 0 & (\underline{\underline{B}}_N)_{\text{angular}} \\ 0 & 0 & 0 \end{bmatrix} \quad (4)$$

Accordingly, a total characterization of a support bearing would include sixteen coefficients which make up the 4 (2 x 2) matrices:

$$(\underline{\underline{K}})_{\text{lineal}} = \begin{bmatrix} K_{xx} & K_{xy} \\ K_{yx} & K_{yy} \end{bmatrix}_{\text{lineal}} \quad (5)$$

$$(\underline{B})_{\text{lineal}} = \begin{bmatrix} B_{xx} & B_{xy} \\ B_{yx} & B_{yy} \end{bmatrix}_{\text{lineal}} \quad (6)$$

$$(\underline{K})_{\text{angular}} = \begin{bmatrix} K_{xx} & K_{xy} \\ K_{yx} & K_{yy} \end{bmatrix}_{\text{angular}} \quad (7)$$

$$(\underline{B})_{\text{angular}} = \begin{bmatrix} B_{xx} & B_{xy} \\ B_{yx} & B_{yy} \end{bmatrix}_{\text{angular}} \quad (8)$$

In the event that the pedestal compliance is significant, then the effective support impedance can be calculated from

$$\underline{Z}_N = (\underline{Z}_b^{-1} + \underline{Z}_p^{-1}) \quad (9)$$

where subscripts "p" and "b" refer to the pedestal and bearing respectively. Note that both pedestal inertia and damping may be included in \underline{Z}_p .

2.2 General Bearing Support Characteristics

The function of a bearing is to restrict the rotor axis to a nominal axis under realistic static and dynamic load environments. Deviation of any particular point of the rotor axis from the nominal line can be characterized by three lineal and two angular displacements. These may be designated as $(\delta_x, \delta_y, \delta_z, \theta_x, \theta_y)$ in accordance with a right-handed Cartesian reference system. The z-coordinate is coincident with the reference axis and is directed toward the spin vector. (θ_x, θ_y) are rotor axis inclinations respectively in the z-x and z-y planes. The x-coordinate is directed toward the predominant static load; e.g., earth gravity. Ideally, the bearing would resist the occurrence of any displacement so that the reaction force system imparted by the bearing to the rotor is generally expressed in matrix notation as

$$\underline{F} = -\underline{Z} \cdot \underline{x} \quad (10)$$

\underline{F} is a column vector comprising the five reaction components (F_x , F_y , F_z , M_x , M_y), while \underline{x} is the displacement vector (δ_x , δ_y , δ_z , θ_x , θ_y). Z is a (5 x 5) matrix containing the elements Z_{ij} with both indices (i, j) ranging from 1 to 5. The values of Z_{ij} characterize how rotor displacements are being resisted by the bearing.

From the standpoint of dynamic perturbation, distinction is made between a static equilibrium component and a dynamic perturbation component for both the displacements and the reactions. Thus,

$$\underline{x} = \underline{x}_0 + \underline{x}'; \quad \underline{F} = \underline{F}_0 + \underline{F}' \quad (11)$$

(\underline{x}' , \underline{F}') are respectively presumed to be infinitesimal in comparison with (\underline{x}_0 , \underline{F}_0). Accordingly, Z_{ij} are regarded as dependent on \underline{x}_0 but not on \underline{x}' . To illustrate the idea of perturbation linearization, one may examine the one-dimensional load-displacement curve shown in Figure 2.

As illustrated, the load-displacement relationship is a 3/2 power law in accordance with the Hertzian point contact formula. It is not possible to describe the entire range by a linear approximation. However, if a small dynamic perturbation is taken around a static equilibrium point, $\delta'_x < \delta_{x_0}$, the small segment of the load-displacement curve can be approximated by a local tangent line. The corresponding force increment is

$$F'_x = \frac{\partial F_x}{\partial \delta x} \delta'_x \quad (12)$$

where δ'_x is the incremental displacement. $\partial F_x / \partial \delta x$ will depend on the amplitude of δ_{x_0} .

The question of history dependence is resolved by regarding \underline{x}' as periodic motions at any frequency v of interest, and Z_{ij} accordingly would have both real and imaginary parts and may also be dependent on both the rotor speed ω and the vibration frequency v .

To avoid notational clumsiness, the primes will be dropped from (\underline{F}' , \underline{x}')

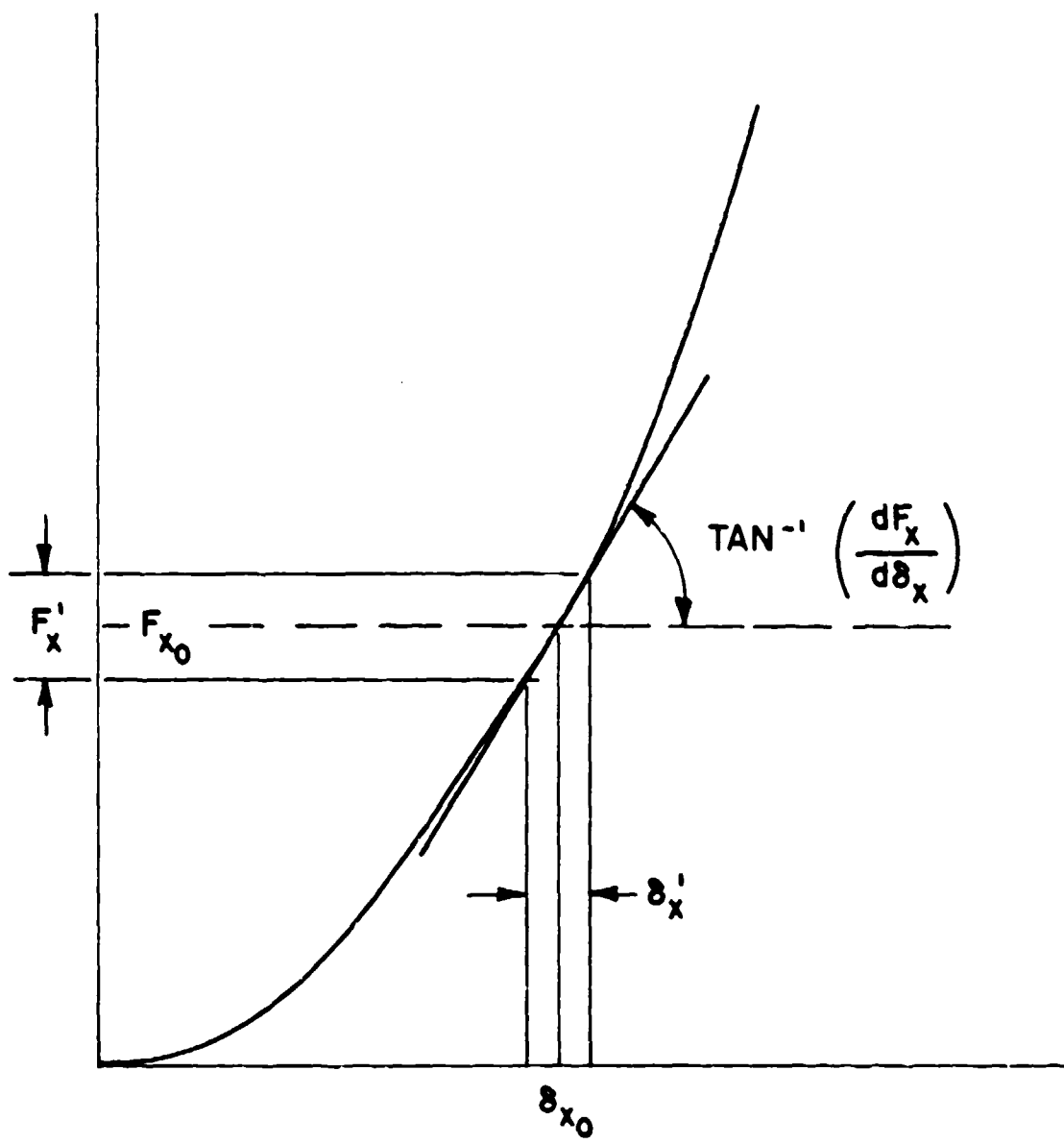


Figure 2 Linearization of Ball Bearing Stiffness

which are understood to be dynamic perturbation quantities unless the subscript "0" is used to designate the static equilibrium condition.

2.3 Ball Bearing Characterization

In many ways the ball bearing is much simpler to model from a rotor dynamics point of view than a fluid film bearing. In general, the following two simplifications can be made:

- The restraining characteristics do not include cross coupling among the various displacement/inclination coordinates.
- The restraining force/moment is normally temporally in phase with the displacement/inclination.

Figure 3 shows a ball bearing referred to in an orthogonal xyz coordinate system. The outer ring is fixed but the inner ring may move with respect to the coordinate system. Both rings are free to rotate about their axes.

Three lineal displacements, δ_x , δ_y , δ_z , and two angular displacements, θ_x , θ_y , are required to define the spatial position and attitude of the inner ring when it is displaced from its initial position. For purposes of derivation the initial situation is that existing when the bearing's end play is just taken up in the thrust direction. Figure 3 shows these displacements in the positive sense.

Figure 4 shows some important dimensions and establishes the convention of the ball-position index q. The contact angle β is the initial mounted contact angle and is shown in the positive sense.

2.3.1 Stiffness

The total characterization of a ball bearing's stiffness can be expressed by the matrix at the top of page 12.

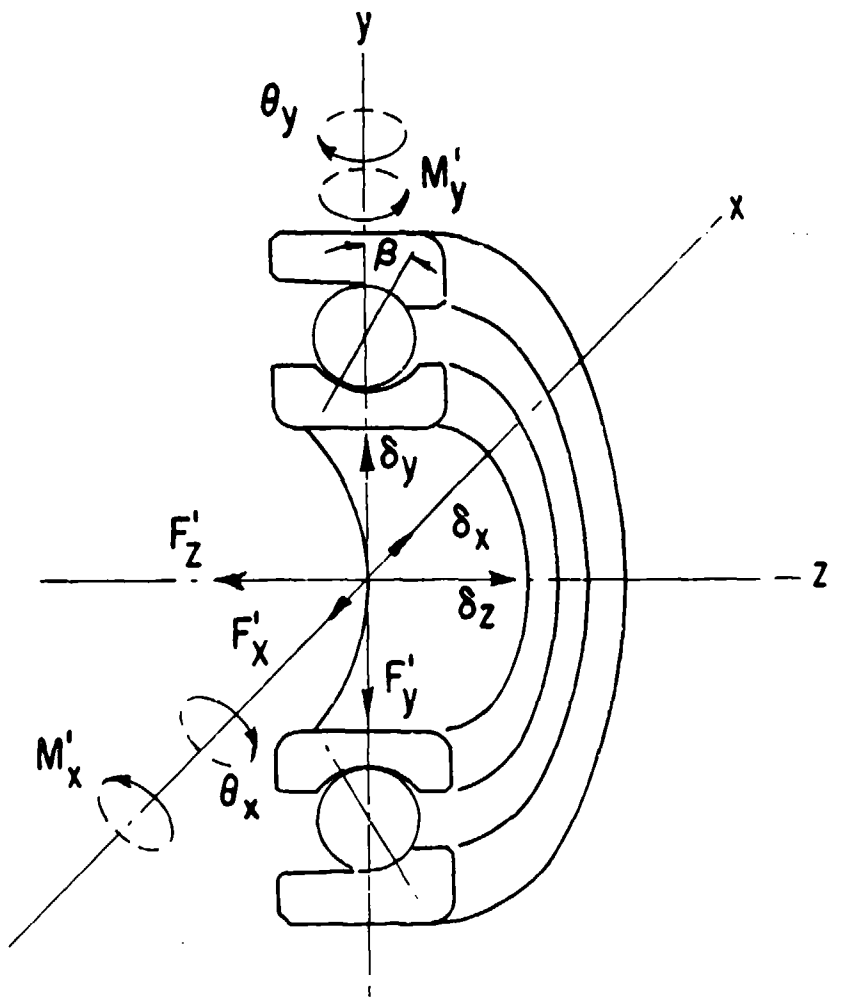


Figure 3 Ball Bearing Coordinate System

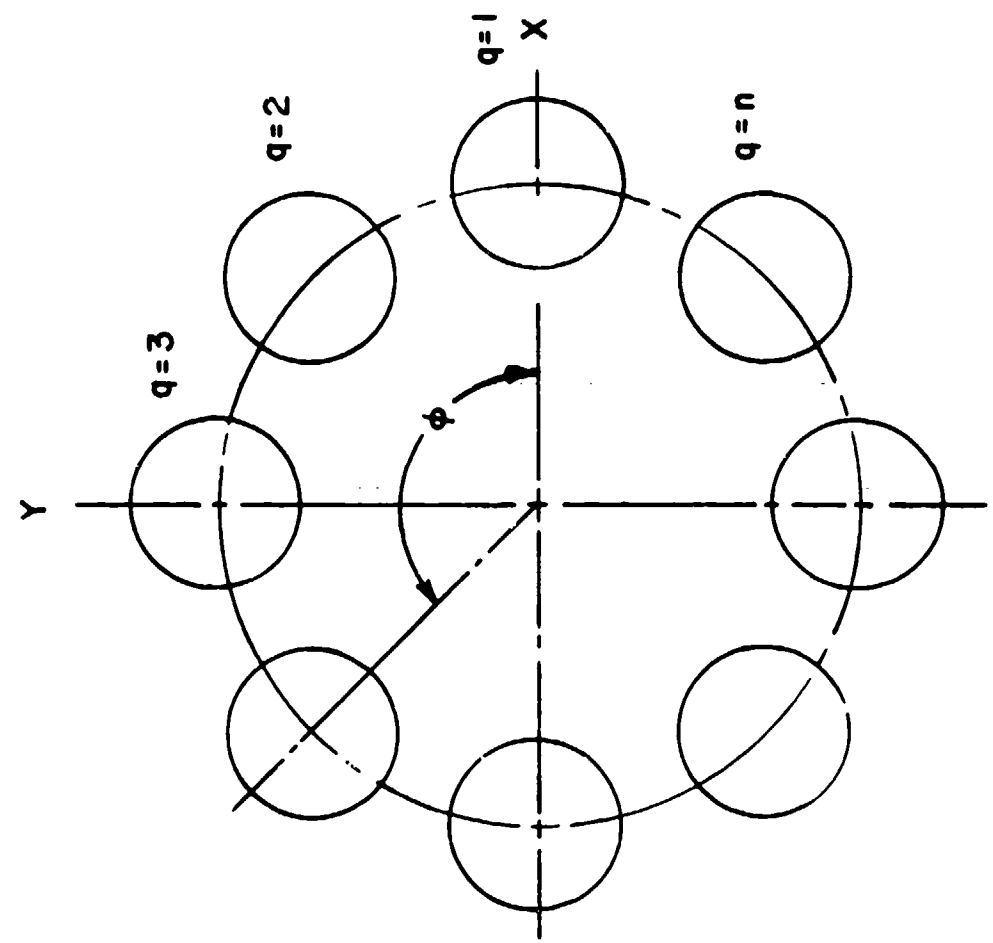
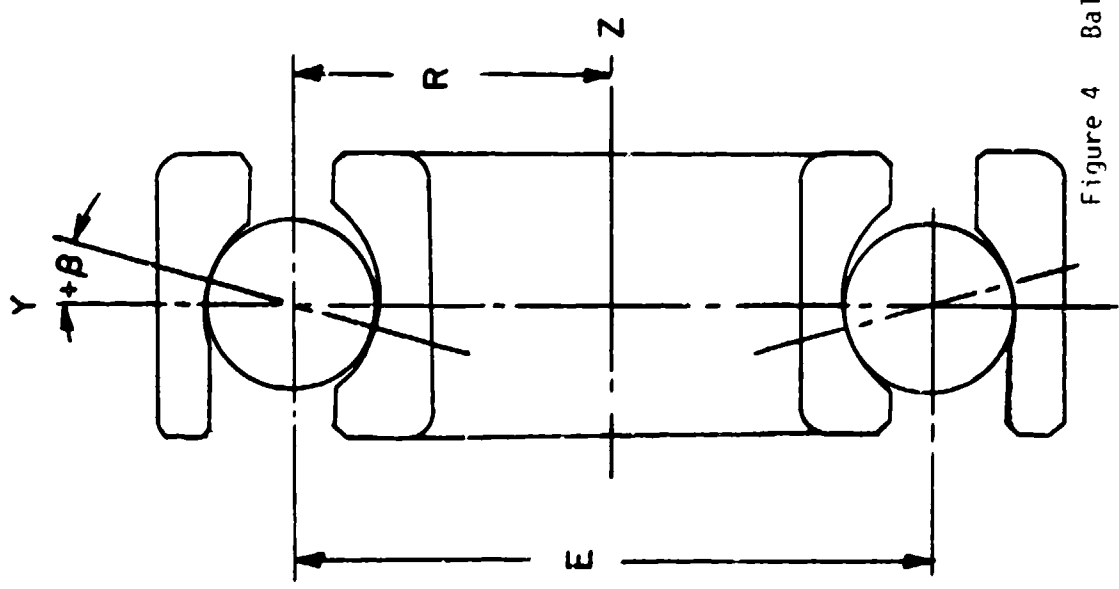


Figure 4 Ball Bearing Dimensions and Index, q

$$[K] = \begin{vmatrix} \frac{\partial F_x}{\partial x} & \frac{\partial F_x}{\partial y} & \frac{\partial F_x}{\partial z} & \frac{\partial F_x}{\partial \theta_x} & \frac{\partial F_x}{\partial \theta_y} \\ \frac{\partial F_y}{\partial x} & \frac{\partial F_y}{\partial y} & \frac{\partial F_y}{\partial z} & \frac{\partial F_y}{\partial \theta_x} & \frac{\partial F_y}{\partial \theta_y} \\ \frac{\partial F_z}{\partial x} & \frac{\partial F_z}{\partial y} & \frac{\partial F_z}{\partial z} & \frac{\partial F_z}{\partial \theta_x} & \frac{\partial F_z}{\partial \theta_y} \\ \frac{\partial M_x}{\partial x} & \frac{\partial M_x}{\partial y} & \frac{\partial M_x}{\partial z} & \frac{\partial M_x}{\partial \theta_x} & \frac{\partial M_x}{\partial \theta_y} \\ \frac{\partial M_y}{\partial x} & \frac{\partial M_y}{\partial y} & \frac{\partial M_y}{\partial z} & \frac{\partial M_y}{\partial \theta_x} & \frac{\partial M_y}{\partial \theta_y} \end{vmatrix} \quad (13)$$

The lineal and angular stiffness matrices (Equations 5 and 7) can be derived from Equation (13). For example:

$$[K]_{\text{lineal}} = \begin{vmatrix} \frac{\partial F_x}{\partial x} & \frac{\partial F_x}{\partial y} \\ \frac{\partial F_y}{\partial x} & \frac{\partial F_y}{\partial y} \end{vmatrix} \quad (14)$$

$$[K]_{\text{angular}} = \begin{vmatrix} \frac{\partial M_x}{\partial \theta_x} & \frac{\partial M_x}{\partial \theta_y} \\ \frac{\partial M_y}{\partial \theta_x} & \frac{\partial M_y}{\partial \theta_y} \end{vmatrix} \quad (15)$$

Note that although the axial components of stiffness are not utilized by the lateral rotor dynamics program (2), they have been retained in the general ball bearing stiffness matrix, Equation (13). The axial stiffness would be required, for example, if the reader was calculating the axial natural frequency of a ball bearing mounted shaft.

2.3.2 Damping

There is very little data on ball bearing damping. The data included in Reference 1, which is for nonrotating grease packed bearings, suggested a value in the order of 15-20 pound sec/in. This should be

used only as an approximate figure since this has not been confirmed.

2.4 Load-Deflection Relationships

For a given ball-raceway contact, the load deflection relationship is given by an equation of the form:

$$P = K \Delta^{3/2} \quad (16)$$

The total normal approach between two raceways under load separated by a rolling element is the sum of the approaches between the rolling element and each raceway. Hence,

$$\Delta = \Delta_1 + \Delta_2 \quad (17)$$

and

$$K = \left[\frac{1}{(1/K_1)^{2/3} + (1/K_2)^{2/3}} \right]^{3/2} \quad (18)$$

where K_1 and K_2 are a function of the ball-race geometry and material properties.

2.5 Ball Bearings Under Radial Load

For a rigidly supported bearing subjected to radial load, the radial deformation at any rolling element angular position is given by

$$\Delta_\phi = \delta_{\max} \cos\phi - (1/2)P_D \quad (19)$$

in which δ_{\max} is the maximum deflection, occurring at $\phi = 0$ and P_D is the diametral clearance. Figure 5 illustrates a radial bearing with clearance.

Equation (19) may be rearranged in terms of maximum deformation as follows:

$$\Delta = \Delta_{\max} \left\{ 1 - \frac{1}{2\zeta} (1 - \cos\phi) \right\} \quad (20)$$

in which

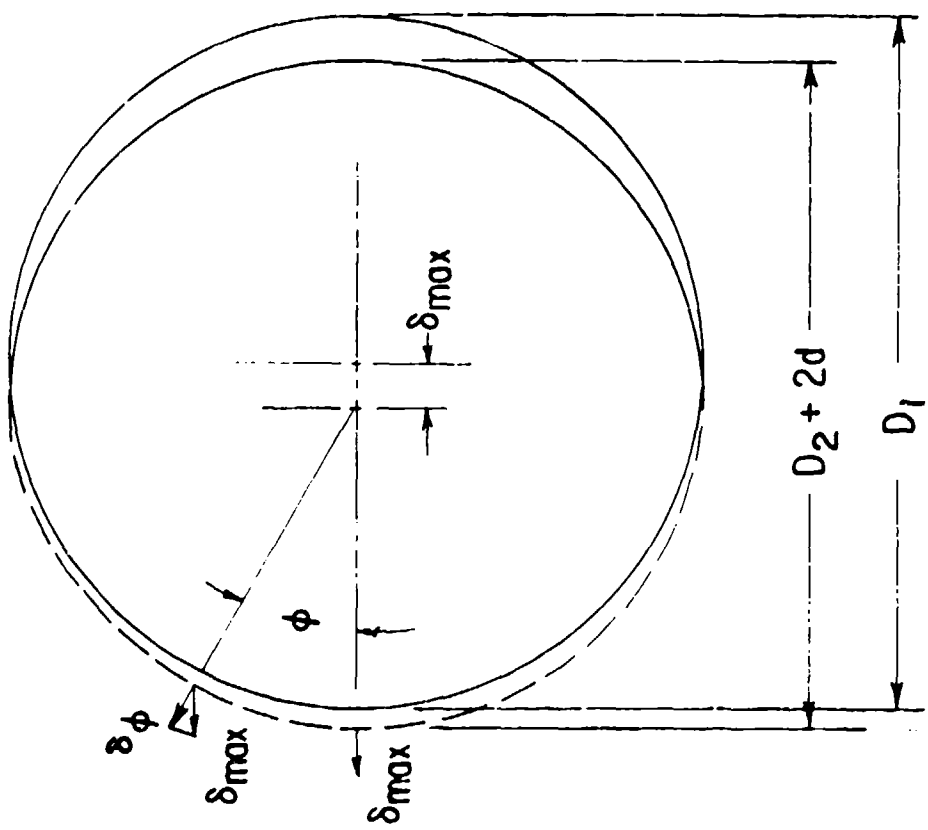
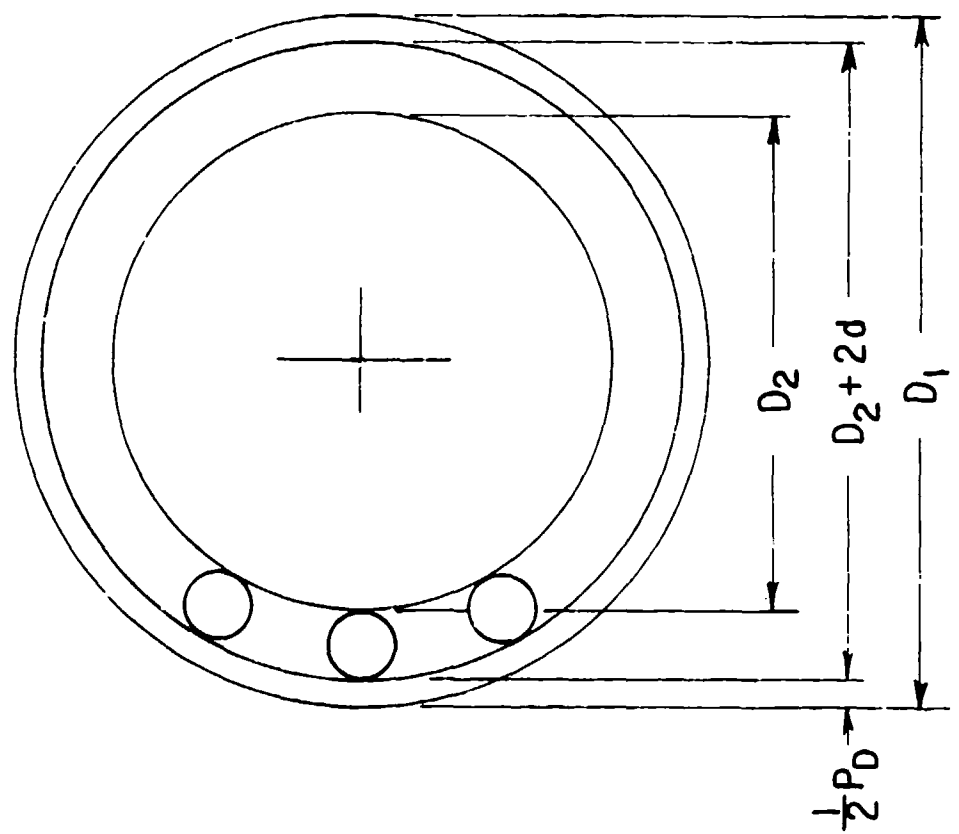


Figure 5 Radially Loaded Ball Bearing

$$\zeta = \frac{1}{2} \left[1 - \frac{P_D}{2\delta_{\max}} \right] \quad (21)$$

It is clear from Equation (21) that the angular extent of the load zone is determined by the diametral clearance such that

$$\phi_L = \cos^{-1} \left[\frac{P_D}{2\delta_{\max}} \right] \quad (22)$$

For zero clearance, $\phi = 90^\circ$

From Equation (16)

$$\left[\frac{P_\phi}{P_{\max}} \right] = \left[\frac{\Delta_\phi}{\Delta_{\max}} \right]^{3/2} \quad (23)$$

Therefore, from Equations (20) and (23)

$$P_\phi = P_{\max} \left[1 - \frac{1}{2\zeta} (1 - \cos\phi) \right]^{3/2} \quad (24)$$

For static equilibrium to exist, the applied radial load must equal the sum of the horizontal (parallel to the load direction) components of the rolling element loads:

$$F_x = \sum_{\phi=-\pi}^{\phi=+\pi} P_\phi \cos\phi \quad (25)$$

$$F_x = P_{\max} \sum_{\phi=-\pi}^{\phi=+\pi} \left[1 - \frac{1}{2\zeta} (1 - \cos\phi) \right]^{3/2} \cos\phi \quad (26)$$

The summation in above equations applies only to the angular extent of the load zone. Equation (26) can also be written in integral form:

$$F_x = nP_{\max} \times \frac{1}{2\pi} \int_{-\phi_L}^{\phi_L} \left[1 - \frac{1}{2\zeta} (1 - \cos\phi) \right]^{3/2} \cos\phi d\phi \quad (27)$$

or

$$F_x = n P_{\max} J_x(\zeta) \quad (28)$$

in which

$$J_x(\zeta) = \frac{1}{2\pi} \int_{-\phi_x}^{+\phi_x} \left(1 - \frac{1}{2\zeta} (1 - \cos\phi)\right)^{3/2} \cos\phi d\phi \quad (29)$$

The radial integral of Equation (29) has been evaluated numerically by Harris (5) for various values of ζ .

From Equation (16),

$$P_{\max} = K \Delta_{\phi=0}^{3/2} = K \left\{ \delta_{\max} - \frac{1}{2} P_D \right\}^{3/2} \quad (30)$$

Therefore,

$$F_x = n K \left\{ \delta_{\max} - \frac{1}{2} P_D \right\}^{3/2} J_x(\zeta) \quad (31)$$

For a given bearing with a given clearance under a given load, Equation (31) may be solved by trial and error.

For ball bearings under pure radial load and zero clearance, $J_x = .2285$, and it can be shown from Reference 6 that

$$P_{\max} = \frac{4.37 F_x}{n \cos \beta} \quad (32)$$

Accounting for nominal diametral clearance in the bearing, one may use the following approximation,

$$P_{\max} = \frac{5 F_x}{n \cos \beta} \quad (33)$$

2.5.1 Approximation to Radial Stiffness

A complete definition of bearing stiffness requires calculation of the stiffness matrix defined by Equation (13). However, for many

applications, simplifications can be made which permit calculation of radial stiffness of a ball bearing under radial load alone.

Palmgren (6) gives a series of formulas to calculate bearing deflection for specific conditions of loading. For slow and moderate speed deep-groove and angular-contact ball bearings subjected to radial load which causes only radial deflection, that is $\delta_z = 0$,

$$\delta_x = 1.58 \times 10^{-5} \frac{P_{\max}^{2/3}}{d^{1/3} \cos \beta} \quad (34)$$

For self-aligning ball bearings,

$$\delta_x = 2.53 \times 10^{-5} \frac{P_{\max}^{2/3}}{d^{1/3} \cos \beta} \quad (35)$$

For this case the maximum rolling element load has previously been shown to be

$$P_{\max} = \frac{5F_x}{n \cos \beta} \quad (33)$$

Substituting for P_{\max} in Equation (34) yields

$$\delta_x = \frac{4.62 \times 10^{-5} F_x^{2/3}}{n^{2/3} d^{1/3} \cos^{5/3} \beta} \quad (36)$$

Transposing, then taking the derivative with respect to x , the stiffness of the bearing is

$$K_{xx} = 4.77 \times 10^6 n d^{1/2} \cos^{5/2} \beta \delta_x^{1/2} \quad (37)$$

For self-aligning ball bearings

$$K_{xx} = 2.36 \times 10^6 n d^{1/2} \cos^{5/2} \beta \delta_x^{1/2} \quad (38)$$

From Equations (37) and (38) it is apparent that the deflection-stiffness relationship is nonlinear because it is dependent on the square

root of radial deflection. In this respect, a ball bearing is unlike a simple spring for which deflection is linear with respect to load.

By substituting for δ_x in Equations (37) and (38), bearing stiffness can be expressed in terms of load as:

Angular Contact Bearings

$$\frac{K_{xx}}{d^{1/3} n^{2/3} \cos^{5/3} \beta} = 3.247 \times 10^4 F_x^{1/3} \quad (39)$$

Self-Aligning Bearings

$$\frac{K_{xx}}{d^{1/3} n^{2/3} \cos^{5/3} \beta} = 2.028 \times 10^4 F_x^{1/3} \quad (40)$$

These expressions are plotted in Figure 6.

2.6 Bearings Under Thrust Load

Thrust ball bearings subjected to a centric thrust load have the load distributed equally among the rolling elements. Hence,

$$P = \frac{F_z}{n \sin \beta} \quad (41)$$

In Equation (41), β is the contact angle which occurs in the loaded bearing. For thrust ball bearings whose contact angles are nominally less than 90 degrees, the contact angle in the loaded bearing is greater than the initial contact angle β' which occurs in the unloaded bearing.

In the absence of centrifugal loading, the contact angles at inner and outer raceways are identical; however, they are greater than those in the unloaded condition. In the unloaded condition, contact angle is defined by

$$\cos \beta' = 1 - \frac{P_D}{2Bd} \quad (42)$$

in which P_D is the mounted diametral clearance. A thrust load, F_z , applied to the inner ring as shown by Figure 7 causes an axial deflection δ_z . This axial deflection is a component of a normal deflection along the line of contact such that from Figure 7

$$\Delta = Bd \left(\frac{\cos\beta'}{\cos\beta} - 1 \right) \quad (43)$$

Since $P = K\Delta^{3/2}$,

$$P = K(Bd)^{3/2} \left(\frac{\cos\beta'}{\cos\beta} - 1 \right)^{3/2} \quad (44)$$

Substitution of Equation (41) into Equation (44) yields

$$\frac{F_z}{nK(Bd)^{3/2}} = \sin\beta \left(\frac{\cos\beta'}{\cos\beta} - 1 \right)^{3/2} \quad (45)$$

Since K is a function of the final contact angle, β , Equation (45) must be solved by trial and error to yield an exact solution for β . Jones (7) has defined an axial deflection constant K_z as follows:

$$K_z = \frac{B}{g(+\gamma) + g(-\gamma)} \quad (46)$$

in which $\gamma = \frac{d \cos \beta}{E}$ and $g(+\gamma)$ refers to the inner raceway and $g(-\gamma)$ refers to the outer raceway. Jones further indicates that the sum of $g(+\gamma)$ and $g(-\gamma)$ remains virtually constant for all contact angles being dependent only on total curvature B . The axial deflection constant K_z is related to K as follows:

$$K = \frac{K_z d^{1/2}}{B^{3/2}} \quad (47)$$

Hence:

$$\frac{F_z}{nd^2 K_z} = \sin\beta \left(\frac{\cos\beta'}{\cos\beta} - 1 \right)^{3/2} \quad (48)$$

Taking K_z from Reference 7, Equation (48) may be solved numerically by the

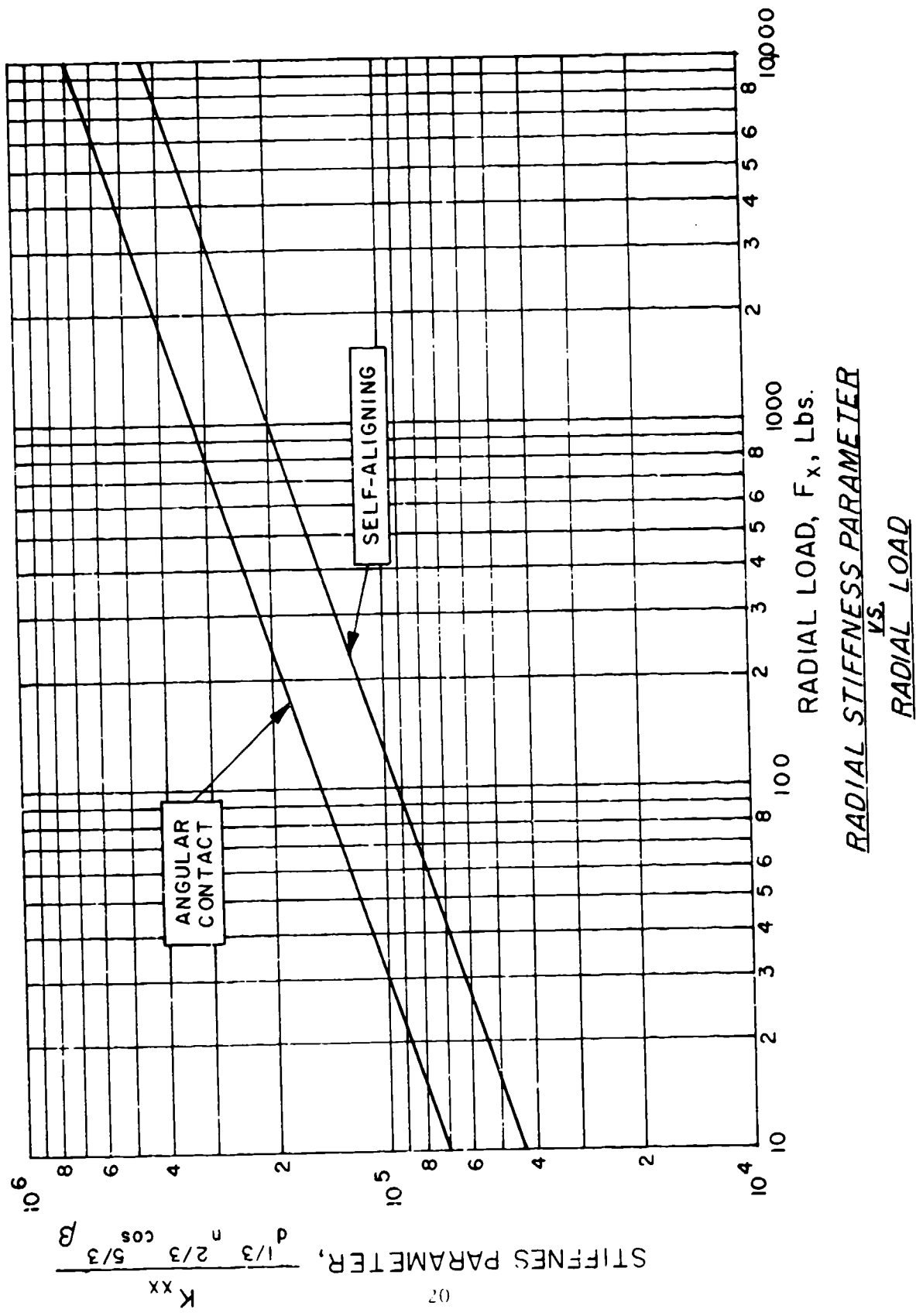


Figure 6 Radial Stiffness Parameter vs. Radial Load

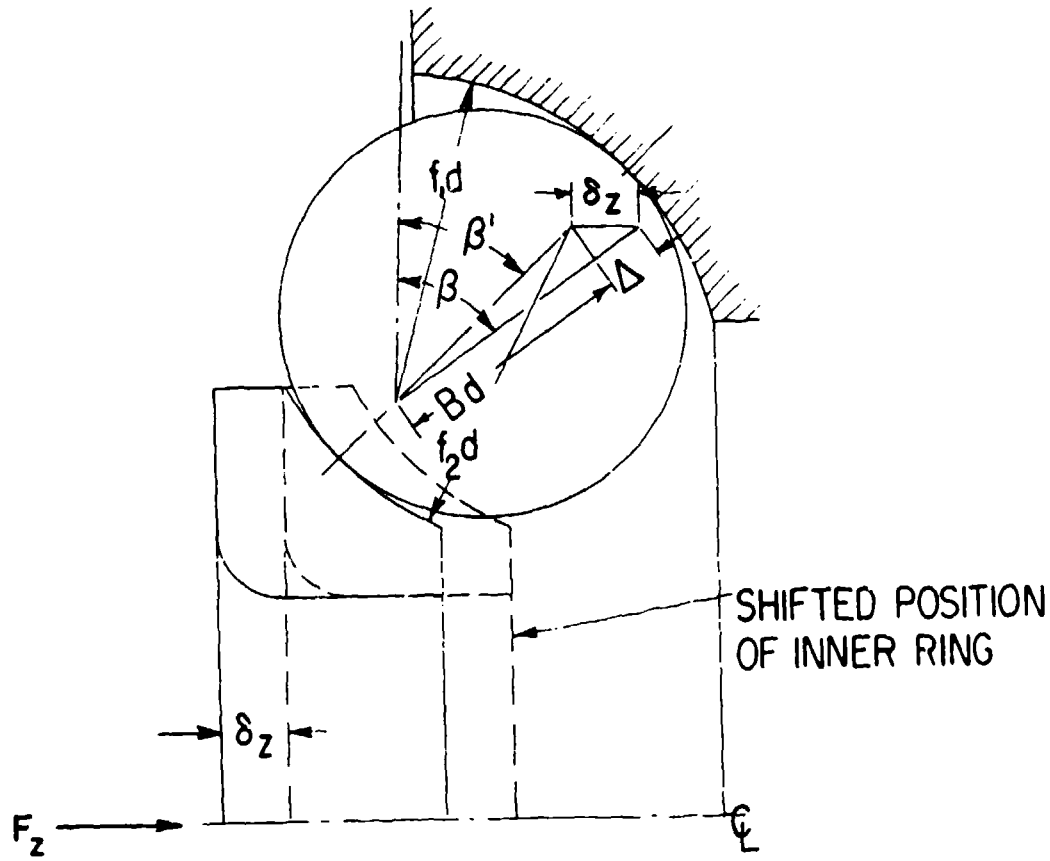


Figure 7 Angular Contact Ball Bearing Under Thrust Load

Newton-Raphson method.

The axial deflection δ_z corresponding to Δ may also be determined from Figure 7 as follows:

$$\delta_z = (Bd + \Delta) \sin\beta - Bd \sin\beta' \quad (49)$$

Substituting Δ from Equation (43) yields

$$\delta_z = \frac{Bd \sin(\beta - \beta')}{\cos\beta} \quad (50)$$

2.6.1 Approximation to Axial Stiffness

From examination of Figure 7, the following approximation can be made:

$$\Delta \sim \delta_z \sin\beta \quad (51)$$

Substituting for Δ in Equation (16) gives

$$\delta_z \sim \frac{1}{K^{2/3}} \frac{P^{2/3}}{\sin\beta} \quad (52)$$

Using the Jones (7) axial deflection parameter, Equation (52) becomes

$$\delta_z \sim \frac{B}{K_z^{2/3} d^{1/3}} \frac{P_{\max}^{2/3}}{\sin\beta} \quad (53)$$

A similar approximation was arrived at by Palmgren (6). Suggested values for axial deflection under pure axial load are:

Angular-Contact Bearings

$$\delta_z = 1.58 \times 10^{-5} \frac{P_{\max}^{2/3}}{d^{1/3} \sin\beta} \quad (54)$$

Self-Aligning Ball Bearings

$$\delta_z = 2.53 \times 10^{-5} \frac{P_{\max}^{2/3}}{d^{1/3} \sin\beta} \quad (55)$$

Thrust Ball Bearings

$$\epsilon_z = 1.9 \times 10^{-5} \frac{p_{\max}^{2/3}}{d^{1/3} \sin \beta} \quad (56)$$

The corresponding stiffnesses are:

Angular-Contact Bearings

$$\frac{K_{zz}}{d^{1/3} n^{2/3} \sin^{5/3} \beta} = 9.5 \times 10^4 F_z^{1/3} \quad (57)$$

Self-Aligning Ball Bearings

$$\frac{K_{zz}}{d^{1/3} n^{2/3} \sin^{5/3} \beta} = 5.9 \times 10^4 F_z^{1/3} \quad (58)$$

Thrust Ball Bearings

$$\frac{K_{zz}}{d^{1/3} n^{2/3} \sin^{5/3} \beta} = 7.9 \times 10^4 F_z^{1/3} \quad (59)$$

These relationships are plotted in Figure 8 for the three types of bearings.

2.7 Ball Bearings Under Combined Loading

Except for ball bearings under simple radial or thrust load, treated previously, there are very few solutions for bearing stiffness that can be evaluated by simple hand computation.

When a ball bearing operates at high speed, the body forces resulting from the ball's motion become significant and must be considered in any analysis. Figure 9 shows the forces and moments acting on the j^{th} ball in a high-speed ball bearing. The operating contact angle at the outer contact is less than that on the inner because of the body forces. Subscript 1 refers to an outer contact and subscript 2 to an inner.

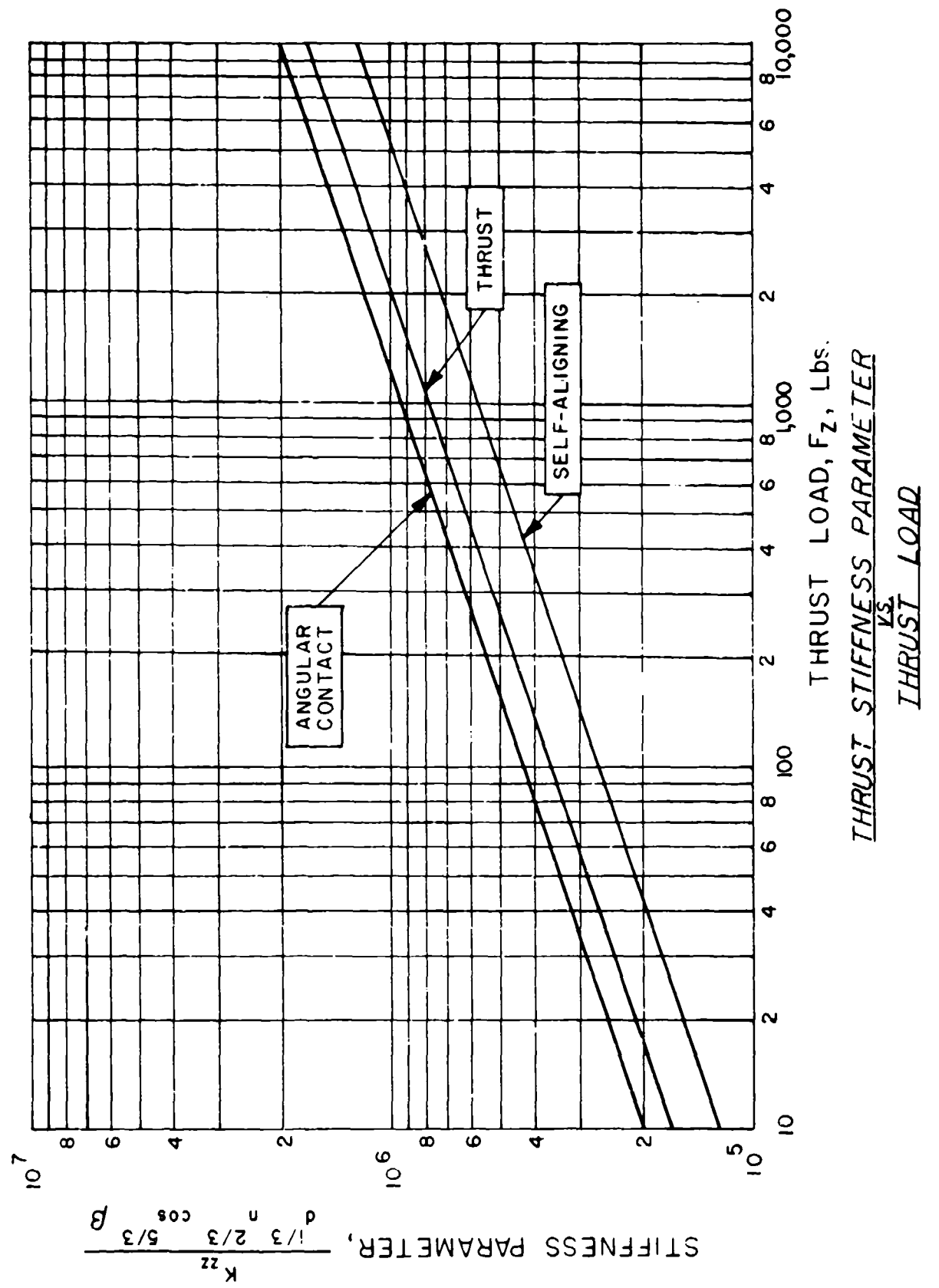


Figure 8 Thrust Stiffness: Parameter vs. Thrust Load

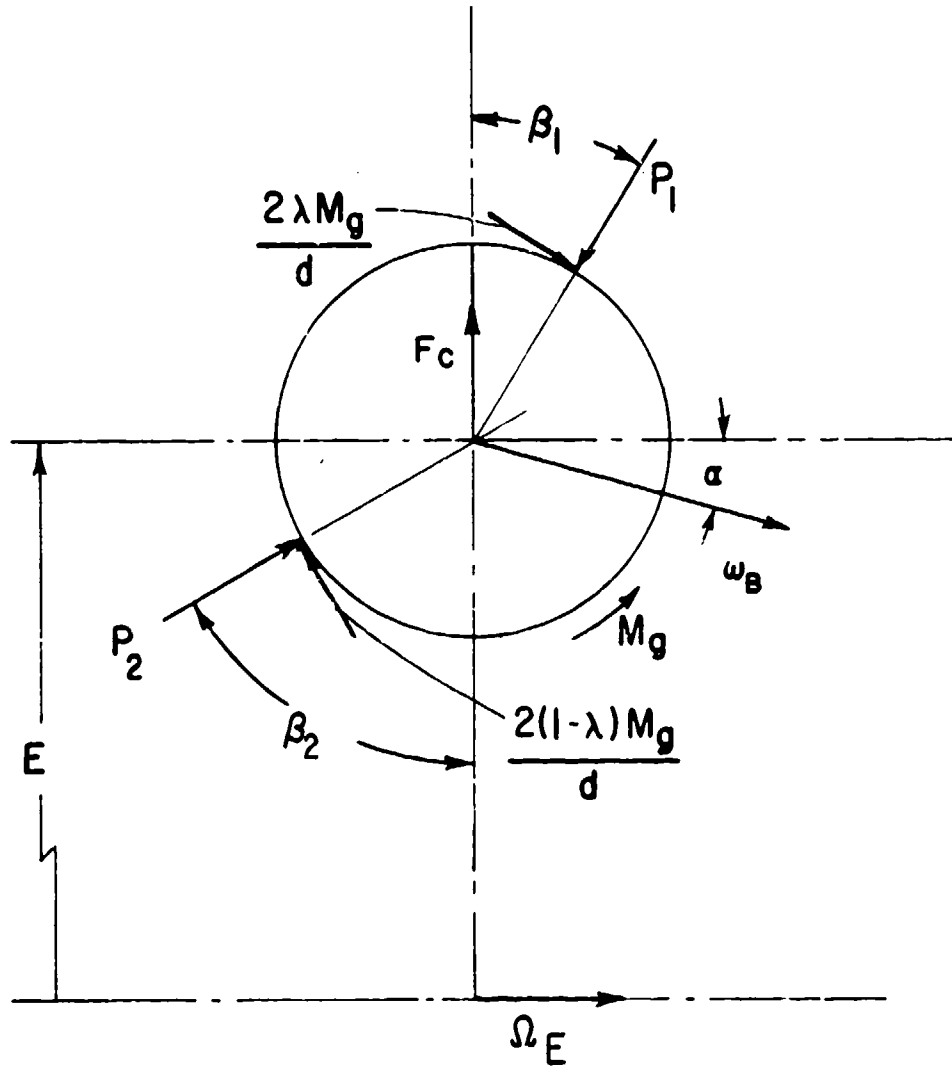


Figure 9 Ball Forces at High Speed Conditions

In Figure 10 the ball center is fixed in the plane of the paper. The ball rotates with the angular velocity ω_B directed at the angle α . The race rotates about the bearing axis with the angular velocity ω_i , $i = 1, 2$ relative to the retainer. For the linear velocity of race and ball to be equal at a contact, the following relation must be satisfied:

$$\omega_B = \frac{C_1 E' (1 + C_1 \gamma_i) \omega_i}{d \cos(\beta_i - \alpha)} \quad (60)$$

where $C_1 = 1$ and $C_2 = -1$

$$\gamma_i = \frac{d \cos \beta_i}{E'} \quad (61)$$

For the i^{th} race to be stationary, the ball must orbit with the angular velocity Ω_E such that

$$\Omega_E = -\omega_i \quad (62)$$

With stationary outer race and rotating inner, the actual angular velocity of the inner race is

$$\Omega_2 = \omega_2 + \Omega_E = \omega_2 - \omega_1 \quad (63)$$

For rotating outer and stationary inner, the actual angular velocity of the outer is

$$\Omega_1 = \omega_1 + \Omega_E = \omega_1 - \omega_2 \quad (64)$$

From Equation (60),

$$\frac{\omega_1}{\omega_2} = \frac{(1-\gamma_2) \cos(\beta_1 - \alpha)}{(1+\gamma_1) \cos(\beta_2 - \alpha)} \quad (65)$$

considering that both races may rotate there results:

$$\omega_1 = \frac{(\Omega_1 - \Omega_2)(1-\gamma_2) \cos(\beta_1 - \alpha)}{(1+\gamma_1) \cos(\beta_2 - \alpha) + (1-\gamma_2) \cos(\beta_1 - \alpha)} \quad (66)$$

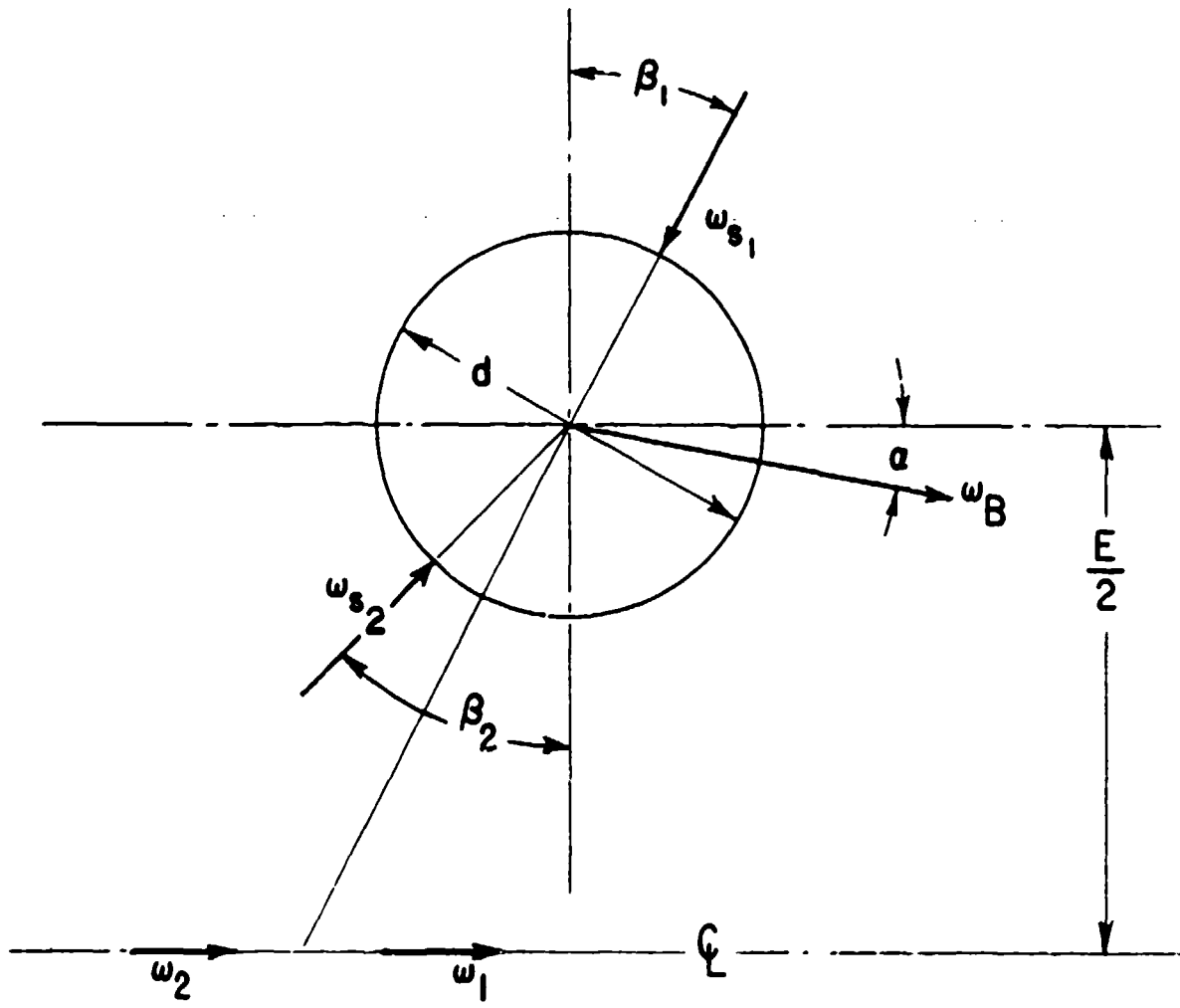


Figure 10 Ball Motion Vectors

$$\omega_2 = - \frac{(\Omega_1 - \Omega_2)(1 + \gamma_1) \cos(\beta_2 - \alpha)}{(1 + \gamma_1) \cos(\beta_2 - \alpha) + (1 - \gamma_2) \cos(\beta_1 - \alpha)} \quad (67)$$

$$\omega_B = \frac{E' \{ (\Omega_1 - \Omega_2)(1 + \gamma_1)(1 - \gamma_2) \}}{d \{ (1 + \gamma_1) \cos(\beta_2 - \alpha) + (1 - \gamma_2) \cos(\beta_1 - \alpha) \}} \quad (68)$$

$$\Omega_E = \frac{\Omega_1(1 + \gamma_1) \cos(\beta_2 - \alpha) + \Omega_2(1 - \gamma_2) \cos(\beta_1 - \alpha)}{(1 + \gamma_1) \cos(\beta_2 - \alpha) + (1 - \gamma_2) \cos(\beta_1 - \alpha)} \quad (69)$$

For an arbitrary choice of α there will be a spin of the ball relative to a race about the normal at the center of the contact area. This is illustrated in Figure 11.

From Figure 10,

$$\omega_{s_1} = C_1 \{ -\omega_i \sin \beta_i + \omega_B \sin(\beta_i - \alpha) \} \quad (70)$$

The controlling race hypothesis assumes that all spin occurs at one contact while no spin occurs at the other. The contact at which no spin exists is called the controlling race. Lightly-loaded bearings may depart somewhat from this situation.

If ω_{s_1} is made zero and Equation (70) solved for α , there results for outer race control:

$$\alpha = \tan^{-1} \frac{\sin \beta_1 \cos \beta_1}{\cos^2 \beta_1 + \gamma_1} \quad (71)$$

and for inner race control:

$$\alpha = \tan^{-1} \frac{\sin \beta_2 \cos \beta_2}{\cos^2 \beta_2 - \gamma_2} \quad (72)$$

The existence of a particular type of control depends on the relative torques required to produce spin at the two contacts.

The torque required to produce spin is:

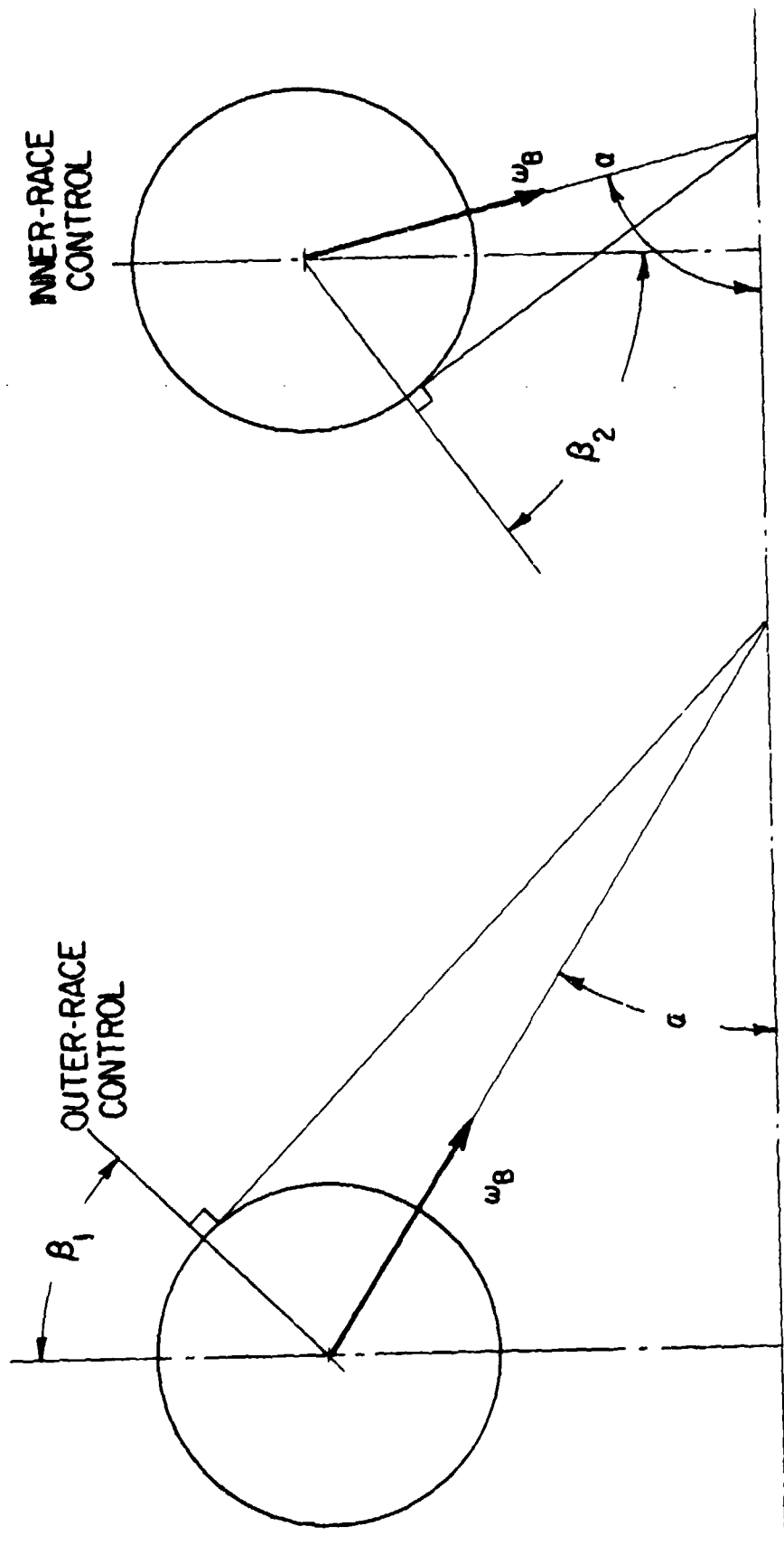


Figure 11 Illustration of Race Control Concept

$$Q = \frac{3\mu P a E(\epsilon)}{8} \quad . \quad (73)$$

Q = spin torque, lb-in
 P = contact load, lbs.
 μ = coefficient of sliding friction
 a = semi-major axis of pressure ellipse, in.
 $E(\epsilon)$ = complete elliptic integral of the second kind formed with the modulus sine where $\cos\epsilon = b/a$, b being the semi-minor axis of the ellipse

Figure 12 shows a ball acted on by the spin torque vectors Q_1 and Q_2 . Outer race control will exist if Q_1 projected on Q_2 is greater than Q_2 . Inner race control will exist if Q_2 projected on Q_1 is greater than Q_1 .

Figure 13 shows the relative positions of ball and race curvature centers before and after the application of the five displacements, δ_x , δ_y , δ_z , θ_x , and θ_y . The outer race curvature center is fixed. The inner race curvature center has moved to (A_1, A_2) and the ball center to (X_1, X_2) .

$$A_1 = B d \sin \beta + \delta_z + \delta''_z + R [(\theta_x + \theta''_x) \sin \phi + (\theta_y + \theta''_y) \cos \phi] \quad (74)$$

$$A_2 = B d \cos \beta + (\delta_x + \delta''_x) \cos \phi + (\delta_y + \delta''_y) \sin \phi - \frac{P_D}{2} \quad (75)$$

$$B = f_1 + f_2 - 1 \quad (76)$$

$$R = E/2 + (f_2 - .5) d \cos \beta \quad (77)$$

P_D = diametral clearance, in.
 δ''_x = initial displacement along x , in.
 δ''_y = initial displacement along y , in.
 δ''_z = initial displacement along z , in.
 θ''_x = initial misalignment about x , rad.
 θ''_y = initial misalignment about y , rad.

For the forces and moments acting on the ball to be in equilibrium, the following must be satisfied:

$$P_1 \sin \beta_1 - P_2 \sin \beta_2 - \frac{2M}{d} \{ \lambda \cos \beta_1 - (1-\lambda) \cos \beta_2 \} = 0 \quad (78)$$

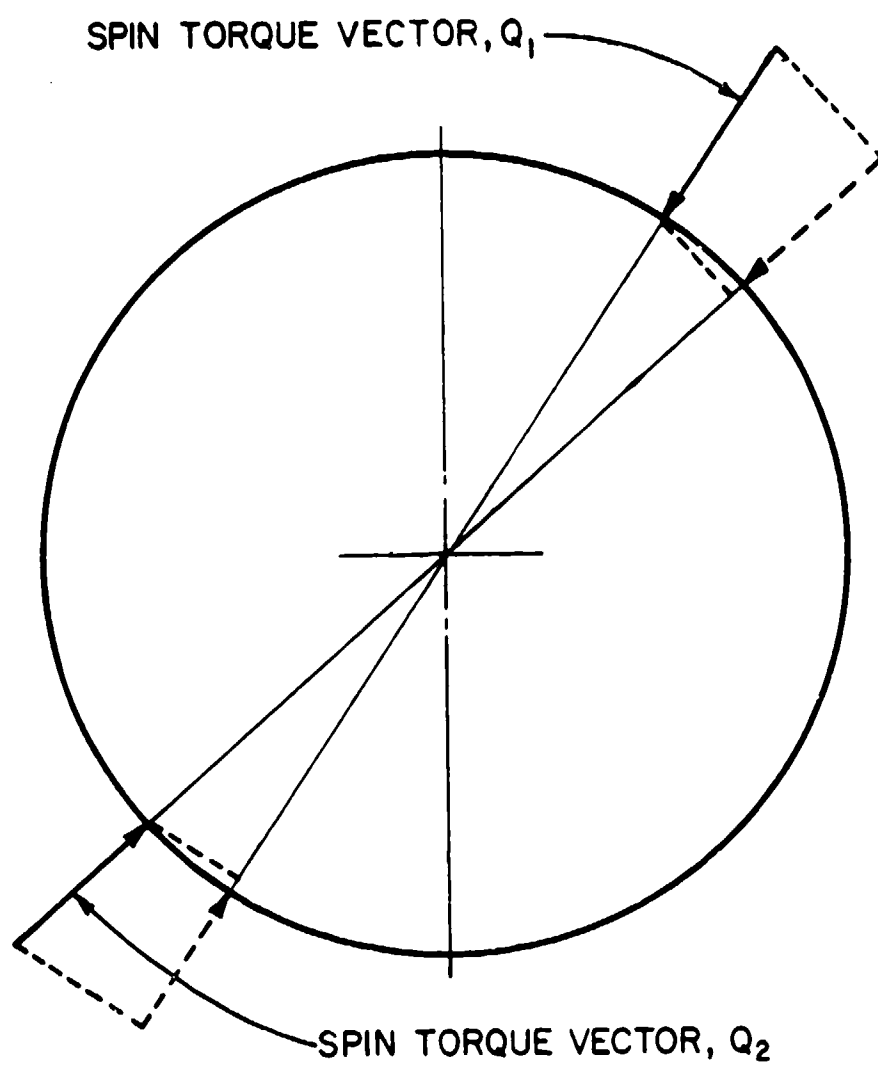


Figure 12 Spin Torque Vectors

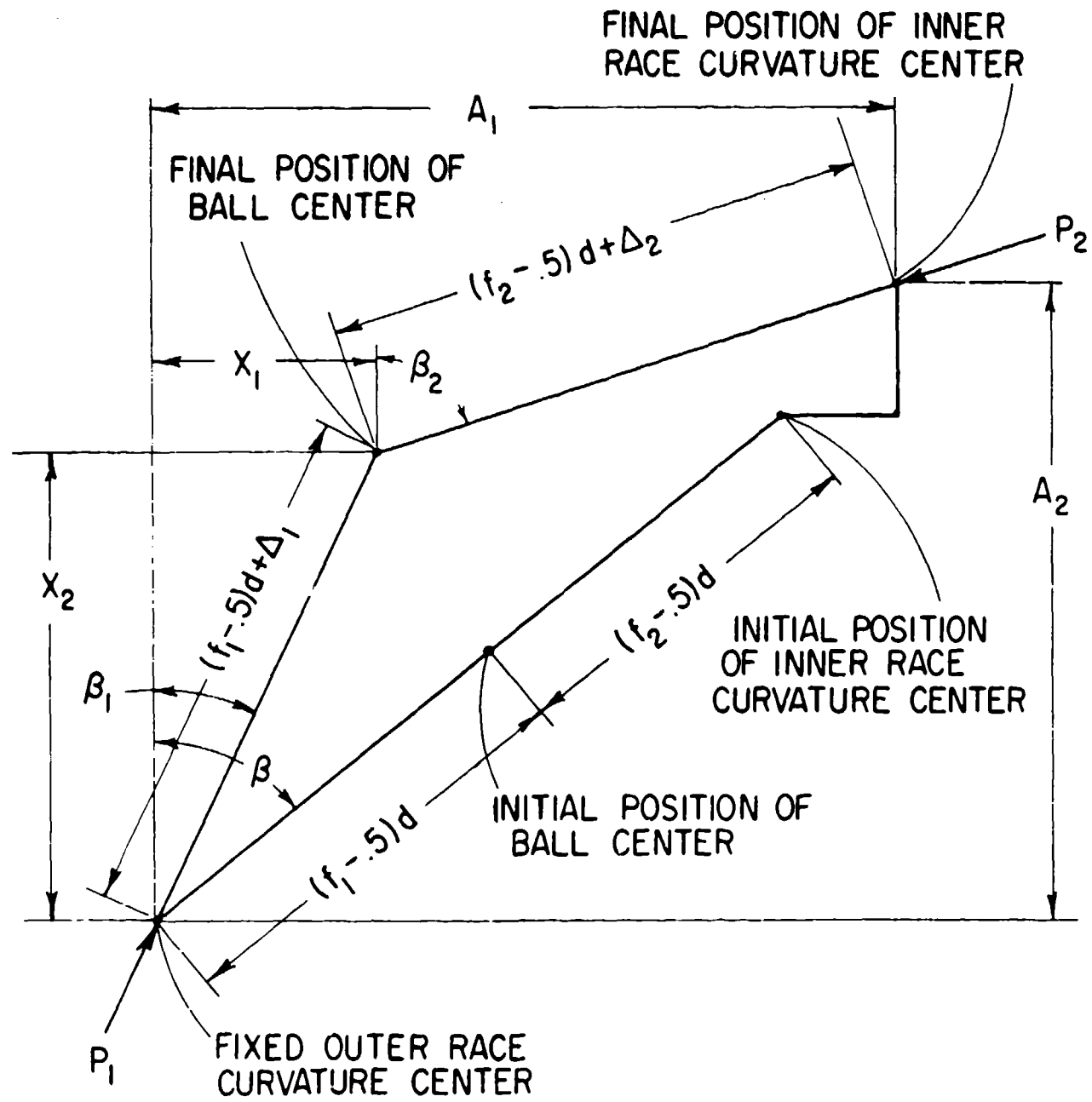


Figure 13 Race Curvature Center Deflection

$$P_1 \cos \beta_1 - P_2 \cos \beta_2 + \frac{2M}{d} \{ \lambda \sin \beta_1 - (1-\lambda) \sin \beta_2 \} - F_c = 0 \quad (79)$$

where λ is 1 for outer race control and 0 for inner race control and

$$F_c = M \Omega_E^2 E' / 2 \quad (80)$$

$$M = I_p \Omega_E \omega_B \sin \alpha \quad (81)$$

E' = Operating Pitch Diameter, in.

$$= E + 2X_2 - (f_1 - .5)d \cos \beta \quad (82)$$

From Figure 13

$$\beta_1 = \tan^{-1} \frac{X_1}{X_2} \quad (83)$$

$$\beta_2 = \tan^{-1} \frac{A_1 - X_1}{A_2 - X_2} \quad (84)$$

Δ_1 and Δ_2 are the elastic approaches of ball and raceways at the contacts

$$\Delta_1 = (X_1^2 + X_2^2)^{1/2} - (f_1 - .5)d > 0 \quad (85)$$

$$\Delta_2 = ((A_1 - X_1)^2 + (A_2 - X_2)^2)^{1/2} - (f_2 - .5)d > 0 \quad (86)$$

The contact loads are related to the elastic approaches through

$$P_i = K_i \Delta_i^{3/2} \quad (87)$$

where

$$K_i = \frac{11.84771}{(n_R + n_B) \cos \epsilon_i} \left[\frac{E(\epsilon_i) d}{\{K(\epsilon_i)\}^3 \{4 - 1/f_i - \frac{2C_i Y_i}{1+C_i Y_i}\}} \right]^{1/2} \quad (88)$$

$$n_R = \frac{4(1-v_R^2)}{E_R} \quad (89)$$

$$n_B = \frac{4(1-\nu_B^2)}{E_B} \quad (90)$$

E_R and E_B are moduli of elasticity for race and ball.

ν_R and ν_B are Poisson's Ratios for race and ball.

$K(\epsilon)$ and $E(\epsilon)$ are the complete elliptic integrals of the first and second kind having the modulus sine.

$$\sin \epsilon_i = \sqrt{1 - \frac{b_i^2}{a_i^2}} \quad (91)$$

b_i and a_i are the semi-minor and semi-major axes of the pressure ellipse
 ϵ is related to the contact geometry through

$$\cot^2 \epsilon_i = \frac{(1-\cos \epsilon_i) E(\epsilon_i)}{2\{K(\epsilon_i) - E(\epsilon_i)\}} \quad (92)$$

$$\cos \epsilon_i = \frac{\frac{1}{f_i} - \frac{2C_i \gamma_i}{1+C_i \gamma_i}}{4 - \frac{1}{f_i} - \frac{2C_i \gamma_i}{1+C_i \gamma_i}} \quad (93)$$

Equations (78) and (79) are a set of nonlinear, simultaneous equations. When the relative ring displacements are held constant, the variables in Equations (78) and (79) are X_1 and X_2 . These are evaluated numerically.

The reactions of the bearing on the shaft are

$$F'_x = \sum_{i=1}^n [P_{2i} \cos \beta_{2i} + \frac{2(1-\lambda_i)M}{d} g_i \sin \beta_{2i}] \cos \phi_i \quad (94)$$

$$F'_y = \sum_{i=1}^n [P_{2i} \cos \beta_{2i} + \frac{2(1-\lambda_i)M}{d} g_i \sin \beta_{2i}] \sin \phi_i \quad (95)$$

$$F'_z = \sum_{i=1}^n [P_{2i} \sin \beta_{2i} - \frac{2(1-\lambda_i)M}{d} g_i \cos \beta_{2i}] \quad (96)$$

$$M'_x = \sum_{i=1}^n [RP_2 \sin\beta_2 - \frac{2(1-\lambda_i)M}{d} (R\cos\beta_2 - f_2 d)] \sin\phi_i \quad (97)$$

$$M'_y = \sum_{i=1}^n [RP_2 \sin\beta_2 - \frac{2(1-\lambda_i)M}{d} (R\cos\beta_2 - f_2 d)] \cos\phi_i \quad (98)$$

Then the equilibrium of external forces

$$\sum_{i=x,y,z} \{F'_i + F_i\} = 0 \quad (99)$$

F_x = external load along x, lbs.

F_y = external load along y, lbs.

F_z = external load along z, lbs.

Equation (99) is a set of three non-linear simultaneous equations in which the variables are δ_x , δ_y and δ_z . They are solved numerically in Appendix A using Newton-Raphson iteration.

If $\delta_{i_{m-1}}$ are current estimates of the three displacements, improved estimates are

$$\delta_{i_m} = \delta_{i_{m-1}} - [K_{ij}]^{-1} \left\{ \Gamma_j \right\}_{m-1} \quad (100)$$

where $\left\{ \Gamma_j \right\}_{m-1}$ are the residues of Equation (99) evaluated at current estimates of δ_i .

The elements K_{ij} of the coefficient matrix are the partial derivatives of the bearing's reactions with respect to the displacements δ_i and comprise the stiffness matrix, Equation (13).

The elements K_{ij} of the stiffness matrix, Equation (13), form the data input for the rotordynamic response computer program described in Reference 2.

SECTION III
APPLICATION OF COMPUTER PROGRAM

The analysis of Section 2.0 has been programmed in Fortran IV for a digital computer and is suitable for use on the CDC 6600. A program listing is presented in Appendix A.

3.1 Input Format

Instructions for preparation of the input cards are included as comment cards in the program listing in Appendix A. To illustrate a typical case consider the bearing in Table 1.

TABLE 1
SAMPLE CASE
DEEP GROOVE BALL BEARING

Number of Balls	=	9
Ball Diameter	=	.1875 inches
Pitch Diameter	=	.9252 inches
Contact Angle	=	0°
Outer-race Curvature	=	.530
Inner-race Curvature	=	.516
Poisson's Ratio	=	.25
Modulus of Elasticity	=	29×10^6 lb/in.
Ball Density	=	0.283 lb/in. ³
RPM of Inner Race	=	1000 rpm
RPM of Outer Race	=	0 rpm
Radial Load	=	1000 lbs.
Axial Load	=	0 lbs.

Figure 14 shows a printout of input for this case.

THIS PAGE IS BEST QUALITY PRACTICABLE
FROM COPY FURNISHED TO DDO

TABLE 1, PAGE 36 OF AFAPL-TR-77, PART II

DESIGN DATA FOR BEARING NO. 1

NO. OF BALLS	PITCH IN	DIA METER IN	INITIAL CONTACT ANGLE DEG	OUTER CURVATURE DEG	INITIAL CURVATURE DEG	INITIAL DEFLECTIONS DEG
9.0003-30	1.875-01	9.2326-C1	3.0000	0.0000	5.3000-01	5.1600-01
OUTER MODULUS OF ELASTICITY LB/IN ²	INNER ELASTICITY LB/IN ²	POISSON'S RATIO	OUTER BALLS	INNER BALLS		
2.9000-37	2.9000-37	0.5000-01	2.5000-01	2.5000-01		

INPUT DATA FOR RUN NO. 1 BEARING NO. 1

TYPE OF LOAD	TYPE OF LOAD	LOADS APPLIED TO SHAFT	INITIAL DISPLACEMENTS ALONG X IN LB	INITIAL DISPLACEMENTS ALONG Z IN LB	INITIAL DEFLECTIONS IN RADIAN	INITIAL DEFLECTIONS IN RADIAN
0.0000	1.0000-03	1.0000-03	0.0000	0.0000	0.0000	0.0000

1: = DEFLECTION PERMITTED
ALONG X, ALONG Y, ALONG Z
1.0000-03 0.0000 0.0000

Figure 14 Input Data for Sample Problem

3.2 Output Format

Figure 15 shows the output format for the sample case of Table 1. The output data includes the internal load distribution and various other stress and dynamic parameters.

The last section of data provides the complete stiffness matrix.

OUTPUT DATA FOR RUN NO. 1 BEARING NO. 1

BALL NUMBER	BALL		CONTACT LOAD		CONTACT ANGLE		CONTACT AREA LENGTH		CONTACT AREA WIDTH		CENTRIFUGAL FORCE
	AZIMUTH	DEG	OUTER INNER	INNER	OUTER	INNER	OUTER	INNER	OUTER	INNER	
4	1.2000+02	1.7117+02	1.7117+02	0.0000	0.0000	0.0000	6.746+02	6.956+02	1.149+02	1.149+02	2.000+02
5	1.6000+02	1.6101+02	1.6101+02	0.0000	0.0000	0.0000	9.2213+02	1.2213+02	1.6105+02	1.6105+02	2.000+02
6	2.0000+02	1.7117+02	1.7117+02	0.0000	0.0000	0.0000	6.956+02	6.956+02	1.149+02	1.149+02	2.000+02
7	2.4000+02	1.7117+02	1.7117+02	0.0000	0.0000	0.0000	6.956+02	6.956+02	1.149+02	1.149+02	2.000+02

MEAN COMPRESSIVE STRESS
BALL NUMBER
OUTER INNER
PSI IN
0.0000 2.9188+05
0.0000 2.9188+05
0.0000 2.9188+05
0.0000 2.9188+05
0.0000 2.9188+05

PARTIAL DERIVATIVES OF REACTIONS WITH RESPECT TO DISPLACEMENTS

DFX/DX LB/IN	DFX/DY LB/IN	DFX/DZ LB/IN	DFX/DALY LB/RAD
7.9779+05	-0.8828+03	0.0000	0.0000
DFY/DX LB/IN	DFY/DY LB/IN	DFY/DZ LB/IN	DFY/DALY LB/RAD
-0.8828+03	0.8828+05	0.0000	0.0000
DFZ/DX LB/IN	DFZ/DY LB/IN	DFZ/DZ LB/IN	DFZ/DALY LB/RAD
0.2000	1.2000	1.2000	-0.5468+04
DMX/DX LB/IN	DMX/DY LB/IN	DMX/DZ LB/IN	DMX/DALY LB/RAD
0.0000	0.0000	0.0000	0.0000
DMY/DX LB/IN	DMY/DY LB/IN	DMY/DZ LB/IN	DMY/DALY LB/RAD
0.0000	0.0000	0.0000	0.0000
DMZ/DX LB/IN	DMZ/DY LB/IN	DMZ/DZ LB/IN	DMZ/DALY LB/RAD
0.0000	0.0000	0.0000	0.0000

aFIN

THIS PAGE IS BEST QUALITY PRACTICABLE
FROM COPY FURNISHED TO DDG

Figure 15 Output Data for Sample Problem

SECTION IV
DESIGN DATA

Three separate sets of design charts were included in the original Part IV report. These were:

- a. Pure Radial Loaded Bearings (Deep Groove) Contact Angle
 $\beta' = 0^\circ$
- b. Pure Thrust Loaded Bearings (Deep Groove) Contact Angle
 $\beta' = 0^\circ$
- c. Angular Contact Bearings with Axial Preload and Applied Radial Load $\beta' = 25^\circ, 15^\circ$

As a check of these design charts shows some differences between the original program prediction and the present program prediction, the design charts have been recalculated and are shown in Appendices B, C, and D.

Table 2 describes the dimensions and symbols used for the deep-grooved ball bearings. Table 3 contains information pertaining to the angular contact bearings. These bearings are identical to those studied previously in Reference 1.

4.1 Radial Stiffness Versus Radial Load

The first set of three charts (Appendix B) contains graphs of radial stiffness versus radial load. Load levels are indicated on the curves. The effects of bearing size and race curvatures are illustrated by these four charts. In general, a bearing with curvatures of $f_1 = .530$, $f_2 = .516$ is stiffer than the same bearing operating with curvatures of $f_1 = f_2 = .570$, for the same radial load. Radial stiffness is higher for a bearing with a larger bore diameter and/or a greater number of balls. Note, for pure radial load, the linear relationship between $\log K_{yy}$ and $\log F_y$. This was previously illustrated in Figure 6.

TABLE 2

DEEP GROOVE BEARINGS

Bearing Symbol	Bore (Inch)	Bore mm	O.D. (Inch)	Ball Diameter, Inch	Number of Balls	f_1	f_o
A1	.5906	15	1.2598	.1875	9	.516	.530
A2	.5906	15	1.2598	.1875	9	.570	.570
B1	.9843	25	1.8504	.250	10	.516	.530
B2	.9843	25	1.8504	.250	10	.570	.570
C1	1.378	35	2.4409	.3125	11	.516	.530
C2	1.378	35	2.4409	.3125	11	.570	.570
D1	2.1654	55	3.5433	.40625	13	.516	.530
D2	2.1654	55	3.5433	.40625	13	.570	.570
E1	2.9528	75	4.5276	.46875	15	.516	.530
E2	2.9528	75	4.5276	.46875	15	.570	.570
AA1	.5906	15	1.378	.2345	8	.516	.530
AA2	.5906	15	1.378	.2345	8	.570	.570
BB1	.9843	25	2.0472	.3125	9	.516	.530
BB2	.9843	25	2.0472	.3125	9	.570	.570
CC1	1.378	35	2.8346	.4375	9	.516	.530
CC2	1.378	35	2.8346	.4375	9	.570	.570
DD1	2.1654	55	3.937	.5625	10	.516	.530
DD2	2.1654	55	3.937	.5625	10	.570	.570
EE1	2.9528	75	5.1181	.6875	11	.516	.530
EE2	2.9528	75	5.1181	.6875	11	.570	.570

TABLE 3

ANGULAR CONTACT BEARINGS

$\beta_o = 15^\circ, 25^\circ$

Basic Static Load (lb)	Bearing Number	Bore (Inch)	Bore mm	O.D. (Inch)	d (in)	Number of Balls	f_i	f_o	Axial Preload (lb)	S.L.	M.	P.H.
630	PA 1 PA 2	.5906	15	1.2598	.1875	11	.516	.530	20	50	100	
	PB 1 PB 2	.9843	25	1.8504	.2500	13	.516	.530	50	100	200	
1400	PC 1 PC 2	1.3780	35	2.4409	.3125	15	.516	.530	50	100	200	
	PD 1 PD 2	2.1654	55	3.5433	.40625	18	.516	.530	100	200	300	
2600	PE 1 PE 2	2.9528	75	4.5276	.46925	21	.516	.530	100	200	300	
	PAA1 PAA2	.5906	15	1.3780	.23425	10	.516	.530	20	50	100	
5100	PBB1 PBB2	.9843	25	2.0472	.3125	12	.516	.530	50	100	200	
	PCC1 PCC2	1.378	35	2.8346	.4375	12	.516	.530	50	100	200	
8600	PDD1 PDD2	2.1654	55	3.9370	.5625	14	.516	.530	100	200	300	
	PEE1 PEE2	2.9528	75	5.1181	.6875	16	.516	.530	100	200	300	
760												
1640												
3750												
7300												
12200												

4.2 Axial Stiffness Versus Thrust Load

The second set of eight charts (Appendix C) contains graphs of axial stiffness and axial deflection versus axial thrust applied load. Load levels are tabulated in Table 4 for bearings undergoing a pure thrust load.

A similar observation as given above for radially loaded bearings, can be made for the thrust loaded bearing, i.e., a bearing operating with curvatures of $f_1 = .530$, $f_2 = .516$, is stiffer than the same bearing operating with curvatures of $f_1 = f_2 = .570$ for the same axial load. For all practical purposes, however, an average curve may be drawn for axial stiffness versus axial load for all bearing sizes. In particular, the bearing with the smaller bore and less balls is less stiff at light loads and more stiff at heavy loads as compared to the larger bore bearing. There is an approximate linear relationship between $\log K_{zz}$ and $\log F_z$ (also see Figure 8).

4.3 Radial Stiffness Versus Radial Load with Preload

The third set of (24) charts (Appendix D) contain graphs of radial stiffness versus radial load with preload. Load levels are indicated on the curves. The effects of bearing size, race curvatures, initial contact angle, and axial preload are illustrated by these 24 charts. For the same radial load and axial preload, a bearing operating with curvatures of $f_1 = .530$, $f_2 = .516$, is stiffer than the same bearing operating with curvatures of $f_1 = f_2 = .570$. The radial stiffness level is higher for a bearing with a larger bore diameter and/or a greater number of balls, and the smaller initial contact angle, ($\beta' = 15^\circ$). In general, the radial stiffness vs. radial load curve for an angular contact bearing is composed of three different behaving regions. One region shows the stiffness to be constant with varying radial load. (This is the light radial load region.) The middle, or moderate radial load region shows a minimum value for radial stiffness. The heavily radial loaded region shows a linear relationship between $\log K_{xx}$ and $\log F_x$. This third region is similar in behavior to that of the characteristics of a pure radial loaded deep grooved bearing. The basic cause for this curve having three separate regions is due to the axial preload. In region one, the axial preload has a great effect in holding the radial stiffness constant. In region two, where the applied radial

TABLE 4

AXIAL LOADED DEEP GROOVE BEARINGS

Table of approximate load values corresponding to C/P = 5 and C/P = 10 load levels.

<u>Bearing Symbol</u>	<u>Load (1b)</u>	
	C/P = 5	C/P = 10
A1	290	100
B1	600	250
C1	1100	450
D1	2250	950
E1	3650	1500
A2	70	30
B2	175	75
C2	300	100
D2	550	250
E2	950	350
AA1	380	155
BB1	800	300
CC1	1550	650
DD1	3000	1250
EE1	5050	2100
AA2	95	50
BB2	200	100
CC2	400	200
DD2	1500	350
EE2	2550	700

load becomes equal in magnitude to the axial preload the radial stiffness tends to decrease with increasing applied radial load to a minimum value. In the third region, the axial preload has little or no effect, and the angular contact bearing reflects the behavior of a pure radially loaded bearing i.e., a linear $\log K_{xx}$ versus $\log F_x$ relationship.

Thus another point one is led to observe is the role of axial preload magnitude on the three regions of a typical stiffness versus load curve. Three different preloads are represented in these charts and are tabulated in Table 3. These preloads are given the names selected light, moderate, and preferred heavy. The effect of increased preload is to increase the region one load range and decrease region three load range. Thus, the ultimate is a constant radial stiffness with varying radial load obtained with an infinite preload. The increased preload also has the effect of increasing the level of stiffness in regions one and two. However, it should be noted particularly that the level of stiffness in region three, for the same radial load, is the same for all preload values. This, as mentioned above, is because the axial preload effect is relieved entirely above a certain (radial load) (axial preload) ratio. (Approximately $F_x/F_z = 3$ for $\delta' = 25^\circ$ and $F_x/F_z = 4$ for $\delta' = 15^\circ$.)

In general, the light and extra light deep grooved ball bearings examined here will have a radial stiffness ranging from 10^5 to 2×10^6 for radial loads of from 10 to 2,000 lbs. The angular contact bearings will have radial stiffness values from 2×10^5 to 2×10^6 for radial loads of from 10 to 2,000 lbs. The deep grooved ball bearings will have an axial stiffness per bearing of from 2×10^4 to 4×10^6 for thrust loads of from 10 to 10^4 lbs. As in the case of the preloaded radial bearing, preloading will increase these values of axial stiffness.

APPENDIX A

COMPUTER PROGRAM FOR CALCULATING THE
STIFFNESS MATRIX OF A BALL BEARING

THIS PAGE IS BEST QUALITY PRACTICABLE
FROM COPY FURNISHED TO DDQ

MAIN PROGRAM

1 CARD 1-10 NUMBER OF BALLS
 1-10 BALL DIAMETER - IN
 1-10 CONTACT DIAMETER - IN
 1-10 CONTACT ANGLE - DEGREE FACTOR (AS .52)
 1-10 INNER-TRACE CURVATURE FACTOR (AS .52)
 1-10 IF CONTACT CLEARANCE IS ZFROM THIS ITEM IS THE TOTAL MOUNTED
 1-10 DIAMETER CONTACT CLEARANCE FROM WHICH THE MOUNTED CONTACT ANGLE IS POSITIVE
 1-10 ANGLE WILL BE CALCULATED. IF CONTACT ANGLE IS POSITIVE
 1-10 IT IS THE INCREMENT IN INTERNAL CLEARANCE FROM WHICH THE
 1-10 MOUNTED CONTACT ANGLE WILL BE CALCULATED. AN INCREASE IN
 1-10 CLEARANCE IS POSITIVE. A REDUCTION IN CLEARANCE IS
 1-10 NEGATIVE.

2 1-80 PUNCH 1 (NO DECIMAL POINT)
 1-80 LITTLE CARD - PUNCH ANYTHING.
 1-80 LEAVE BLANK.

3 1-10 SECOND TITLE CARD - PUNCH ANYTHING. IF BLANK PROGRAM ASSUMES
 1-10 POSITION'S RATIO FOR OUTER RING. IF BLANK PROGRAM ASSUMES

4 1-10 .25 POSITION'S RATIO FOR INNER RING. IF BLANK PROGRAM ASSUMES
 1-10 .25 MODULUS OF ELASTICITY FOR BALLS. IF BLANK PROGRAM ASSUMES .25
 1-10 MODULUS OF ELASTICITY FOR OUTER RING. IF BLANK PROGRAM ASSUMES .25
 1-10 ASSUMES .25 MODULUS OF ELASTICITY FOR INNER RING. IF BLANK PROGRAM ASSUMES .25
 1-10 ASSUMES .25 MODULUS OF ELASTICITY FOR BALLS. IF BLANK PROGRAM ASSUMES .25
 1-10 MODULUS OF ELASTICITY FOR BALLS. IF BLANK PROGRAM ASSUMES .25

5 1-70 BALL DENSITY - LB/IN*3. IF BLANK PROGRAM ASSUMES .25
 1-70 IF INNER-TRACE CONTROL IS SUSPECTED PUNCH 2 HERE. IF
 1-70 BLANK PROGRAM ASSUMES 1. CORRESPONDING TO OUTER-TRACE
 1-70 CONTROL. IF ASSUMPTION IS INCORRECT PROGRAM WILL CORRECT

6 1-10 RING OF OUTER RING
 1-10 LOAD OF INNER RING ALONG X - Lb. MUST BE
 1-10 LOAD APPLIED TO INNER RING ALONG Z - Lb. MUST BE
 1-10 NEGATIVE
 1-10 INITIAL DISPLACEMENT OF INNER RING ALONG X - IN
 1-10 INITIAL DISPLACEMENT OF INNER RING ALONG Y - IN
 1-10 INITIAL DISPLACEMENT OF INNER RING ALONG Z - IN.
 1-10 A POSITIVE VALUE LOADS THE BEARING.
 1-10 INITIAL DISPLACEMENT OF INNER ABOUT X - RADIAN
 1-10 INITIAL DISPLACEMENT OF INNER ABOUT Y - RADIAN
 1-10 A 1. HERE PERMITS REFLECTION ALONG X
 1-10 A 1. HERE PERMITS REFLECTION ALONG Y
 1-10 A 1. HERE PERMITS REFLECTION ALONG Z
 1-10
 1-10 IF INITIAL DISPLACEMENTS EXIST ALONG X, Y OR Z
 1-10 IF REFLECTIONS IN THOSE DIRECTIONS DUE TO EXTERNAL LOADS ARE

UNIVERSITY OF TORONTO LIBRARIES

IF EXTERNAL LOADS ALONG X AND Y ARE PERMITTED
IN THIS MANNER, WHAT ARE THE REFLECTIONS IN
FACT ENTRE BOTH INITIAL DISPLACEMENT AND EXTERNAL LOAD

TURN ADDITIONAL LOOMS WITH SAME BEARING REPEAS CARDS 5 AND 6 DIRECTLY AFTER LAST CARD 6

11. MCF THRE: "LAR'S LAST CARD 6 10 STUP

THIS PAGE IS BEST QUALITY PRACTICABLE
FROM COPY FURNISHED TO DDC

THIS PAGE IS BEST QUALITY PRACTICABLY
FROM COPY FURNISHED TO DDC

```
10      DGA(1,1)=0.
      DGA(1,2)=0.
      DGEA(1,1)=0.
      DGEA(1,2)=0.
      TARE=0
      REAU(5,20)YN,0,E,BETA,F(1),F(2),PD
      IF(XN.EQ.0.)STOP
      NEXN=0
      ISTUP=0
      REAU(5,30)
      FORMAT(1H1,79H
      /1X,79H
      )
      20      WPIIE(0,30)
      WFAU(5,20)PR(1),PR(2),PR,YN(1),YN(2),YC,DFNS,XIC
      IF(XIC.EQ.0.Y.)XIC=1.
      30      D(35,J)=1
      ICTL(J)=XIC
      ILOAD=0
      IPRE=1
      IPR=1
      RDE=(F(1)+F(2)-1.)*D
      D(40)=0
      CRV(K)=F(K)-5)*D
      RET=CETA/57.295780
      TEMP=CCUS(RLT)
      AI=2.*LD*(1.-TFMP)
      PX=0.
      PCW=AI+PD
      TF(4D)-2.*PD)70,50,50
      40      WPII(0,6)
      50      FORMAT(474U THIS BEARING HAS TOO MUCH INTERNAL LOOSENESS)
      60      ISTUP=1
      Q(10,275
      70      TF(4D)75,75,80
      RET=0.
      SINB=0.
      COSB=1.
      PX=PD
      80      SINTC=0
      RETM=ALOS((2.*BD-PLM)/(2.*BD))
      90      SINDESIN(RTM)
      COSDECS(RET)
      100     RETM=RET*37.29578
      110     IF(YR(K))110,110,120
      120     IF(YR(K))130,130,140
      130     PR(K)=25
      140     CNT1=0
      CNT2=5*LCRV(2)*COSB
      IF(YR)150,150,160
```

THIS PAGE IS BEST QUALITY PRACTICABLE
FROM COPY FURNISHED TO DDO

1 F(P(2,J)*LE.0.)GO TC 590
 PHI=PHL(J)*57.2957A
 PHI=F(6.5P(J).PHI(1,J)*P(2,J).RT(1,J).RT(2,J).AMAJ(1,J).AMAJ(2,J)
 1) BMIN(1,J).EMIN(2,J).XCX(J)
 1) FORMAT(17.3X.1P10E12.)
 530 CONTINUE
 540 WRITE(6,600)
 600 1 IN 1 FORMAT(132H0 H/D VALUE MFAN COMPRESSIVE STRESS CONTACT DEFLECT
 2 GYKOSCOPE/130H NUMBER TYPE OF ROTATIONAL ORBITAL
 3 INNER CUTTER INNER CONTROL OUTER VELOCITY
 4 ITY MOMENT/17X.3HPSI.0X.3HPSI.10X.2HIN.10X.2HIN.45X.3HPSI.0X.3
 5HPPM.8X.5ULP*IN)
 600 830 J=1 ON
 7 IF(P(2,J);LE.0.)GO 630
 8 WRD=WRD(J)
 9 IF(LCTL(J).EQ.2)WRD=WRD(2)
 10 K=1
 11 STR3(K)=1.273240*P(K,J)/(AMAJ(K,J)*BMIN(K,J))
 12 STRP=ASTN(5*AMAJ(J)/(F(K)*D))+AT(K,J)/5.2957A
 13 HDP(K)=F(K)*(1.5*STR3(K)*STR3(K)*STR3(K))
 14 HDP(K)=F(K)*(1.5*STR3(K)*STR3(K)*STR3(K))
 15 END, BREL(J), E2FV(J), XF1(J), XF2(J), XFEL(1,J), XFEL(2,J), HUU(1), HUU(2),
 16 FORMAT(17.5X.1P6E12.4.3X, A4, 2HEP, 3X, 1P7E12.4)
 17
 18 WRITE(6,610)
 19 FORMAT(1H0,15X.29REACTIONS OF BEARING ON SHAFT.21X.49HTOTAL DISPL
 20 LACEMENT OF INNER WITH RESPECT TO OUTER/11H ALONG X ALONG Y AL
 21 30 1G Z ALONG < ABOUT ABOUT Y/11RH L7 L8 L9
 22 620 CONTINUE
 23 630 CONTINUE
 24 640 5 FAULTS AND AIDS
 25 DC 050 K=1,3
 26 DFL(K)=DFL(K)+DFL11(K)
 27 4) DFL11(6.260)XF1(2),XF1(3),XF1(4),XF1(5),DFL(2),DFL(3),DFL(1
 28 1) DFL11(4),DFL11(5)
 29 650 650 PARTIAL DERIVATIVES OF REACTIONS WITH RESPECT TO JISP
 30 1) LACEMENTS
 31 660 FORMAT(6,6U)
 32 670 FORMAT(5A,U) RX/UX DFX/DY RFY/DZ RFX/DZ RFY/DZ
 33 680 FORMAT(5R,U) LR/IN LB/IN LB/RAD LB/RAD L3/R
 34 690 1A1 1E(6.250)RTV(2,02),RTV(2,03),RTV(2,04),RTV(2,05)
 35 1A2 1E(6.670)RFY/UX DFY/DY RFY/DZ RFY/DZ
 36 701 1A3 1E(6.670)RTV(3,02),RTV(3,03),RTV(3,04),RTV(3,05)
 702 1A4 1E(6.250)RTV(3,02),RTV(3,03),RTV(3,04),RTV(3,05)

THIS PAGE IS BEST QUALITY FRACTICABLE
FROM COPY FURNISHED TO DDO

```

50      T6=1
60      IF((A2-CRV(1))**2+A1**2-CRV(2)**2)70,70,80
70      NOL0AD=NOL0AD+1
P(2,J)=0.
80      RETURN
80      A1=ARS(A1)/R2
90      AY=H1*CRV(1)/SQT
100     AY=H2*CRV(1)/SQT
100     XX=HAX*TR+AY-A2)/TR
110     X(1)=X(1)+10*110
110     X(1)=X(1)+6*(AX-X(1))*T6
120     X(2)=A2-6*(A2-AY)
120     G0=10190
130     CLM=(CRV(1)**2+A1**2-CLM*(2)**2)/(2.*CRV(1)*SQT)
130     ALAM=ATAN(SQRT(1.-CLM**2)/CLM)
130     A1=ATAN(T1)-ALAM
130     AY=CRV(1)*SIN(R1)
130     AY=SQRT(COV(1)**2-AX**2)
140     G0=100
140     X(2)=AY*T6
140     G0=10120
150     DC=80 L=1,2
150     G=0*SQT((1.+TR**2))*C(L)/E
150     T1=1./E(L)-2.*G/(1.+G)
150     T2=-2./E(L)+T1
150     CALL ELIPN(T1,T2,E,E,K,CST2,TOUT)
150     TOUT=109,180,160
160     FORMAT(6,170,L)
170     RETURN
180     YX(L)=1.047791*EL(L)+SQT(EF*U)/(EK**3*CSE2*T2))
180     AP1=(P1-N-PU)/(1.+(X(2)/X(1))*666666667)
180     AP0=SQRT-B-AP1
180     AY=CRV(1)+AP0*TR/SQRT(1.+TR*AP0)*2-AY**2)
180     G0=10100
190     DC=60 IT=1,2
190     CYR2=CYR3*2+2
200     CYR2=CYR62-1.)*210,210,200
200     B(1)=ALAN(X(1)/X(2))/((2-X(2)))
210     B(2)=A1*AN((1-X(1))/((2-X(2)))
210     DC=20 X=1,2
220     SC(K)=2IN(B(K))
220     DC=X(1,2)=X(1)*2/X(2)
220     DC=X(2,1)=X(1)*3BX(1,2)/X(2)

```


310 C¹AL(K)=C¹NS(T¹MP)
 $T^1 = S^1(L) * C^1AL(?)$
 $T^2 = S^2(L) * C^2AL(?)$

```

RVE11+12*(RPM(1)-RPM(2))*GC(1)*GC(2)/(n*nn)
RVE11*(1+DP*(1)+T2*RP*(2))/DN
CYR11*CS*REVE**C**C
CYR11*CE*REVRS*SEL
H(1)*2*GYR11
H1*(2)*H1*(1)
Y1*2*(IC)*2+C(IC)*G2(IC)*
Y2*2*(IC)*2-5*(IC)*
Y3*2*(IC)*2+C(IC)

```


THIS PAGE IS BEST QUALITY PRACTICABLE
FROM COPY FURNISHED TO DDC

2.1 FORMAT (12.0FLPN - 10)

TER1

DETUR1

3.0 CTE=CSE2/2^15

3.1 X16=AL06(1.0/CSF2^15
+CSF2^15*0.479204+CSF2^15*0.85099193+CSF2^15*0.400905094)+CSE2*(0.0
+CSE2*(0.479494+CSF2^15*0.81507240+CSF2^15*0.13829090)*XL6
+CSF2^15*0.32891+CSF2^15*(0.97032891+CSF2^15*0.545444094+0.3204666*CSE2))
+CSF2^15*(0.134750742+CSF2^15*(0.060111519+0.10944912*CSE2))*XL6
EUKEFKFE
ECK=(1.0-CTAU-2.0*(EUK-1.0)*CTE2)*SNES*SNIF/((8.0-4.0*SNES)*EUK-2.0*CSE2*

3.2 CTE=CSE2-CR-5.0E-7)60.40.40

4.0 CHTUE

4.1 CHTF(6.0-1.0)

5.0 FCRWOT(12.0FLPN - 4.0)

6.0 FTR2

6.1 DETUR1

6.2 FDIR01INT SIMULT(A+N:8,X^KX),R(3),X(3),K0L(3)

6.3 K0L(1)=1

6.4 K0L(2)=1

6.5 K0L(3)=1

6.6 K0L(4)=1

6.7 K0L(5)=1

6.8 K0L(6)=1

6.9 K0L(7)=1

6.10 K0L(8)=1

6.11 K0L(9)=1

6.12 K0L(10)=1

6.13 K0L(11)=1

6.14 K0L(12)=1

6.15 K0L(13)=1

6.16 K0L(14)=1

6.17 K0L(15)=1

6.18 K0L(16)=1

6.19 K0L(17)=1

6.20 K0L(18)=1

6.21 K0L(19)=1

6.22 K0L(20)=1

6.23 K0L(21)=1

6.24 K0L(22)=1

6.25 K0L(23)=1

6.26 K0L(24)=1

6.27 K0L(25)=1

6.28 K0L(26)=1

6.29 K0L(27)=1

6.30 K0L(28)=1

6.31 K0L(29)=1

6.32 K0L(30)=1

6.33 K0L(31)=1

6.34 K0L(32)=1

6.35 K0L(33)=1

6.36 K0L(34)=1

6.37 K0L(35)=1

6.38 K0L(36)=1

6.39 K0L(37)=1

4055

4056

4057

4058

4059

4060

4061

4062

4063

4064

4065

4066

4067

4068

4069

4070

4071

4072

4073

4074

4075

4076

4077

4078

4079

4080

4081

4082

4083

4084

4085

4086

4087

4088

4089

4090

4091

4092

4093

4094

4095

4096

4097

4098

4099

4100

4101

4102

4103

4104

4105

4106

4107

4108

4109

THIS PAGE IS BEST QUALITY PRACTICABLE
FROM COPY FURNISHED TO DDC.

APPENDIX B
BEARING STIFFNESS DESIGN CHARTS
PURE RADIAL LOAD

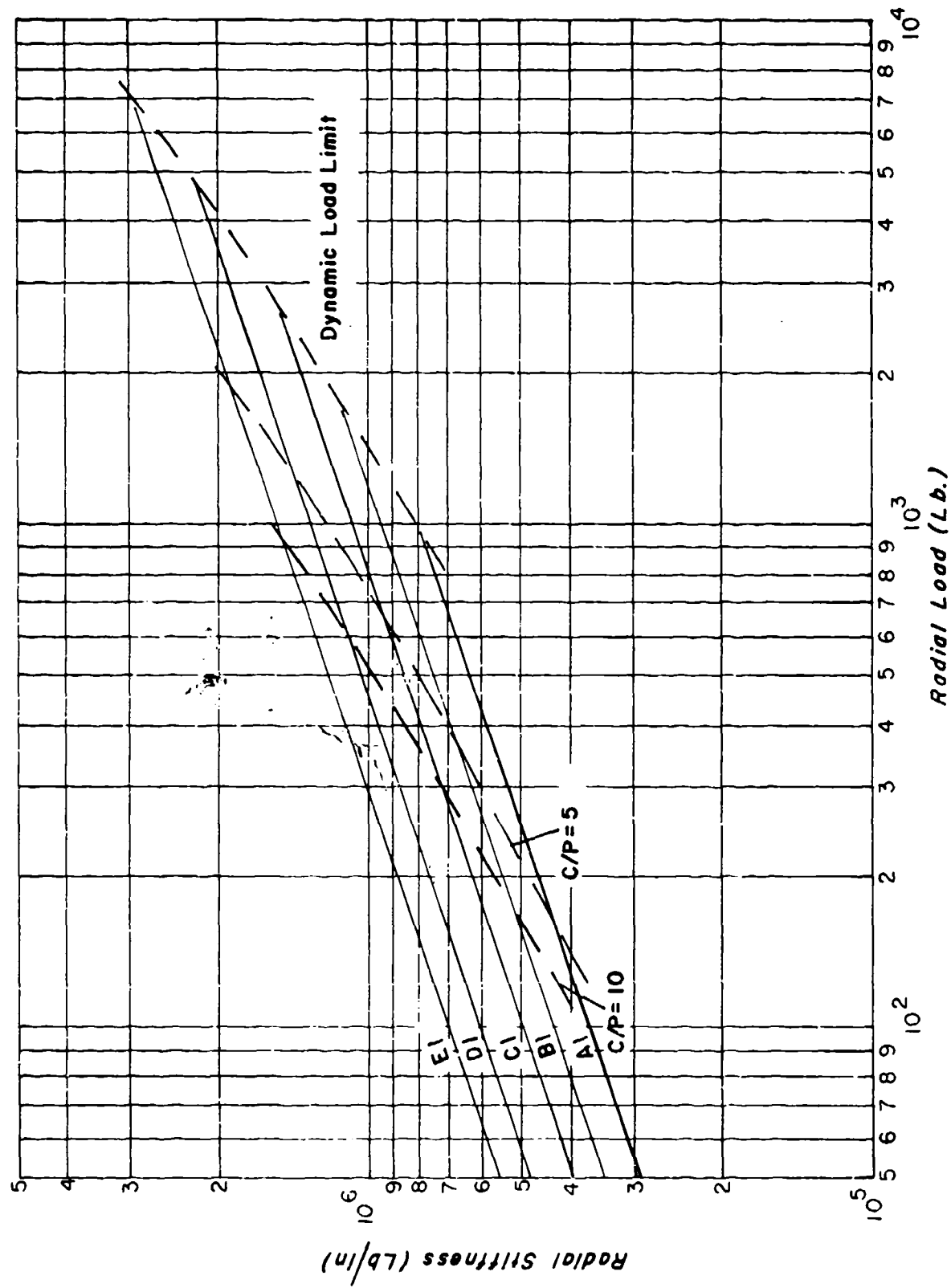


Fig. B-1 Radial Stiffness for Deep Groove Ball Bearing, Pure Radial Load

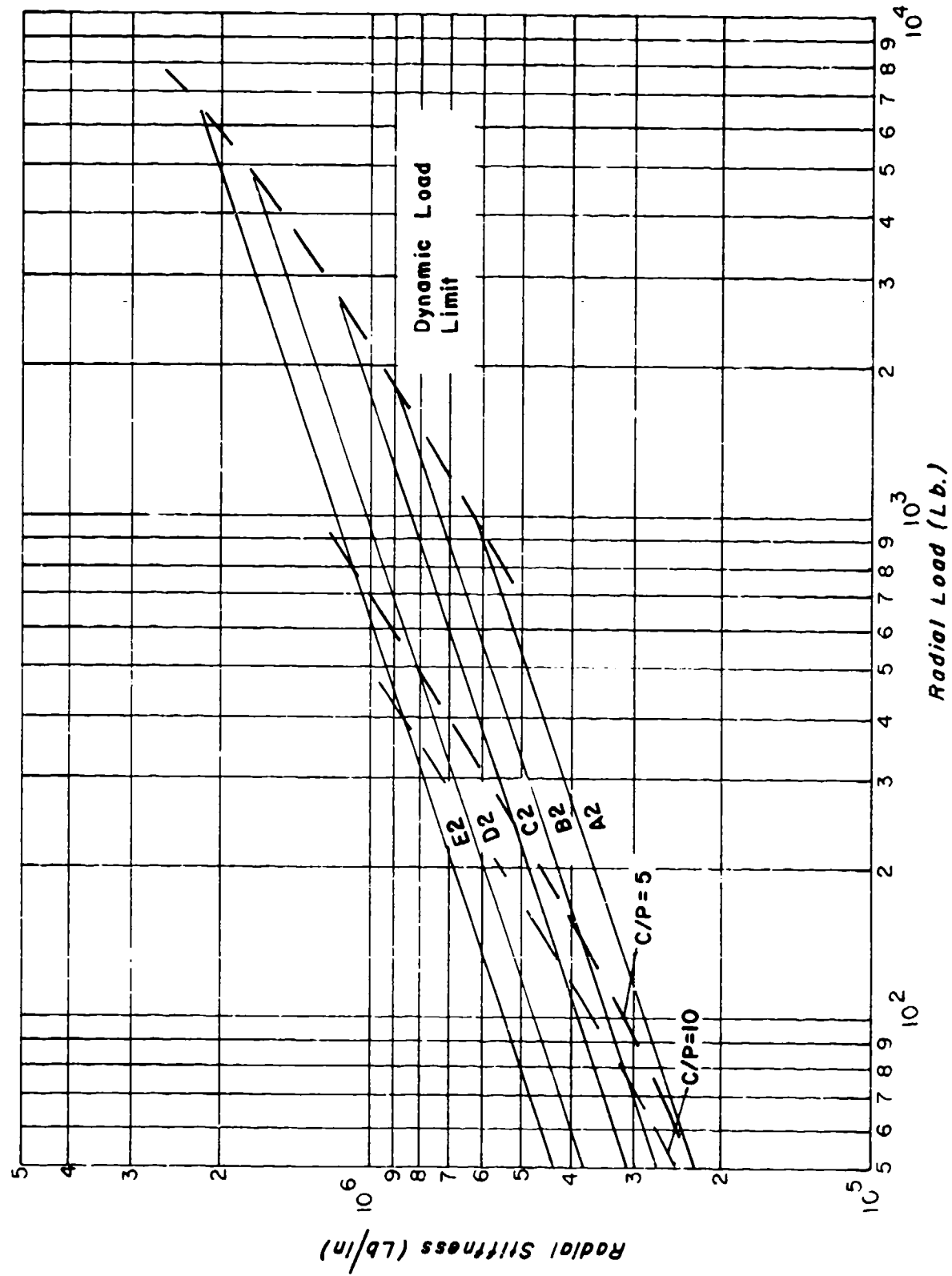


Fig. B-2 Radial Stiffness for Deep Groove Ball Bearings, Pure Radial Load

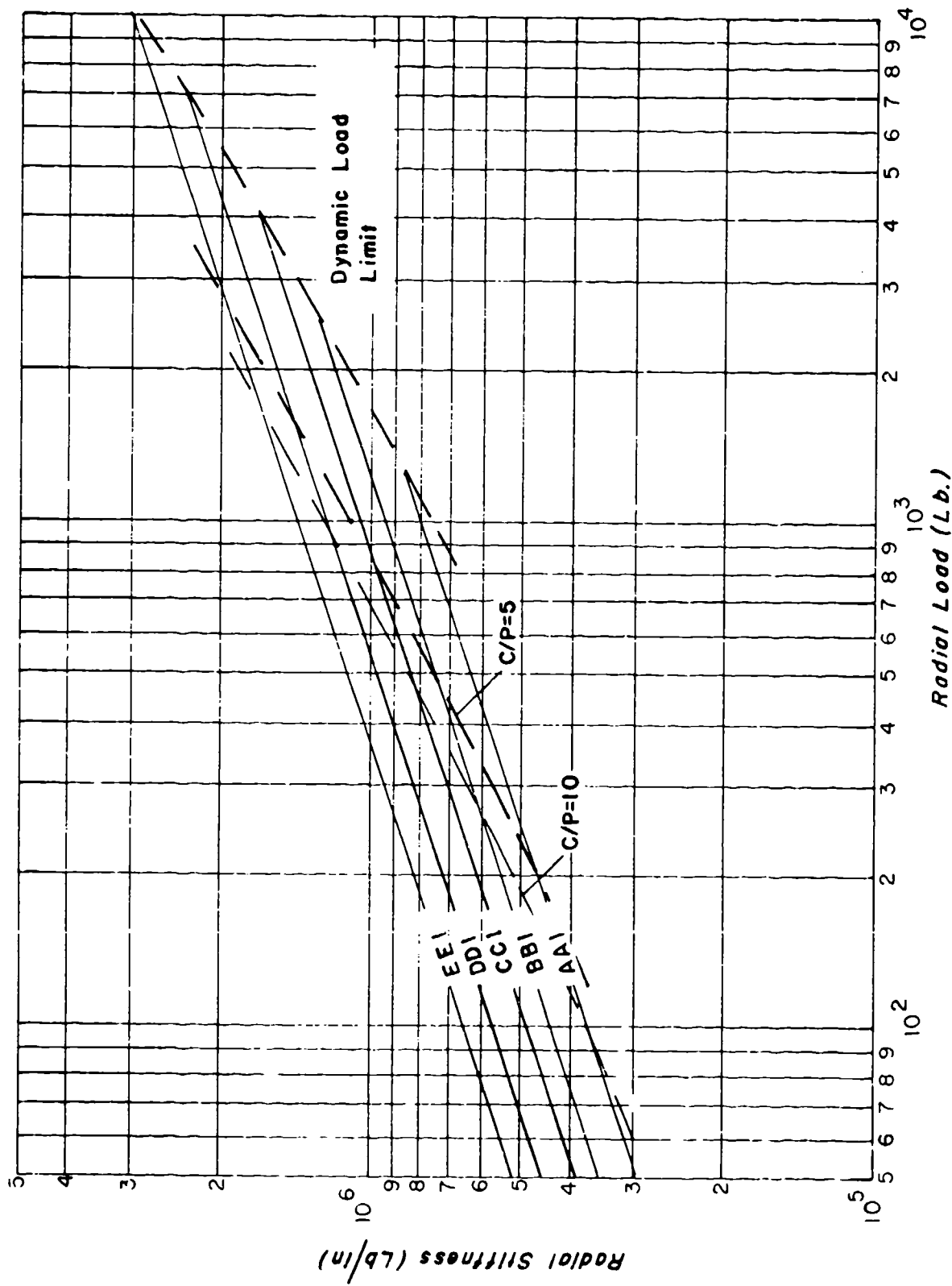


Fig. B-3 Radial Stiffness for Deep Groove Ball Bearings, Pure Radial Load

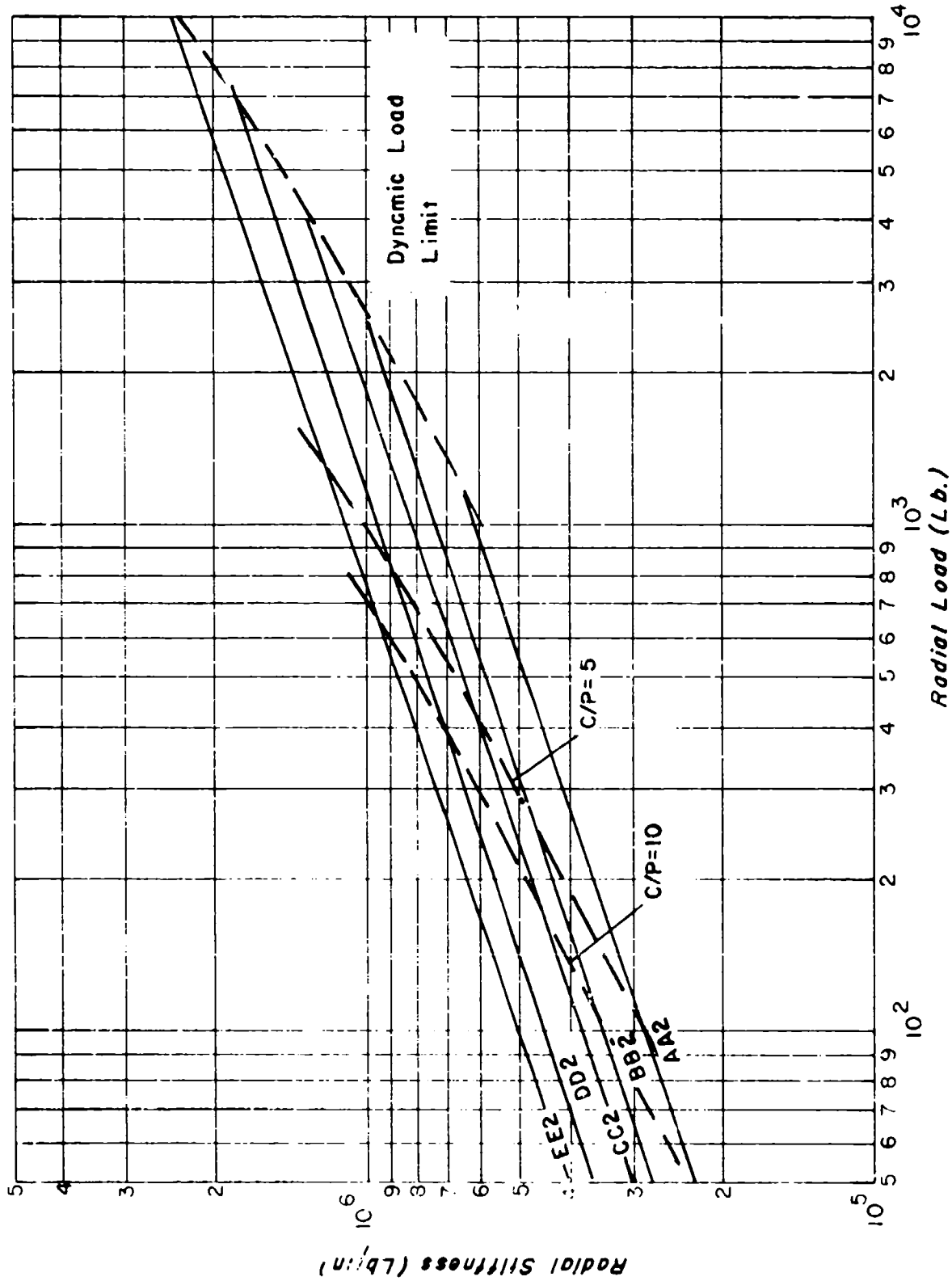


Fig. B-4 Radial Stiffness for Deep Groove Ball Bearings, Pure Radial Load

APPENDIX C
BEARING STIFFNESS DESIGN CHARTS
PURE THRUST LOAD

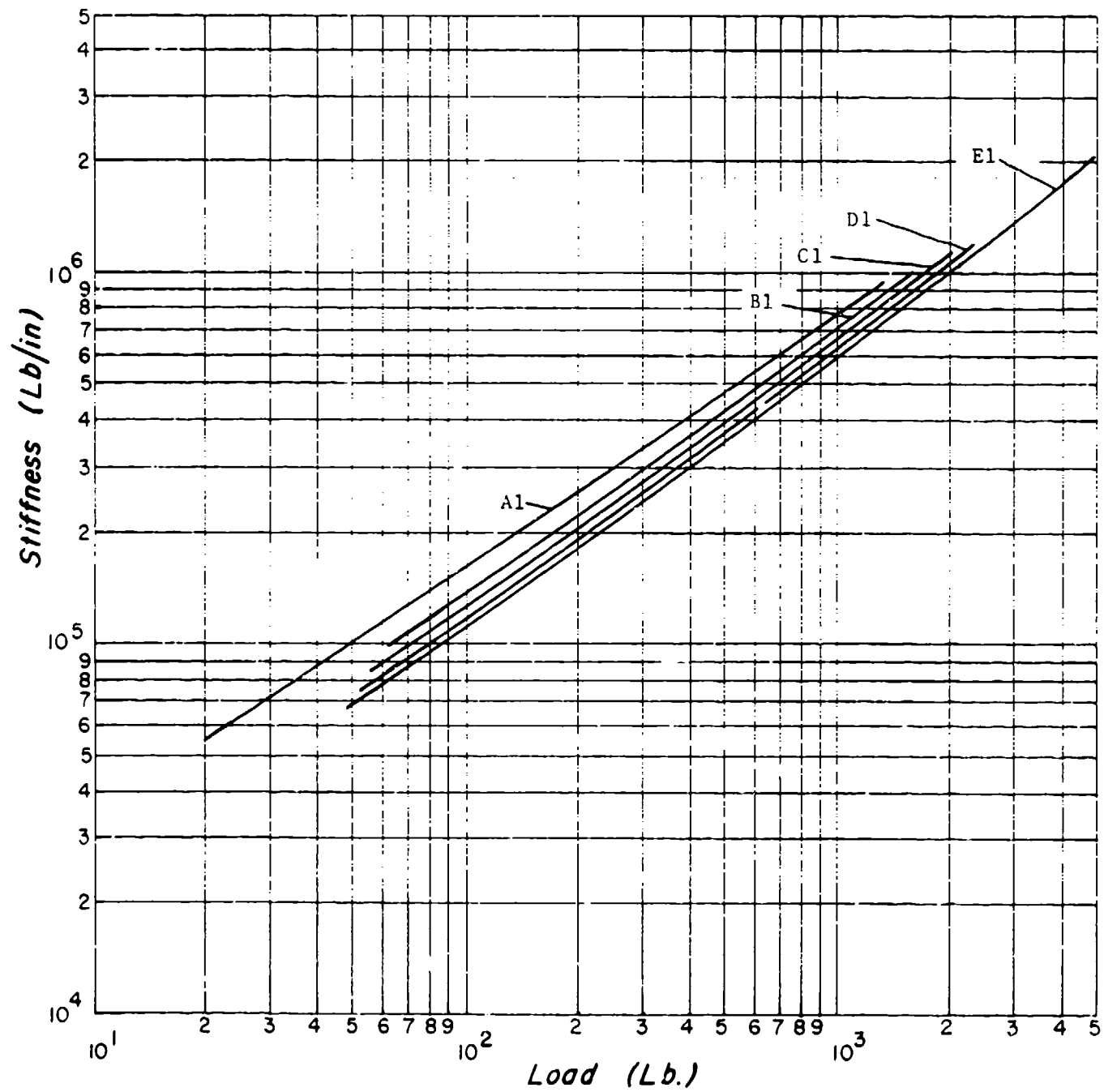


Fig. C-1 Axial Stiffness versus Axial Load,
No Radial Load

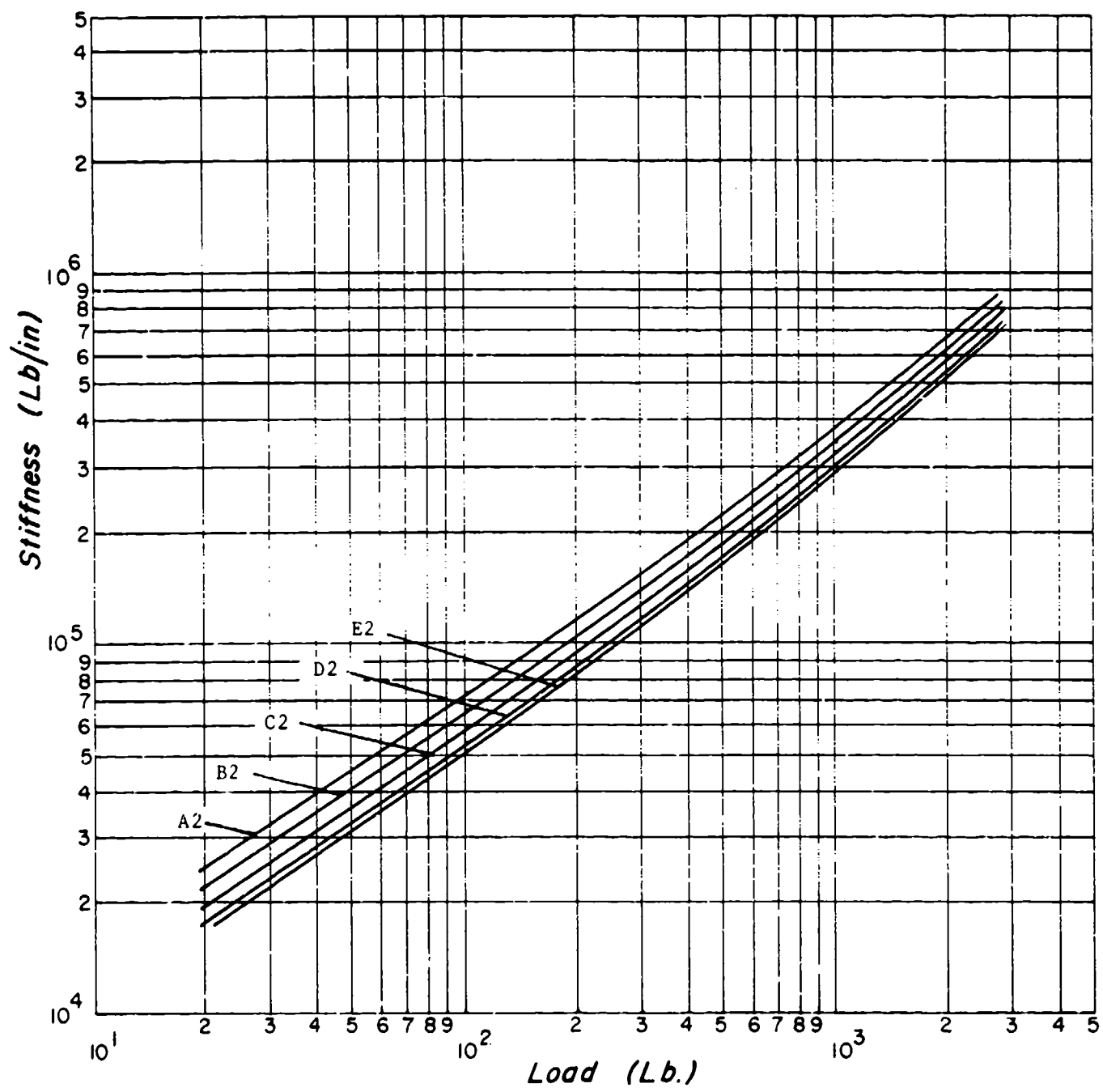


Fig. C-2 Axial Stiffness versus Axial Load,
No Radial Load

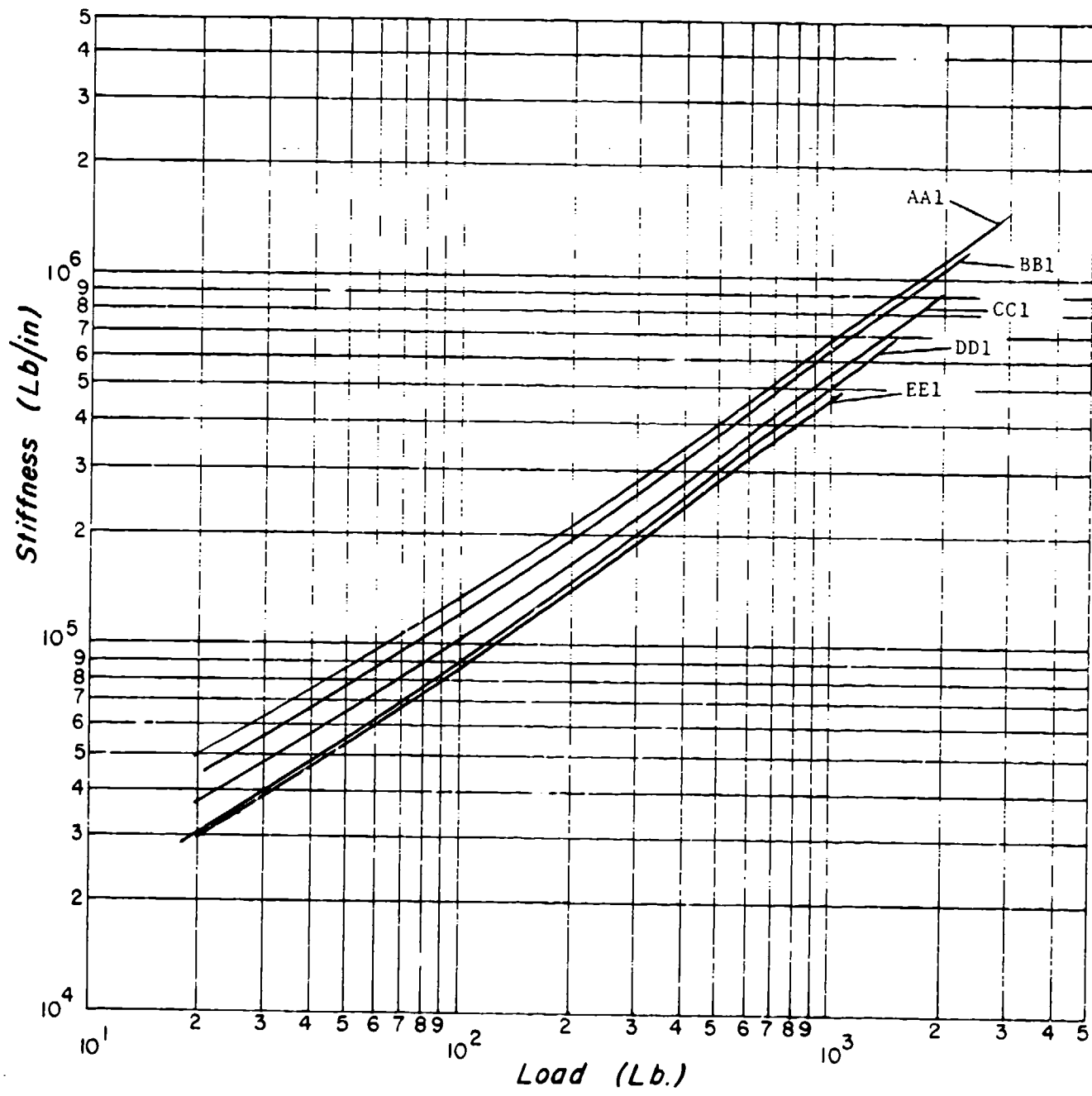


Fig. C-3 Axial Stiffness versus Axial Load,
No Radial Load

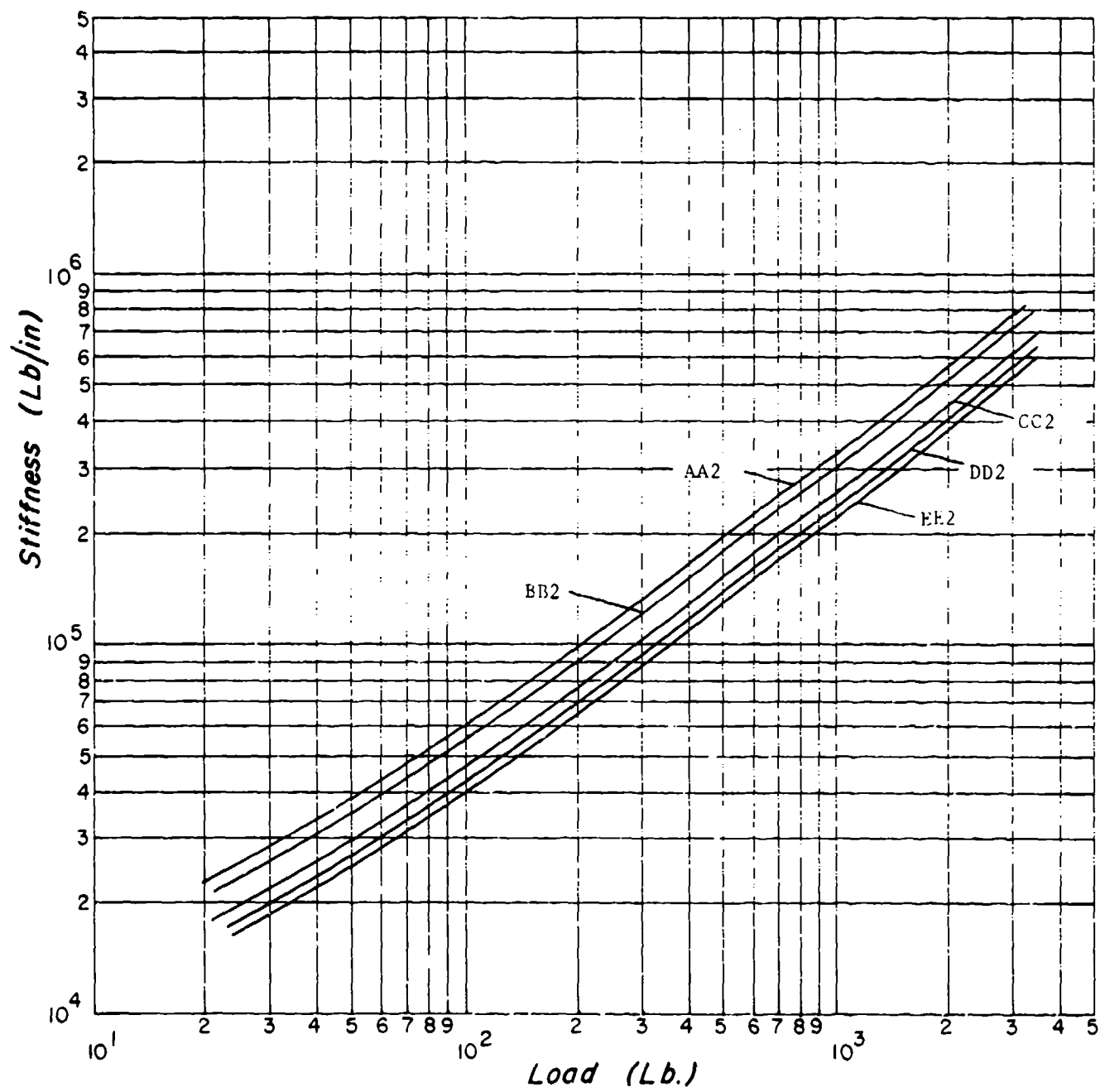


Fig. C-4 Axial Stiffness versus Axial Load,
No Radial Load

APPENDIX D
BEARING STIFFNESS DESIGN CHARTS
ANGULAR CONTACT BEARINGS WITH PRELOAD

$$\beta = 25^\circ$$

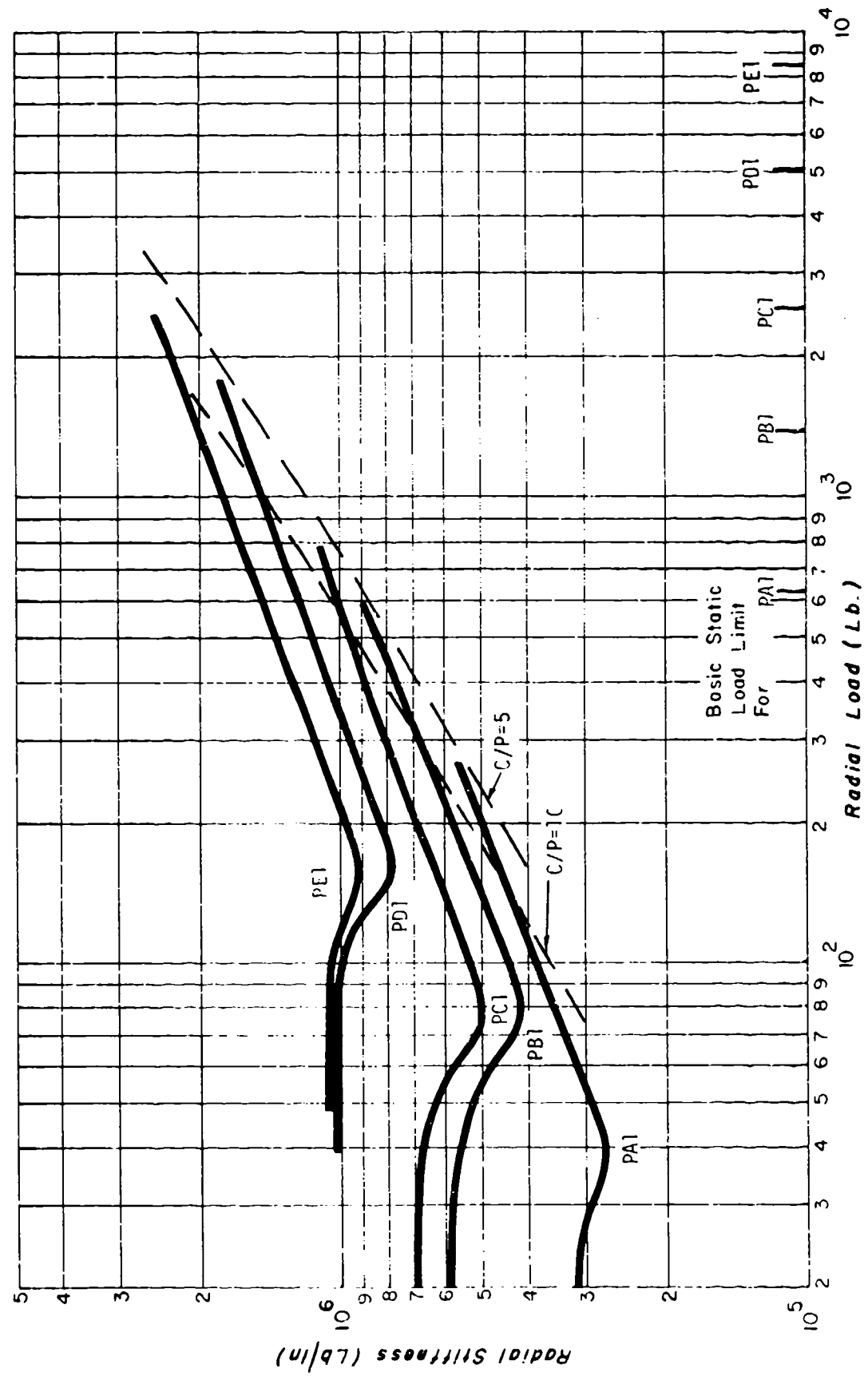


Fig. D-1 Radial Stiffness for Angular Contact Bearing,
 Preload -- Selected Light,
 $R = 250$

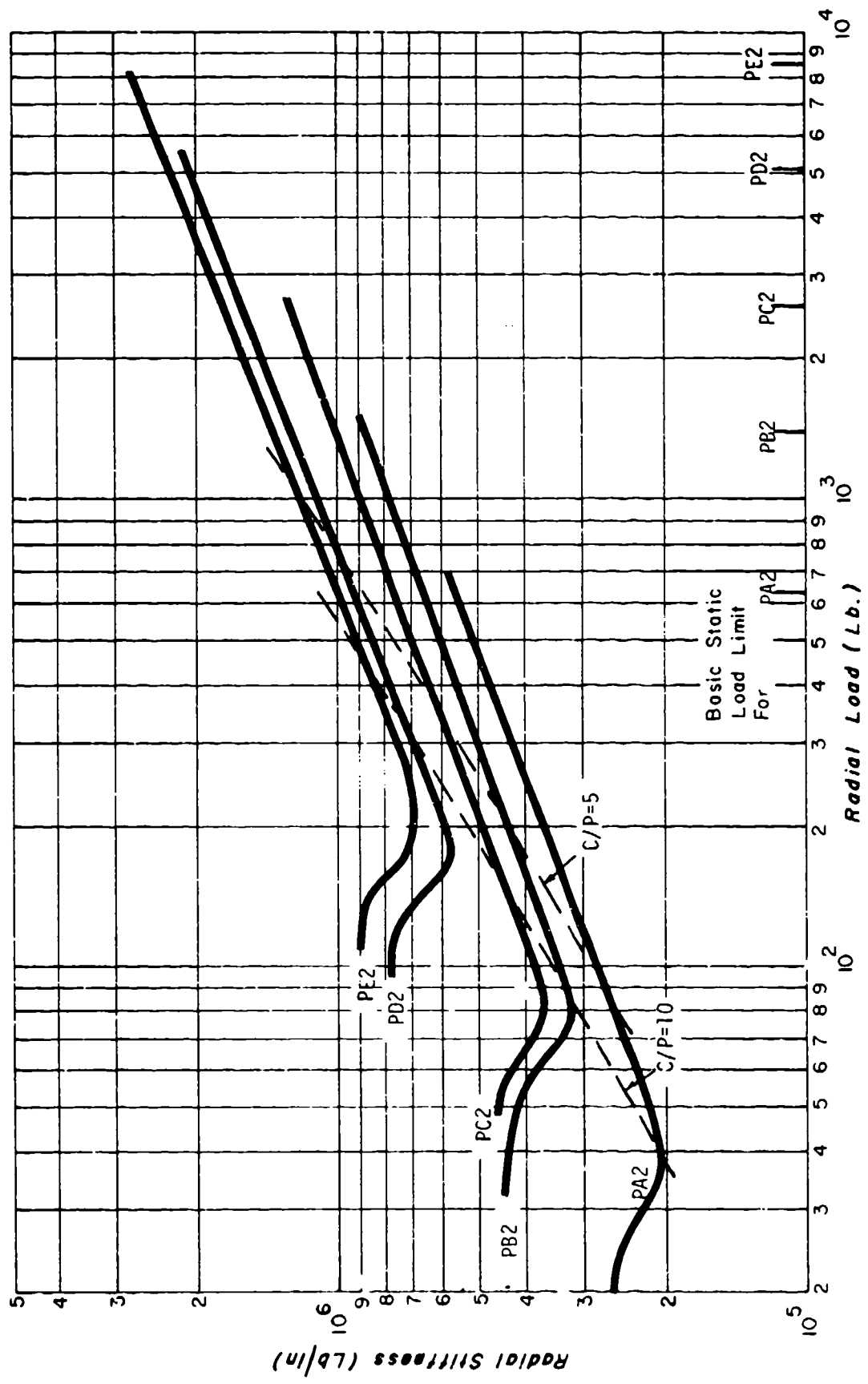


Fig. D-2 Radial Stiffness for Angular Contact Bearing,
Preload - Selected Light,
 $\beta = 25^\circ$

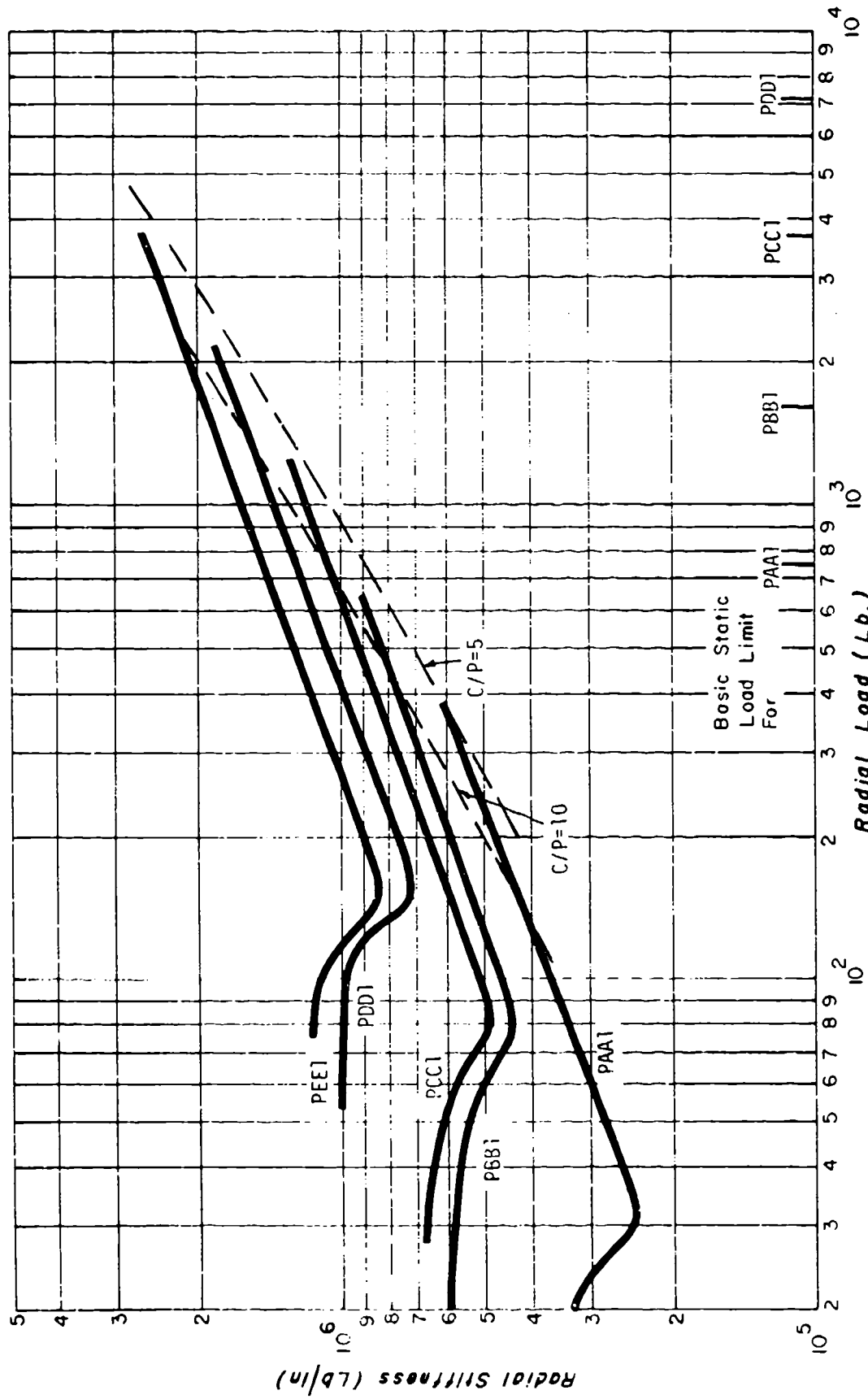


Fig. D-3 Radial Stiffness for Angular Contact Bearing,
 Preload -- Selected Light,
 $\epsilon = 250$

(41/97) 55011111005 (41/97)

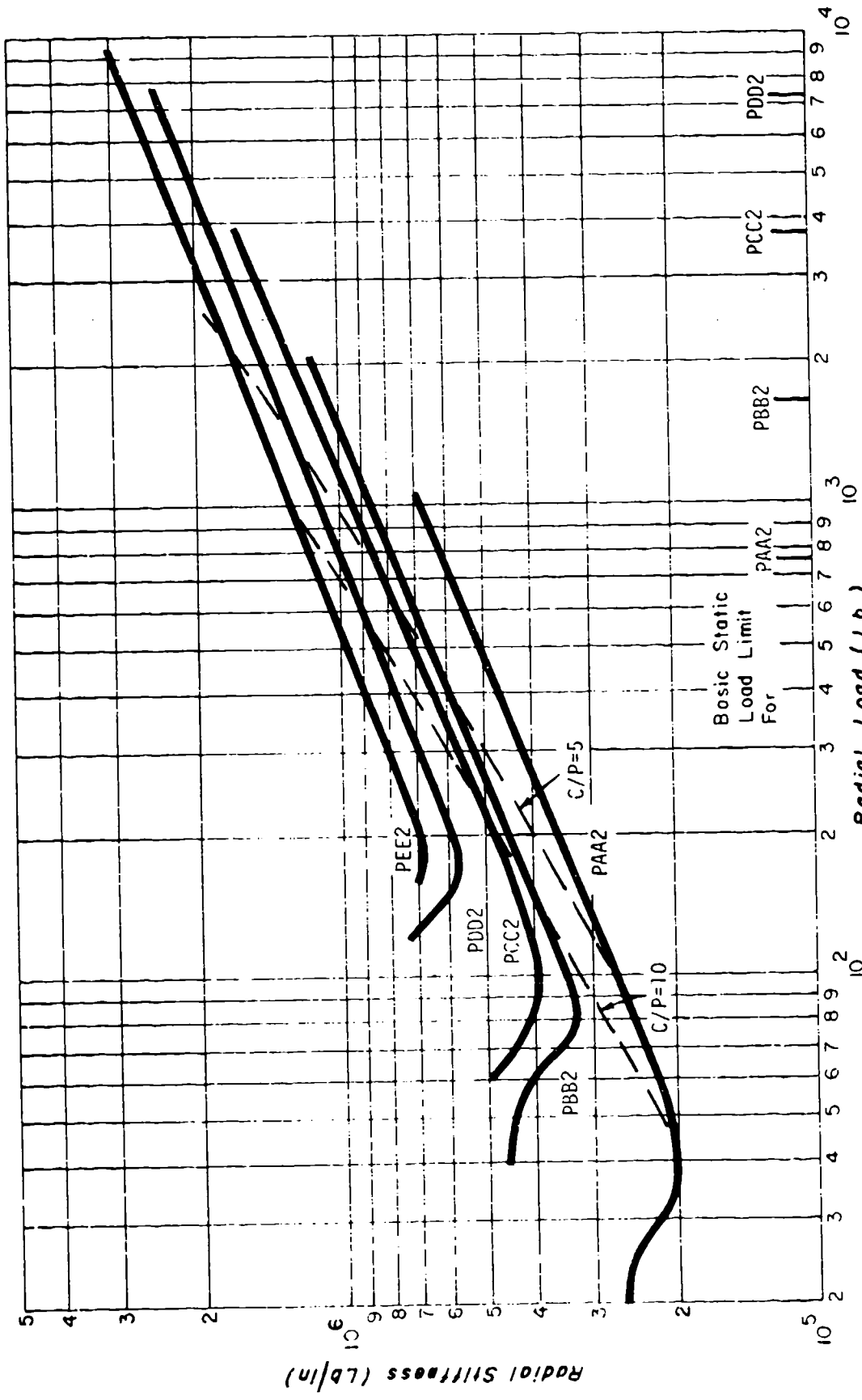


FIG. D-5 Radial Stiffness for Angular Contact Bearings,
 Preload -- Selected Light,
 $P = 250$

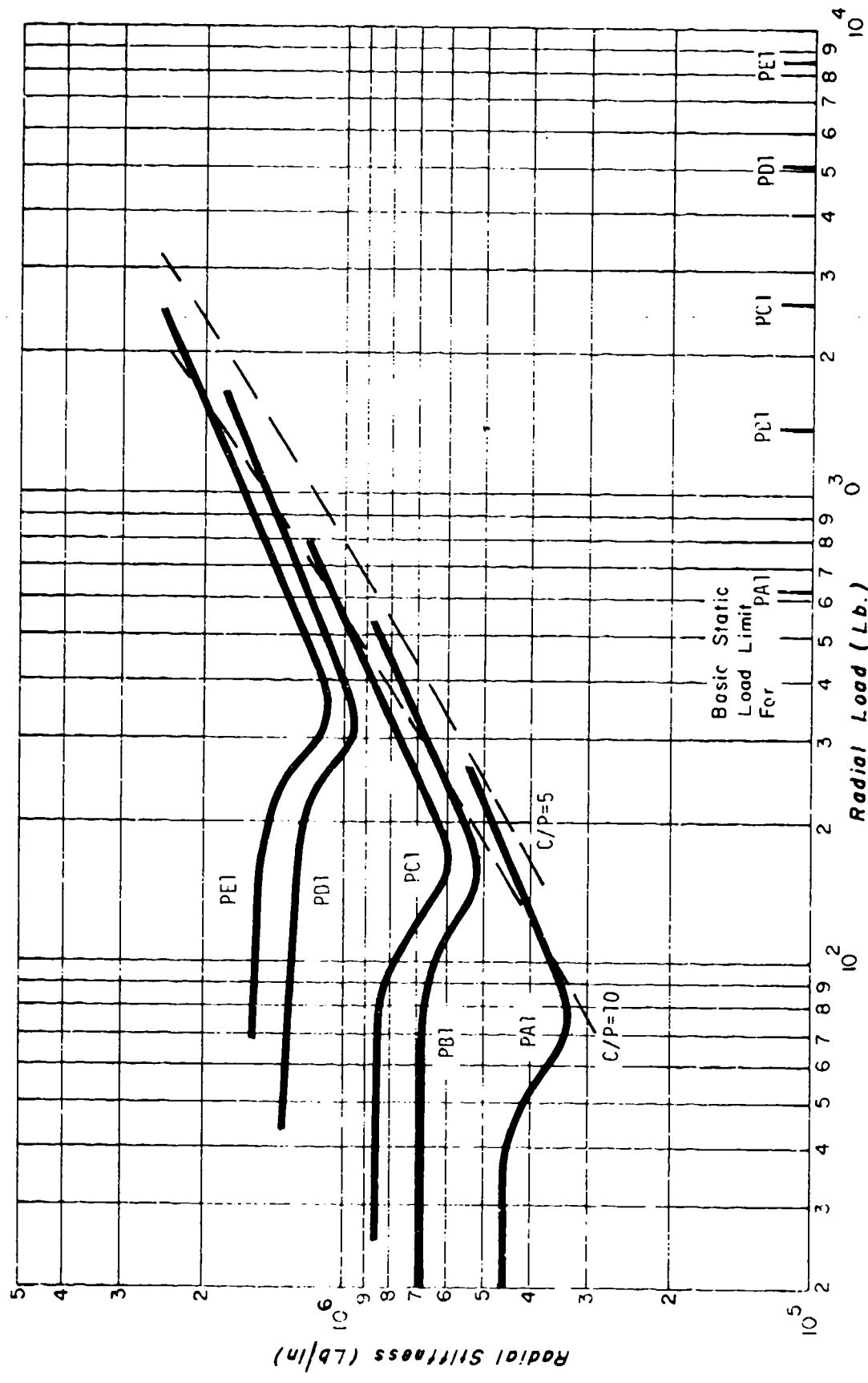


Fig. D-5 Radial Stiffness for Angular Contact Bearing,
Preload -- Moderate,
 $\beta = 250$

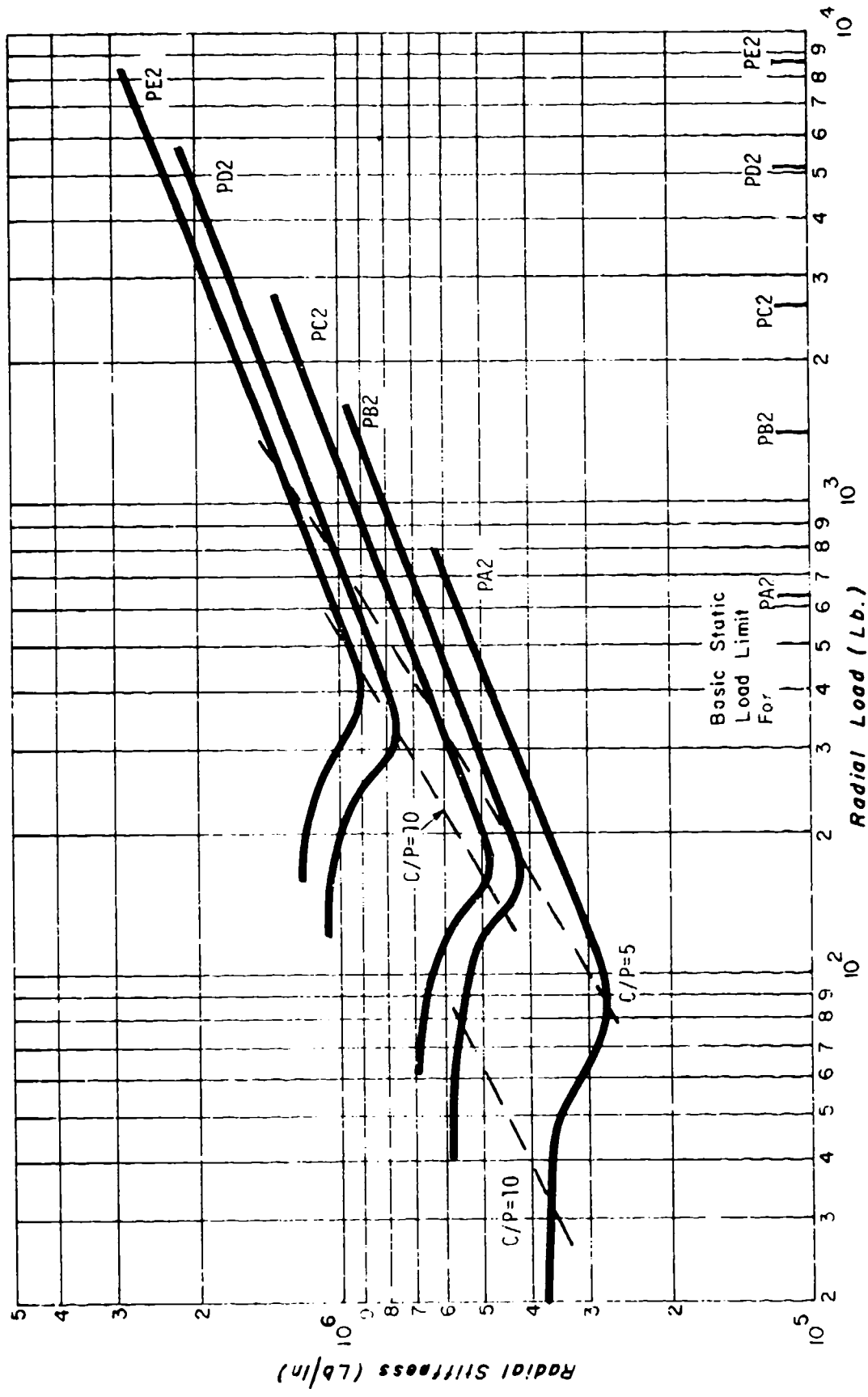


Fig. E-6 Radial Stiffness for Angular Contact Bearing,
Preload -- Moderate,
 $\alpha = 25^\circ$

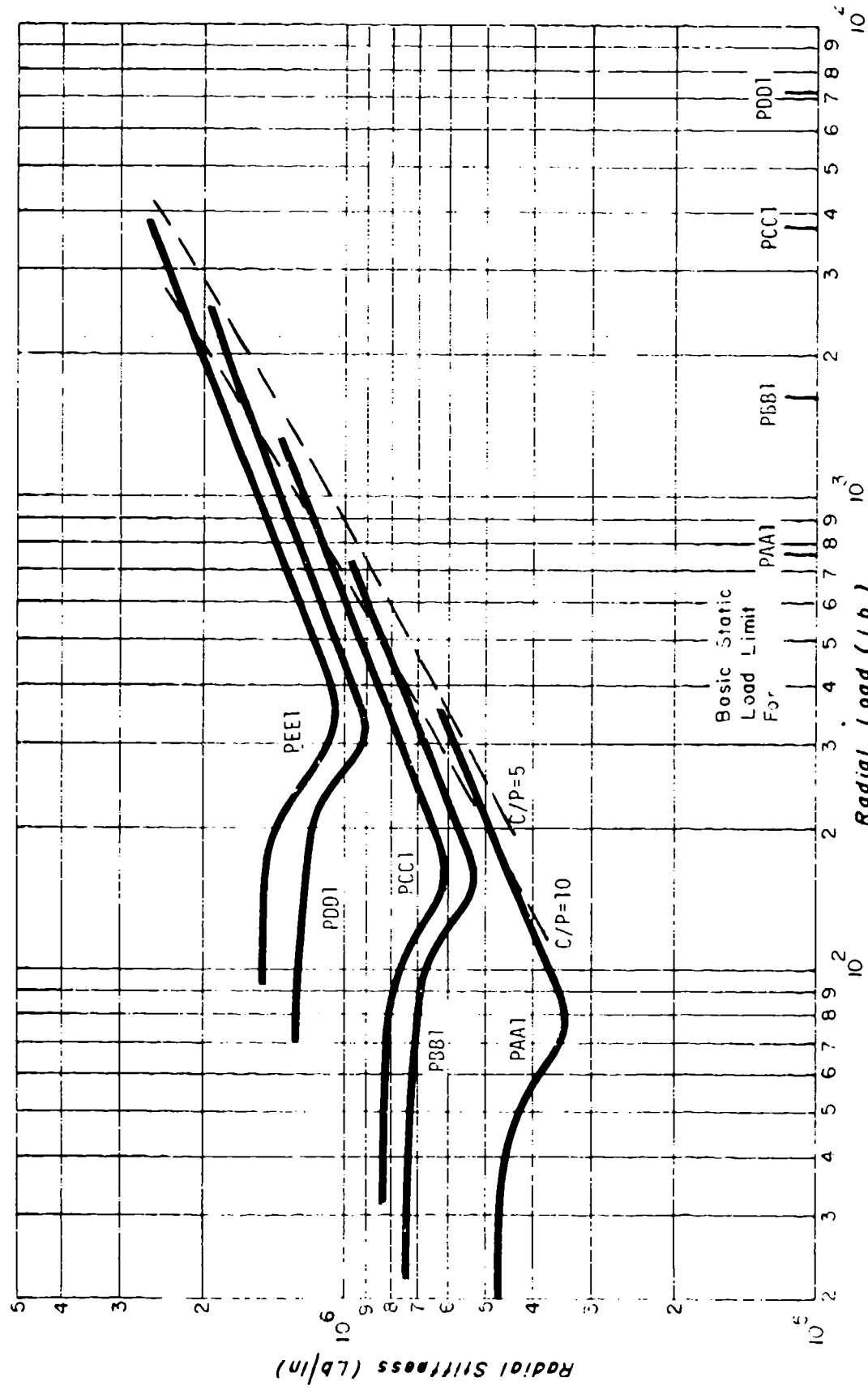


Fig. D-7 Radial Stiffness for Angular Contact Bearing,
Preload -- Moderate,
 $\beta = 30^\circ$

Radial Stiffness (lb/in)

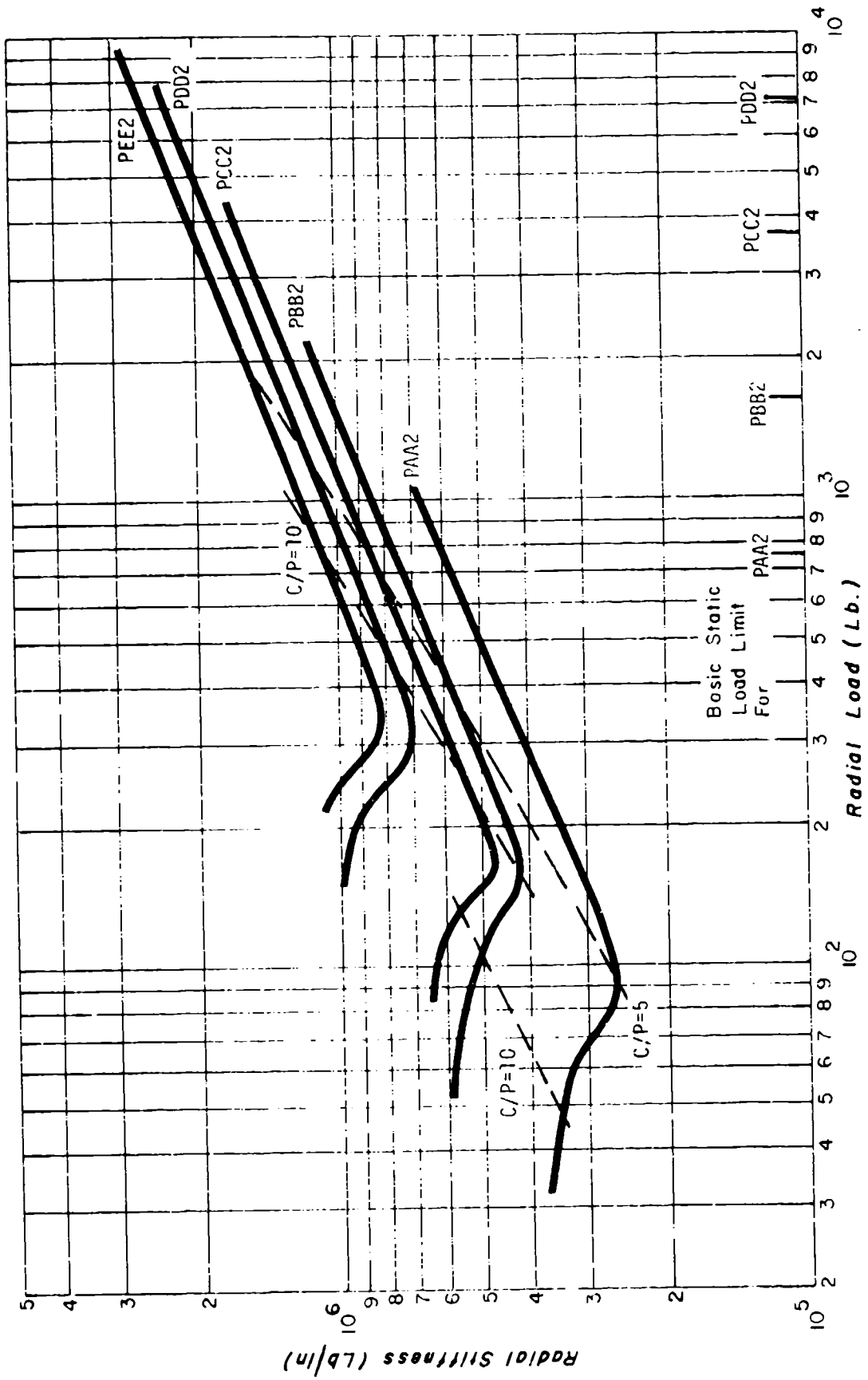


Fig. B-8 Radial Stiffness for Angular Contact Bearing,
 Preload -- Moderate,
 $\mu = 25.0$

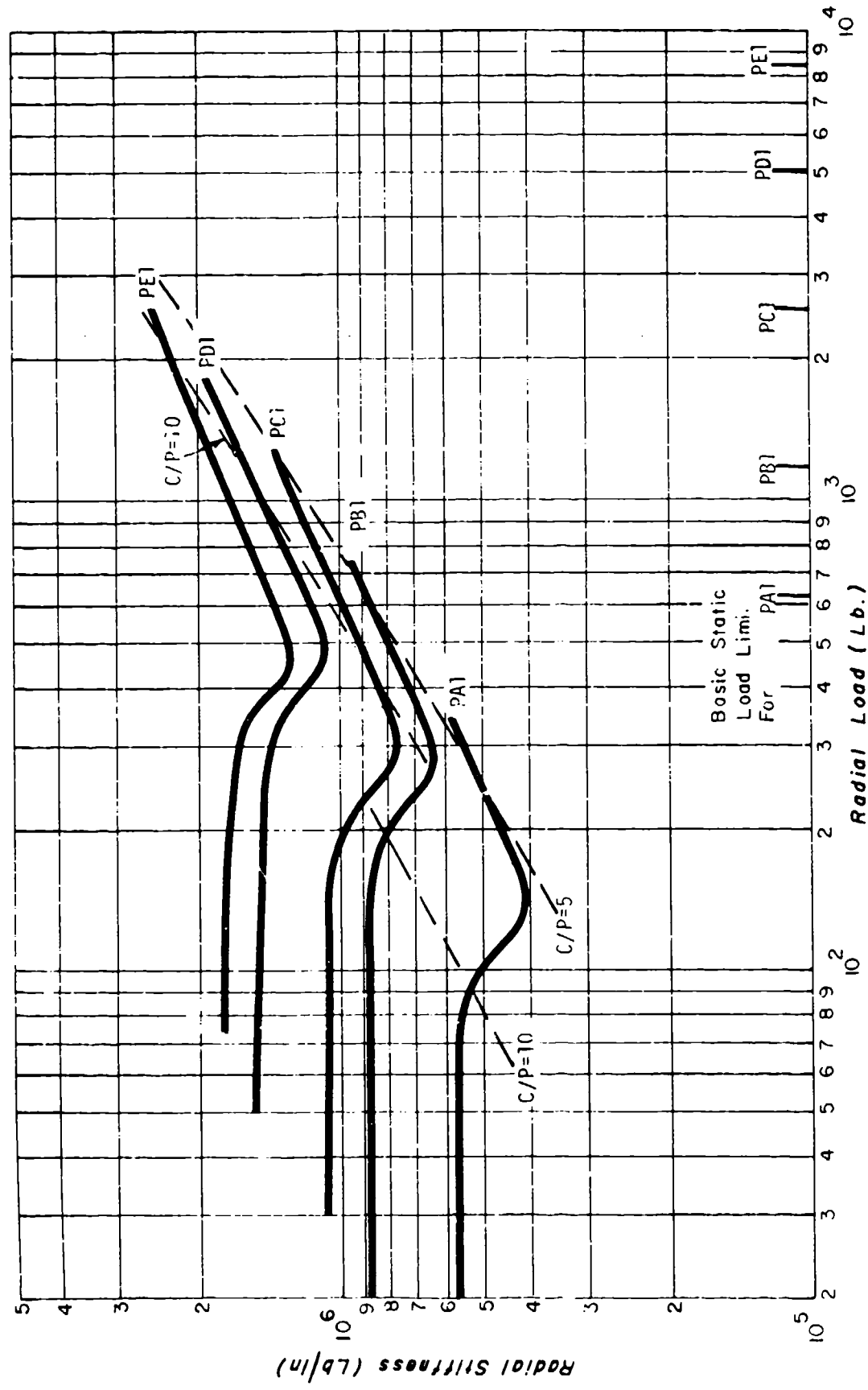


Fig. D-9 Radial Stiffness for Angular Contact Bearing,
 Preload -- Preferred Heavy,
 $\beta = 25^\circ$

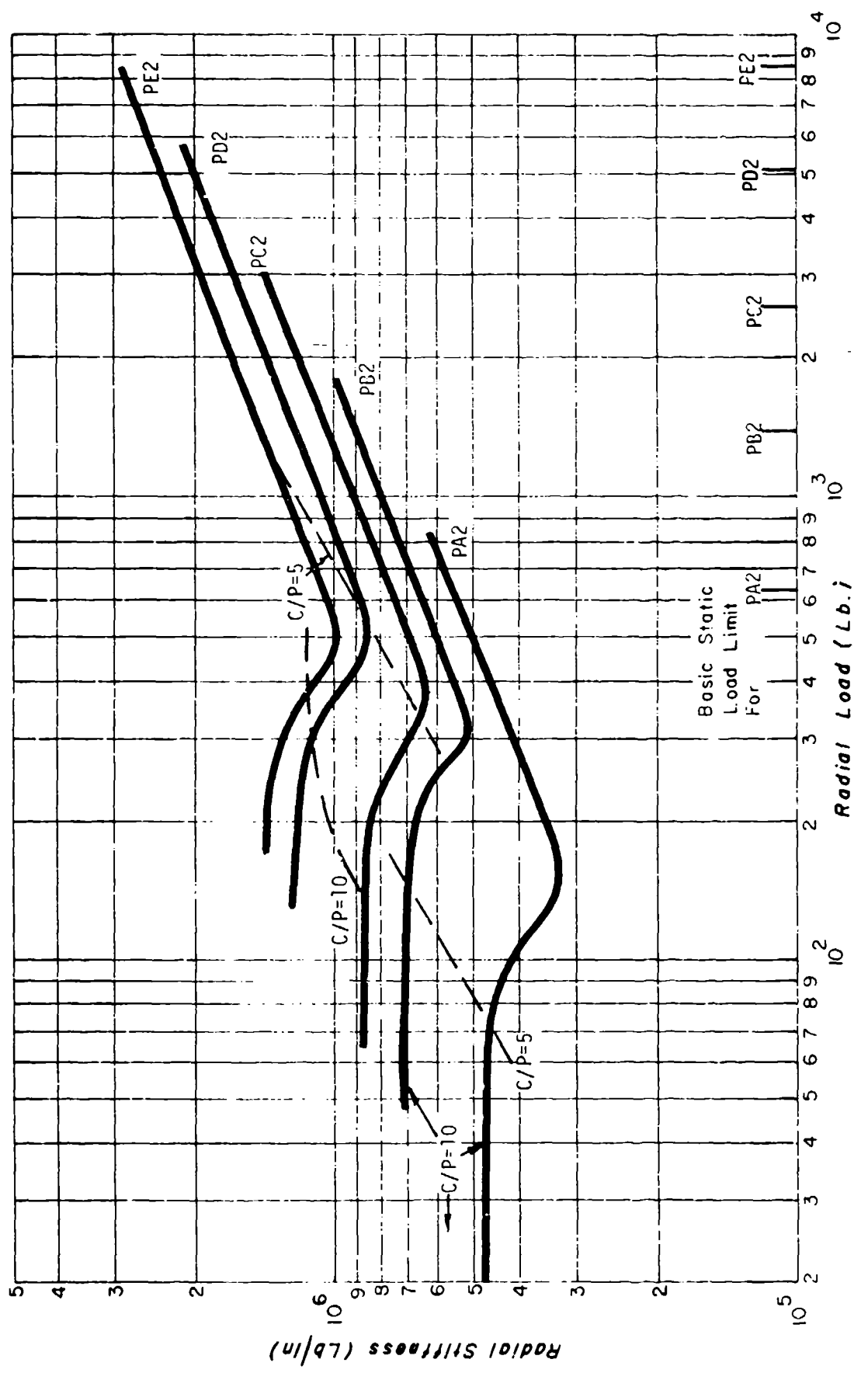


Fig. D-10 Radial Stiffness for Angular Contact Bearing,
 Preload -- Preferred Bearing,
 $\beta = 25^\circ$

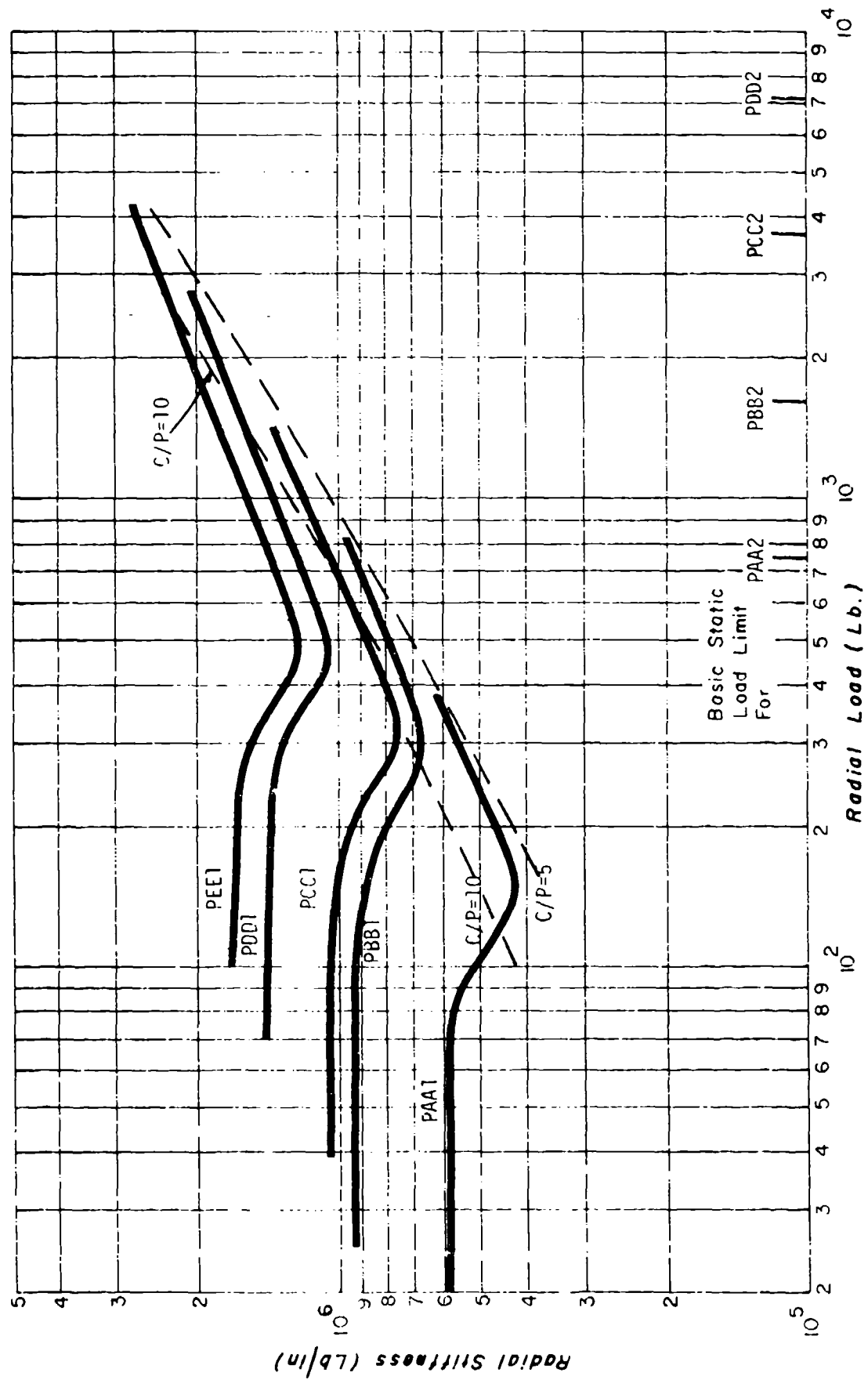


Fig. D-11 Radial Stiffness for Angular Contact Bearing,
Preload -- Preferred Heavy,
 $\epsilon = 25^\circ$

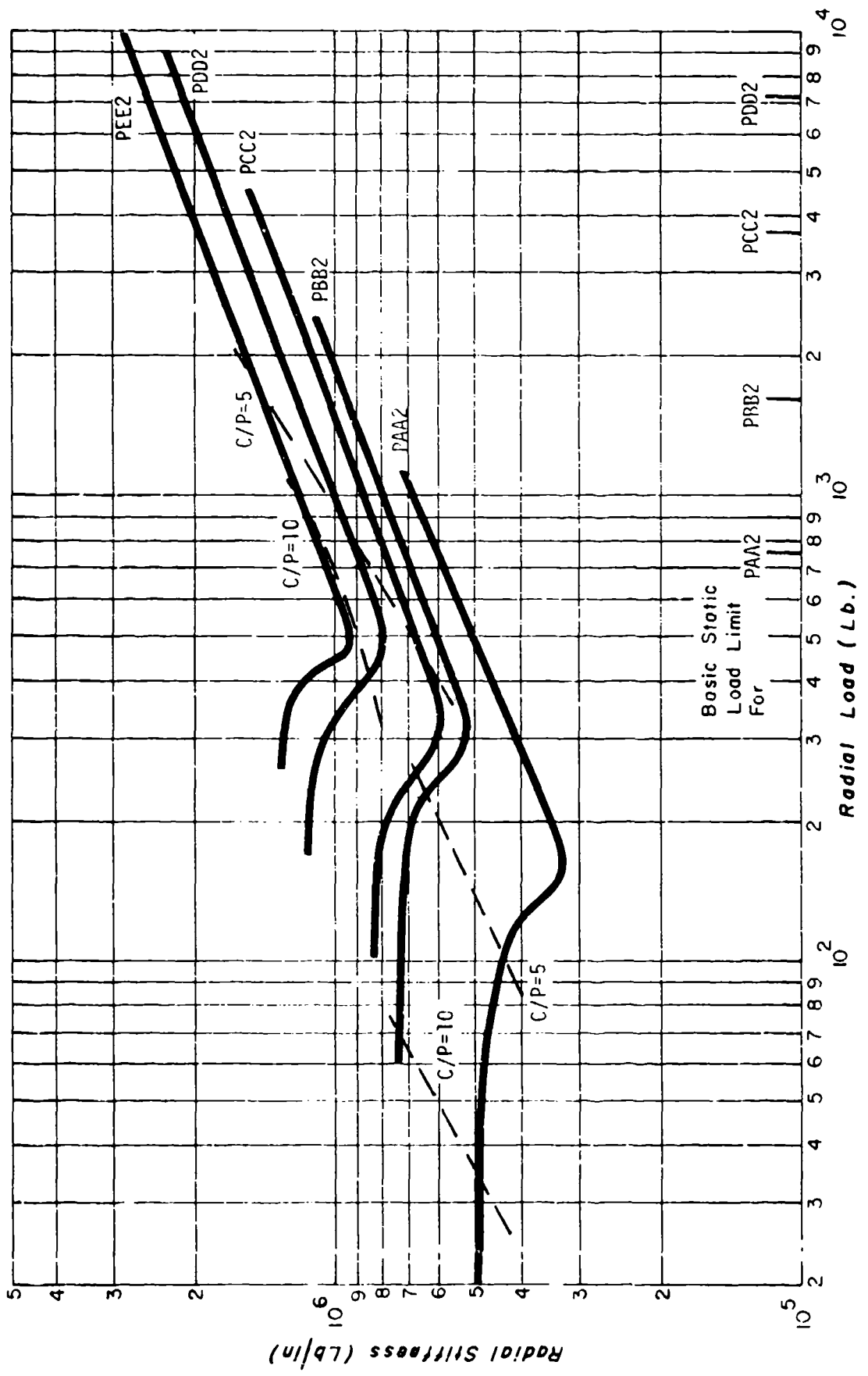


Fig. D-1.2 Radial Stiffness for Angular Contact Bearing,
 Preload -- Preferred Heavy,
 $\beta = 25^\circ$

APPENDIX E

BEARING STIFFNESS DESIGN CHARTS
ANGULAR CONTACT BEARING WITH PRE-LOAD

$$\beta = 15^\circ$$

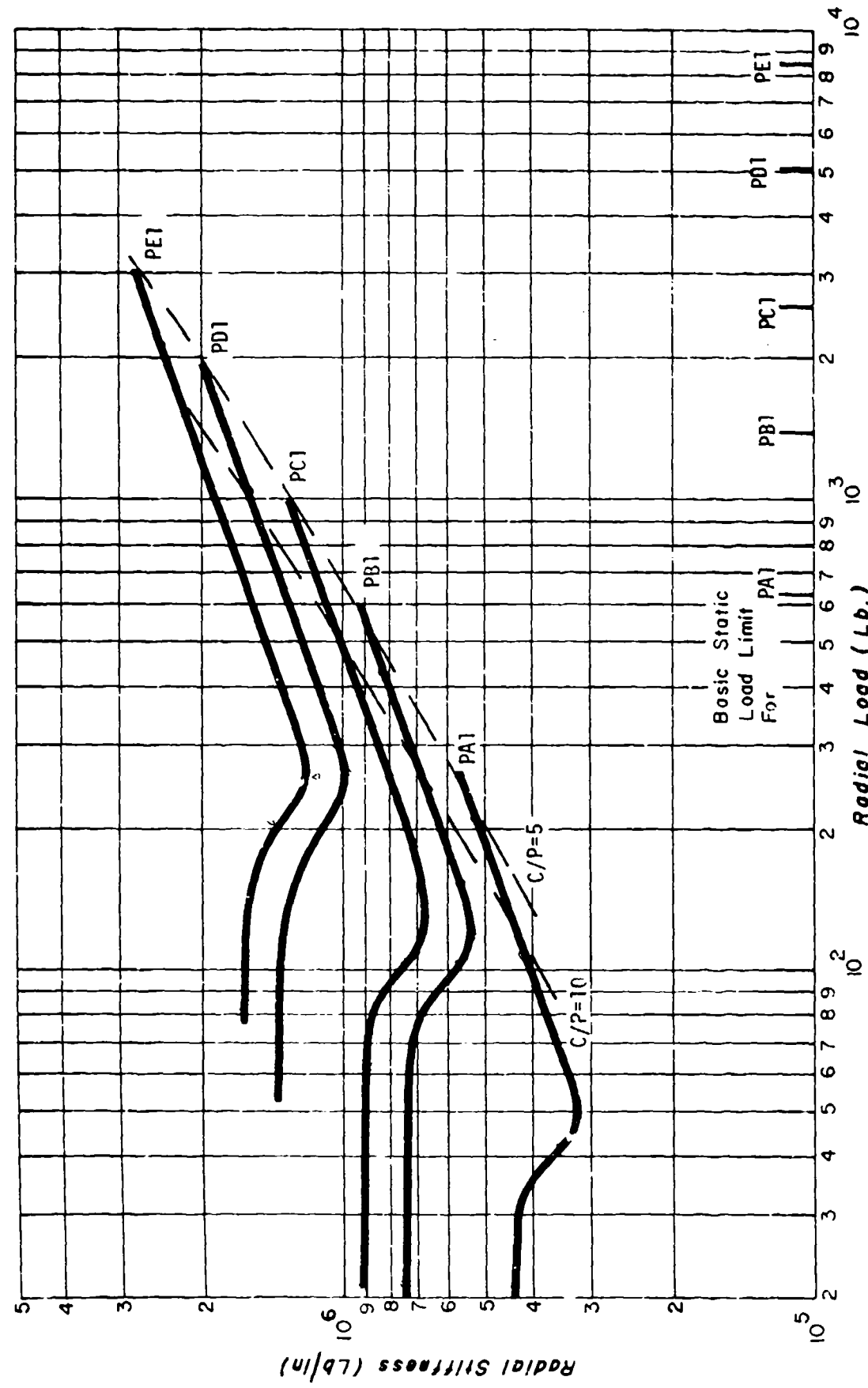


Fig. E-1 Radial Stiffness for Angular Contact Bearing,
Preload — Selected Light,
 $\beta = 15^\circ$

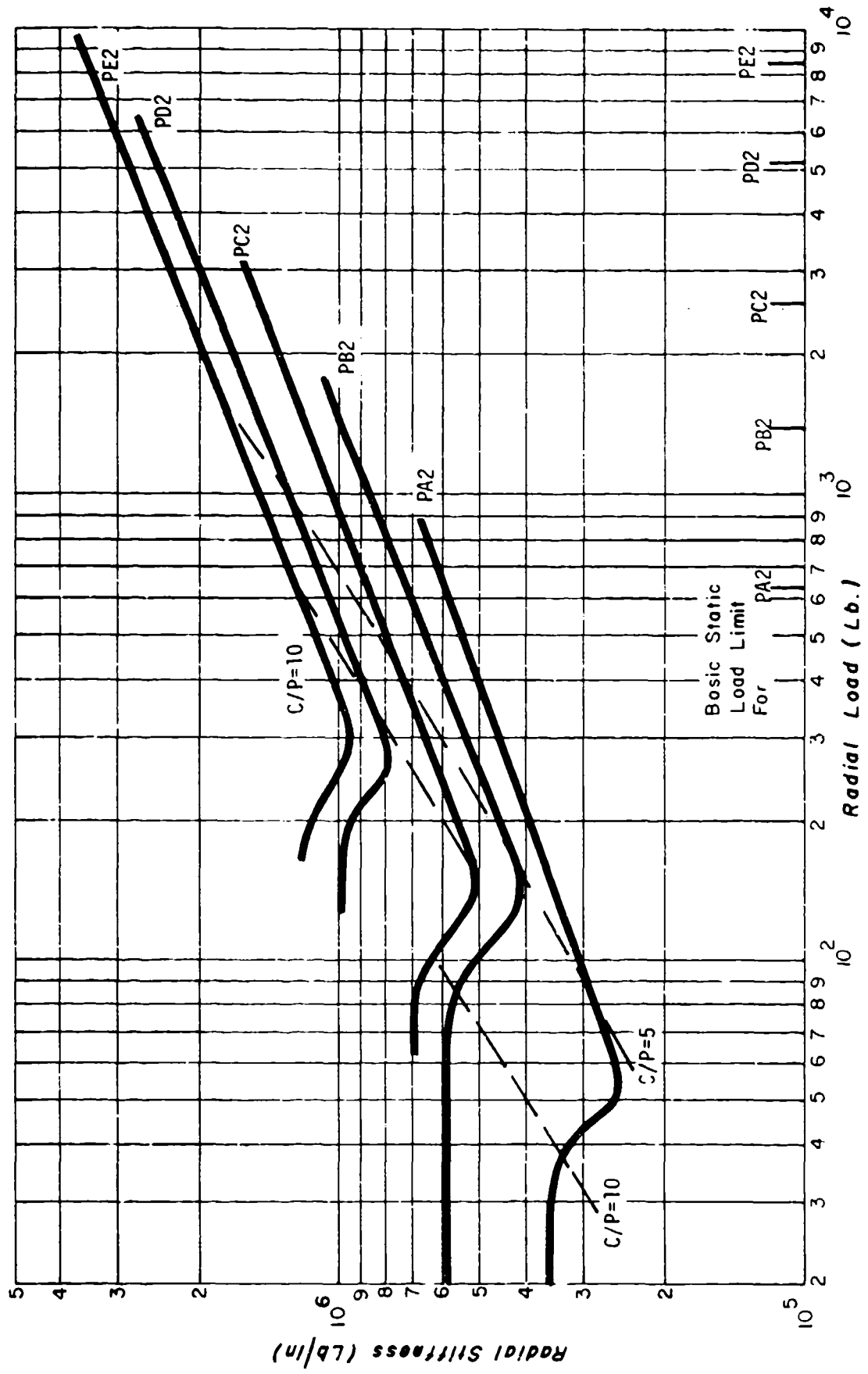
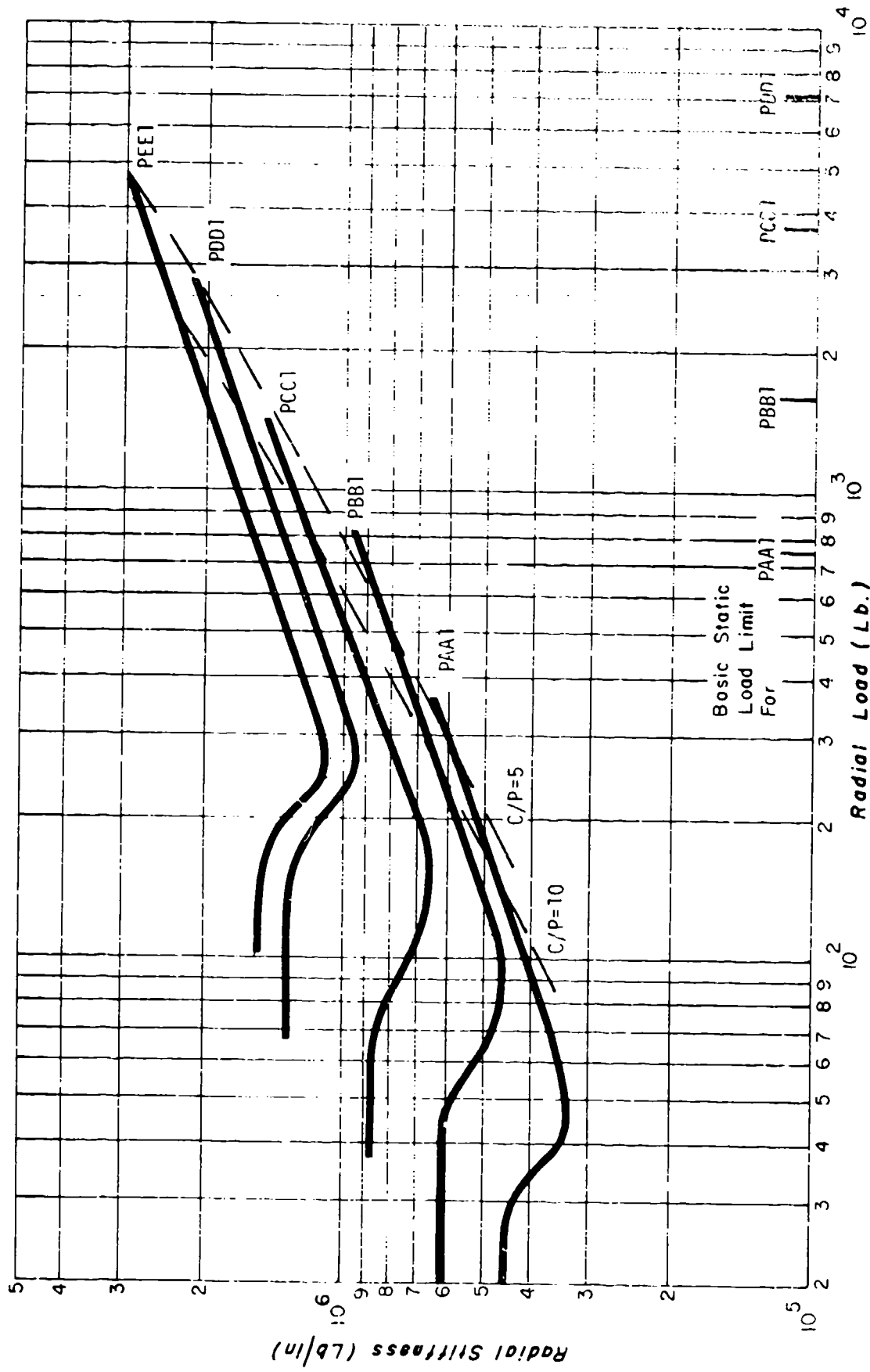


Fig. E-2 Radial Stiffness for Angular Contact Bearing,
 Preload -- Selected light,
 $K = 150$



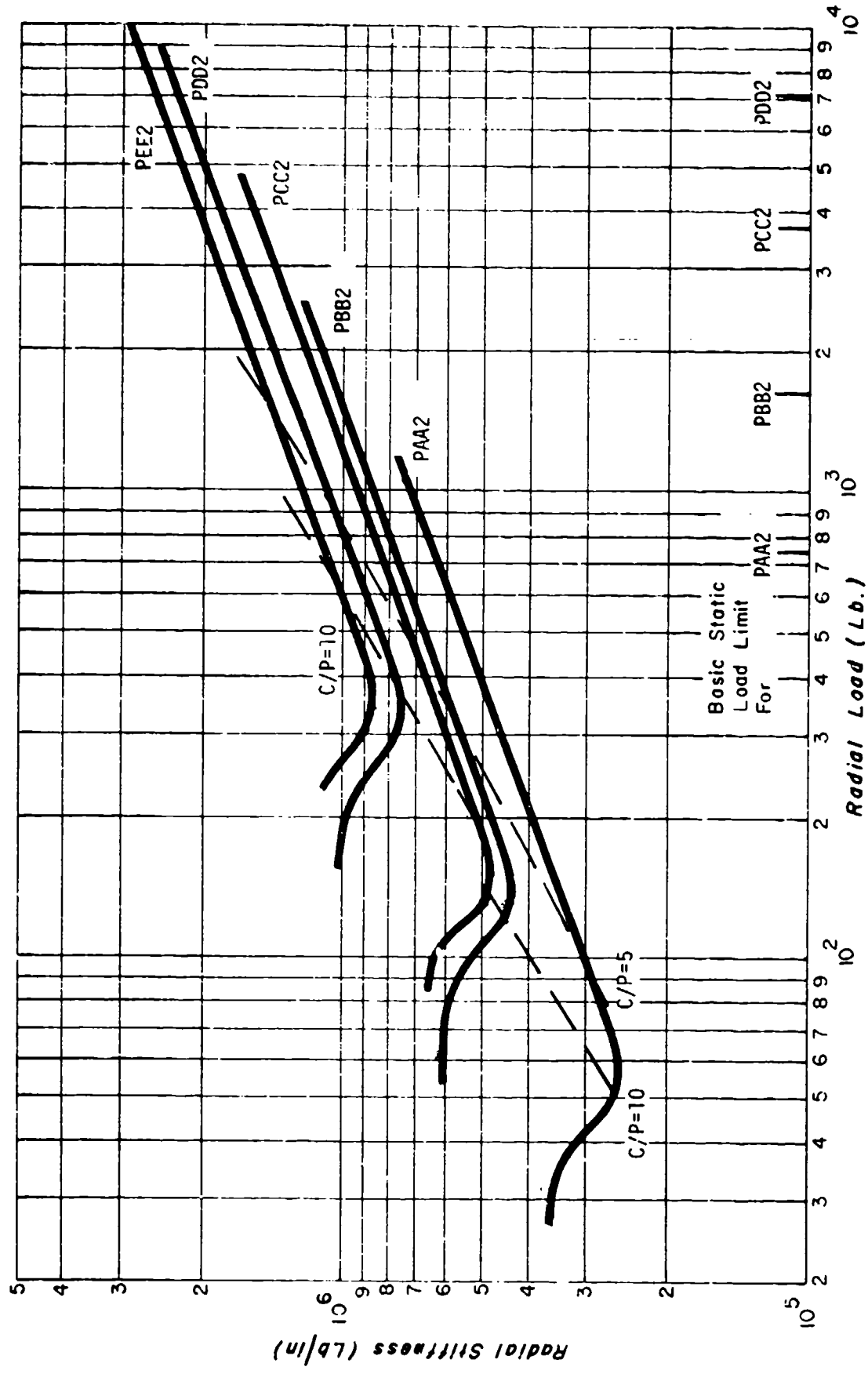


Fig. E-4 Radial Stiffness for Angular Contact Bearing,
 Preload -- Selected Light,
 $\beta = 150$

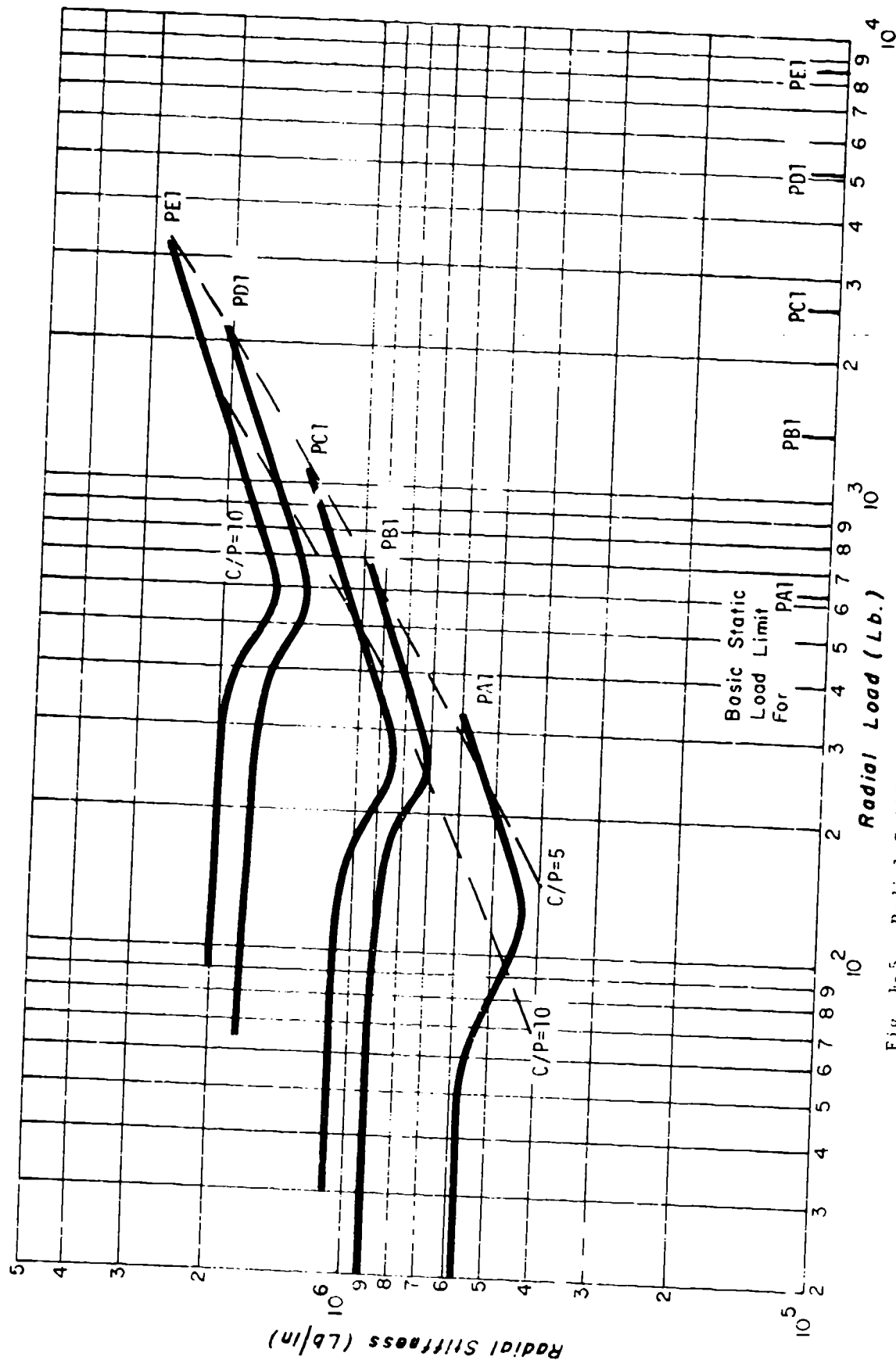


Fig. E-5 Radial Stiffness for Angular Contact Bearing,
Preload -- Moderate,
 $\beta = 1.50$

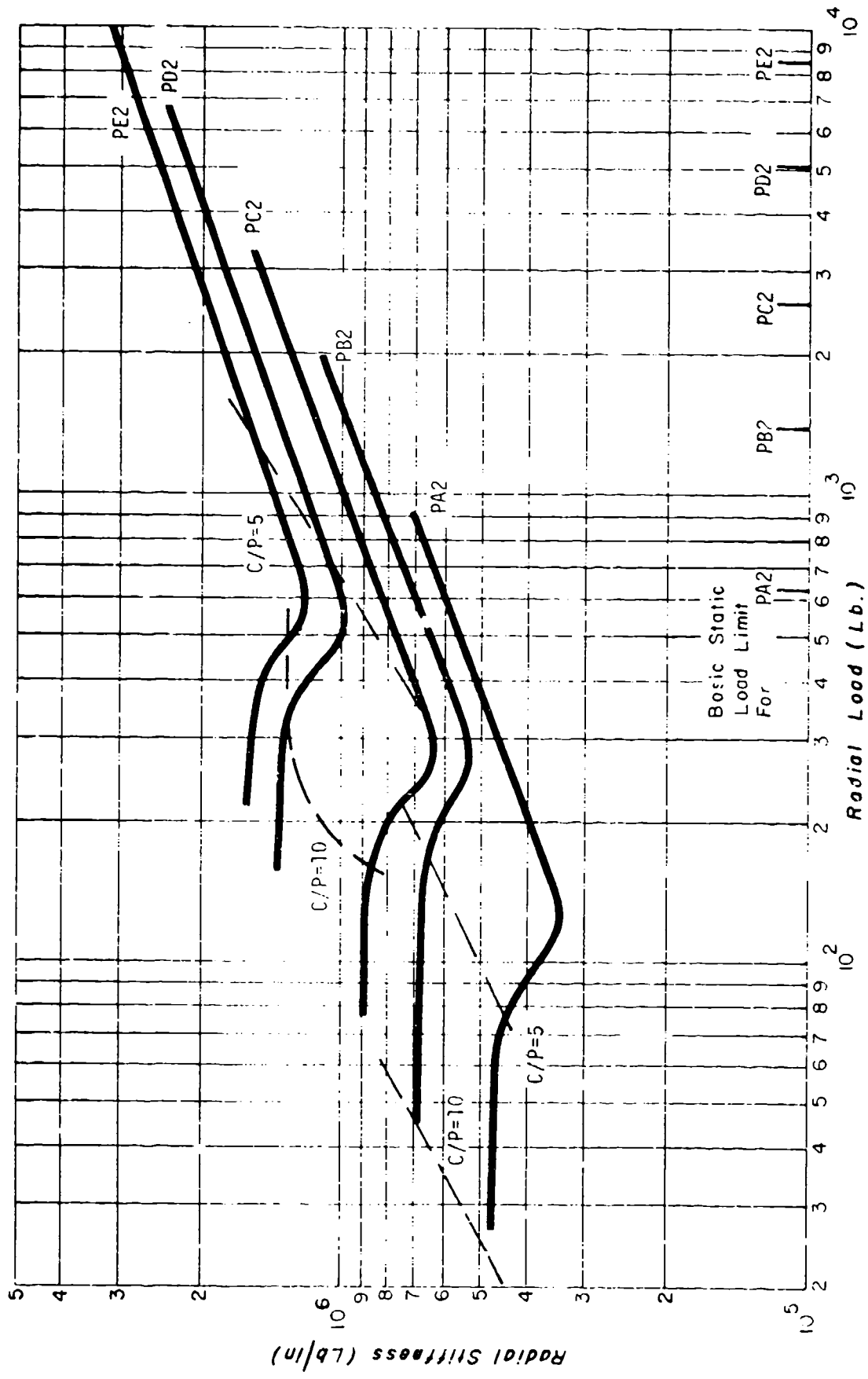


Fig. E-6 Radial Stiffness for Angular Contact Bearing,
preload -- Moderate
R 17.1

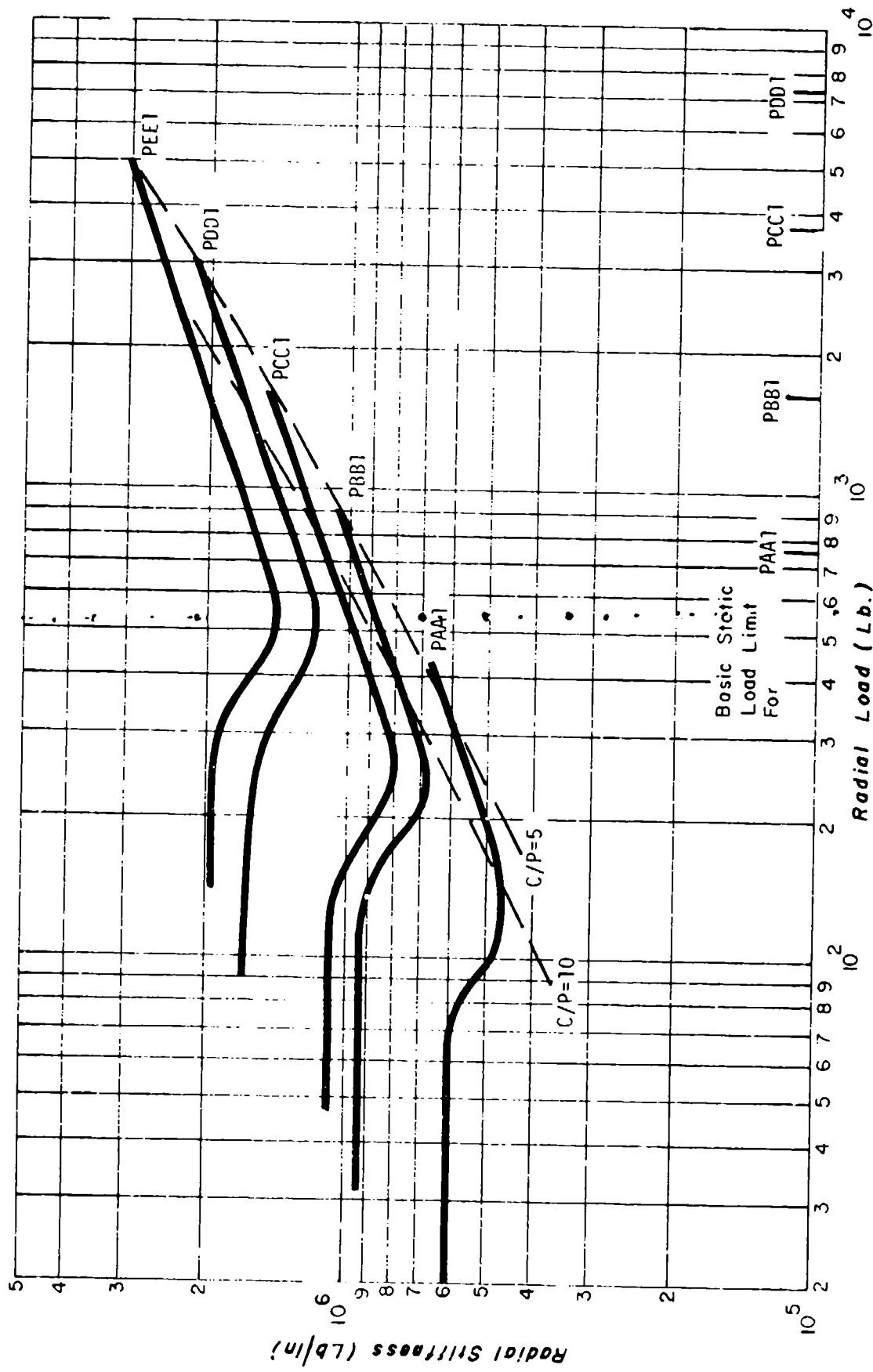


Fig. E-7 Radial Stiffness for Angular Contact Bearing,
 Preload — Moderate,
 $B = 150$

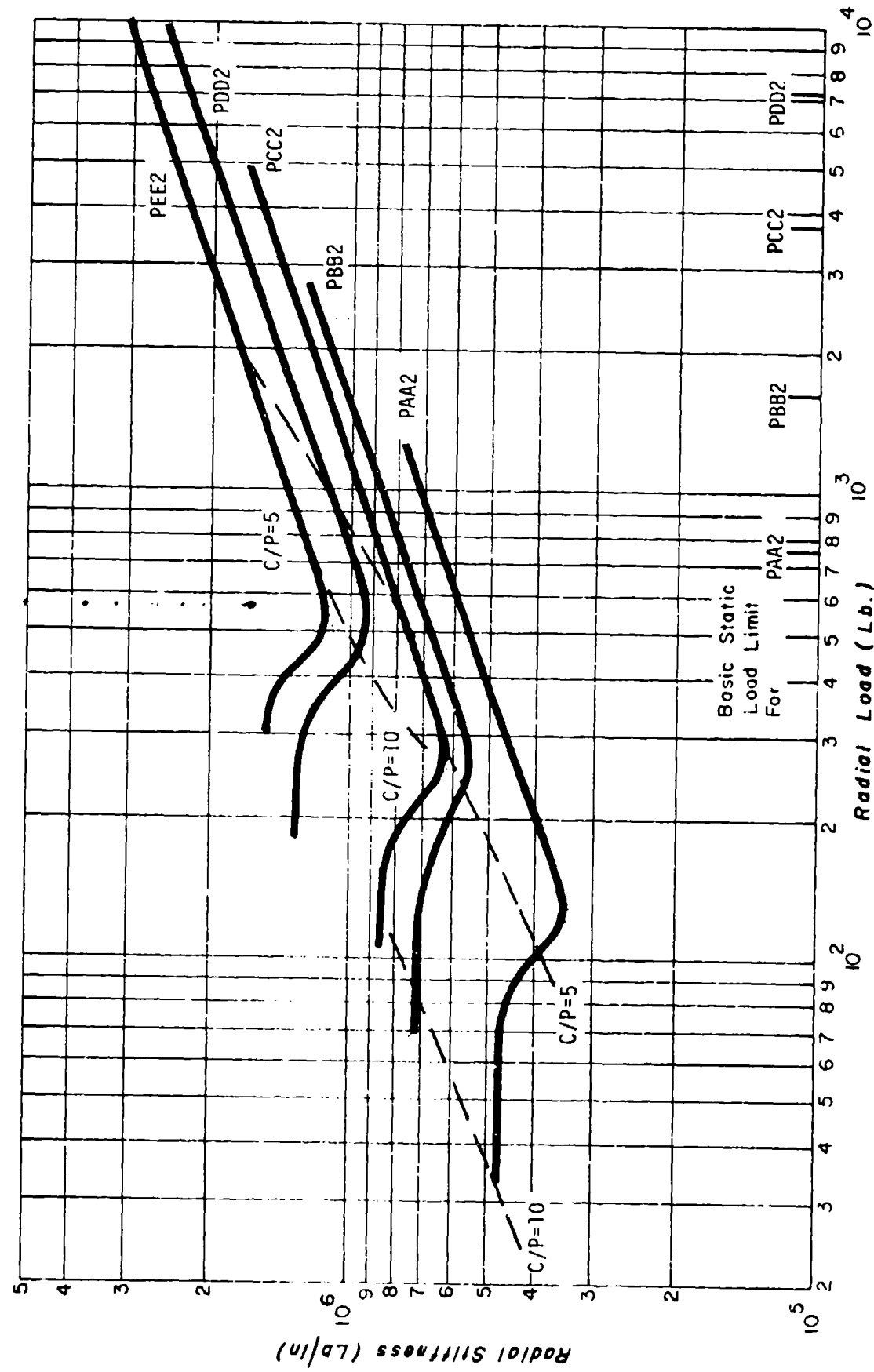


Fig. E-8 Radial Stiffness for Angular Contact Bearing,
Preload — Moderate,
 $\beta = 150$

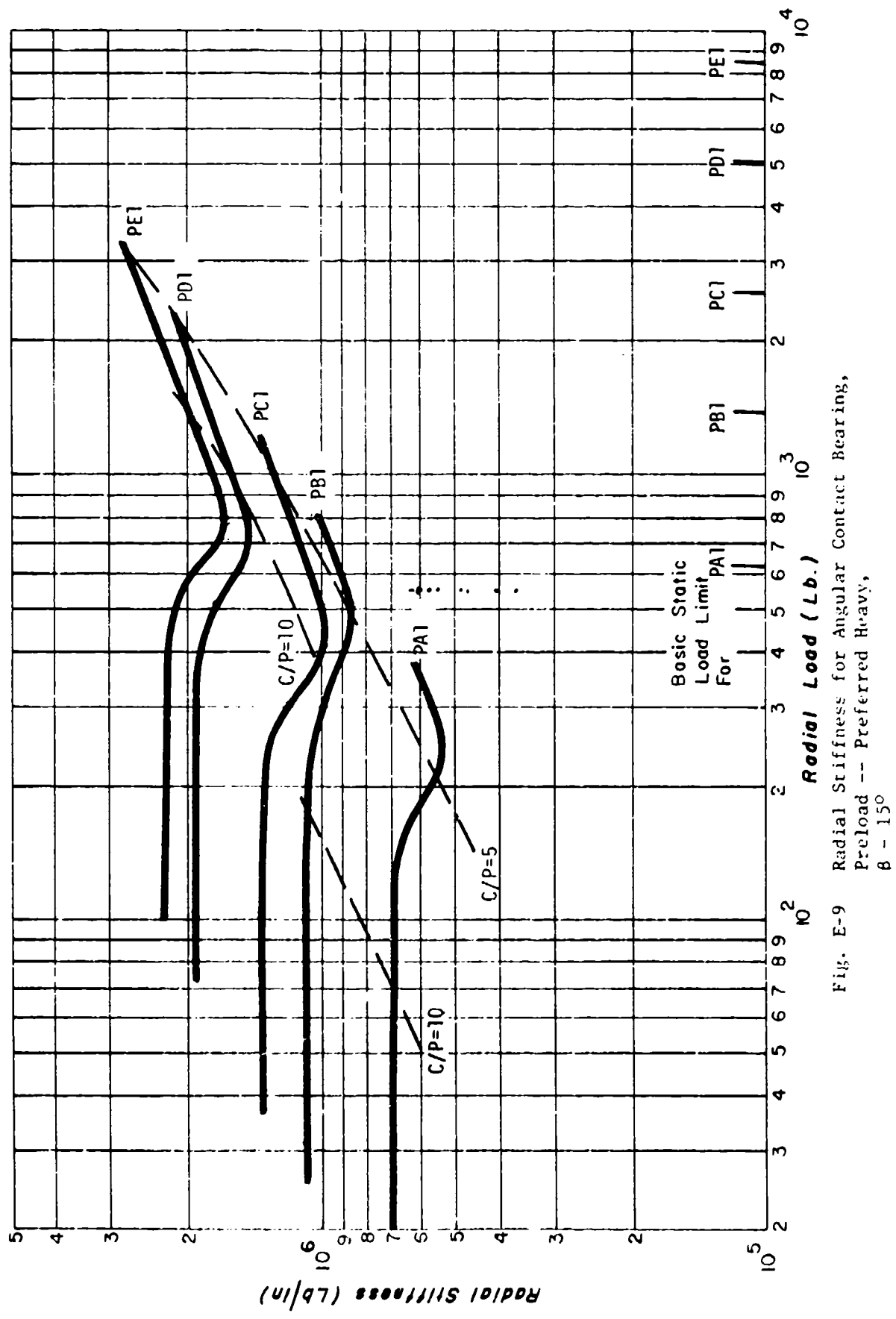


Fig. E-9 Radial Stiffness for Angular Contact Bearing,
 Preload -- Preferred Heavy,
 $\beta = 15^\circ$

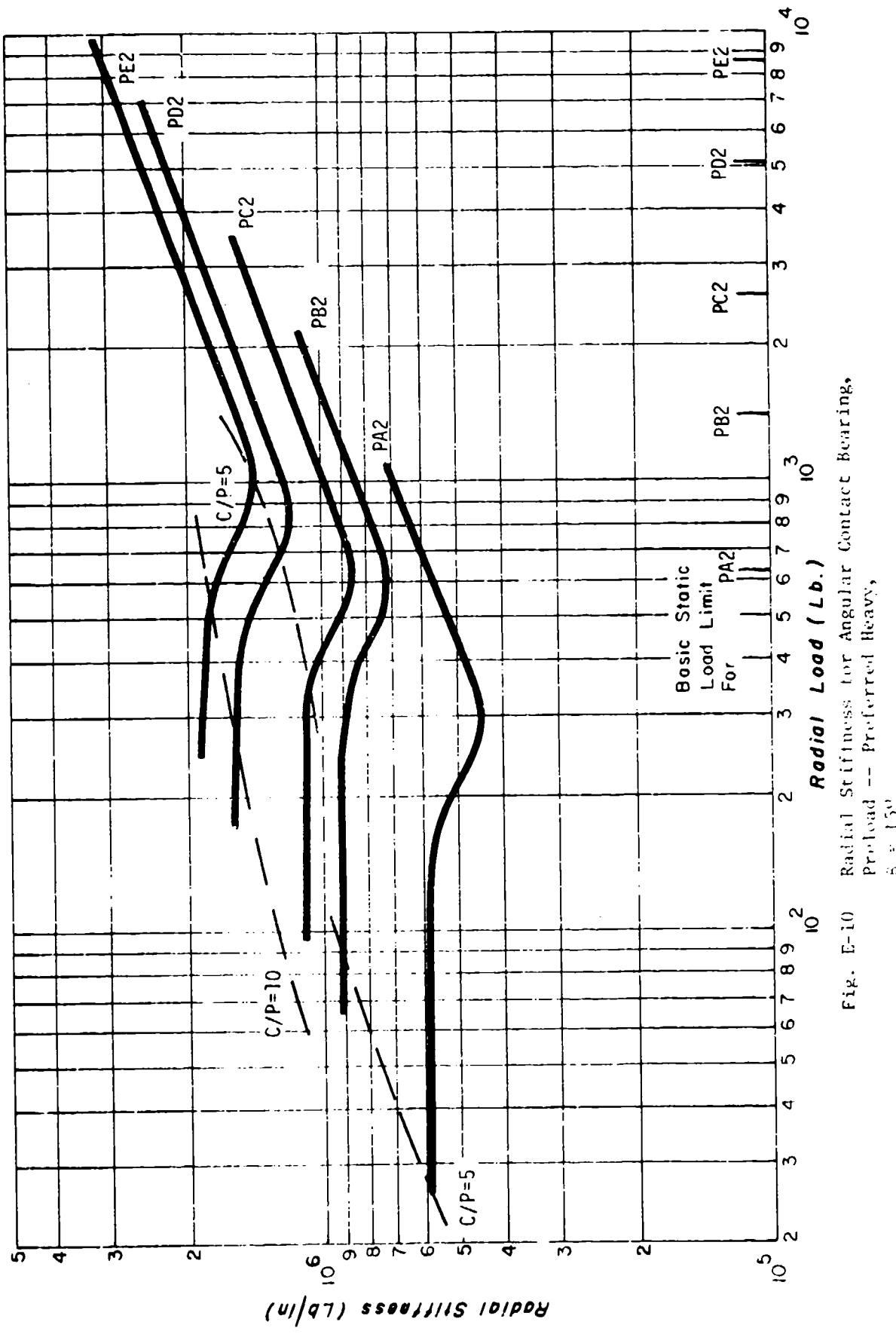


Fig. E-10 Radial Stiffness for Angular Contact Bearing,
 Preload -- Preferred Heavy,
 $n = 1500$

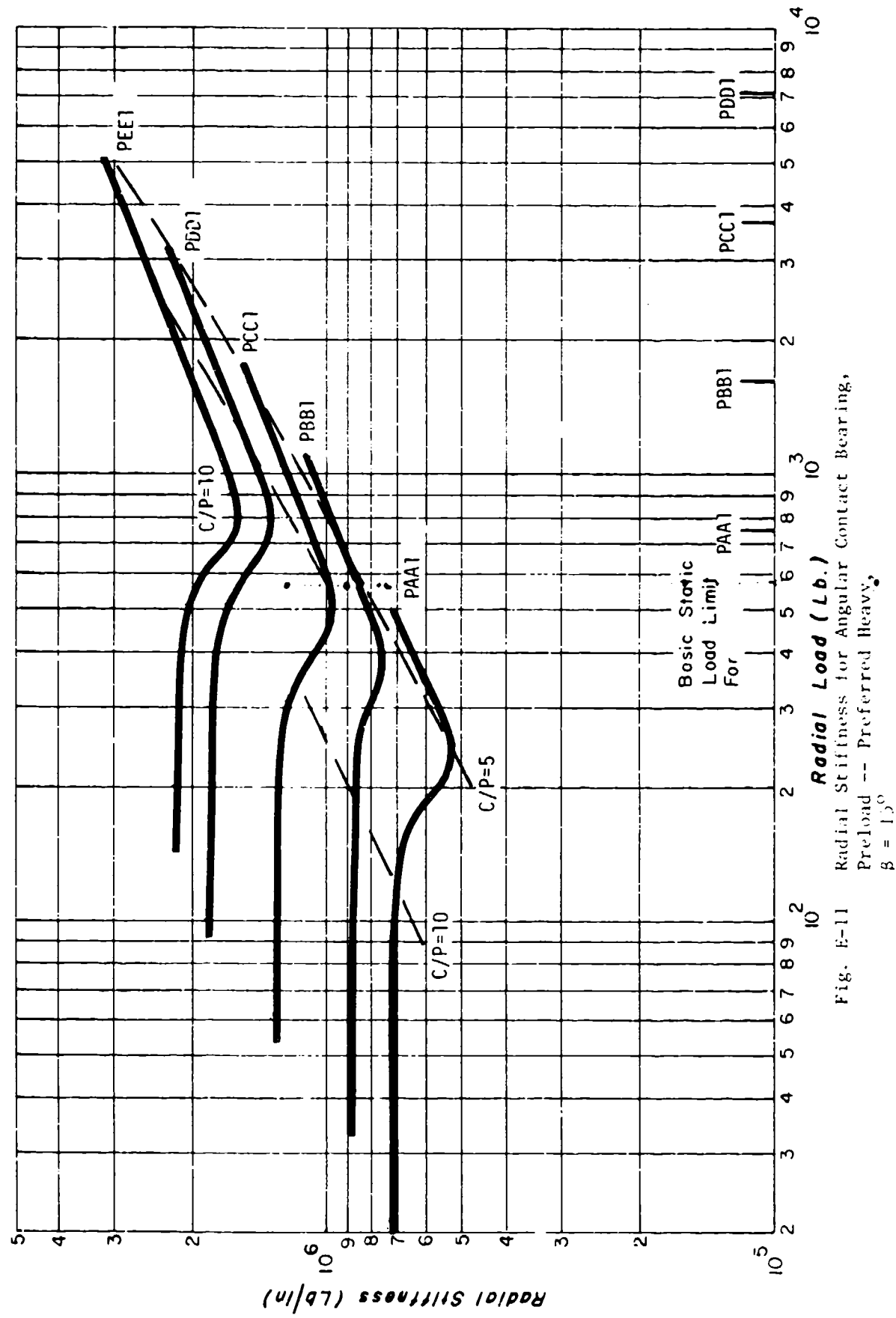


Fig. E-11 Radial Stiffness for Angular Contact Bearing,
 Preload -- Preferred Heavy,
 $\beta = 1.0$

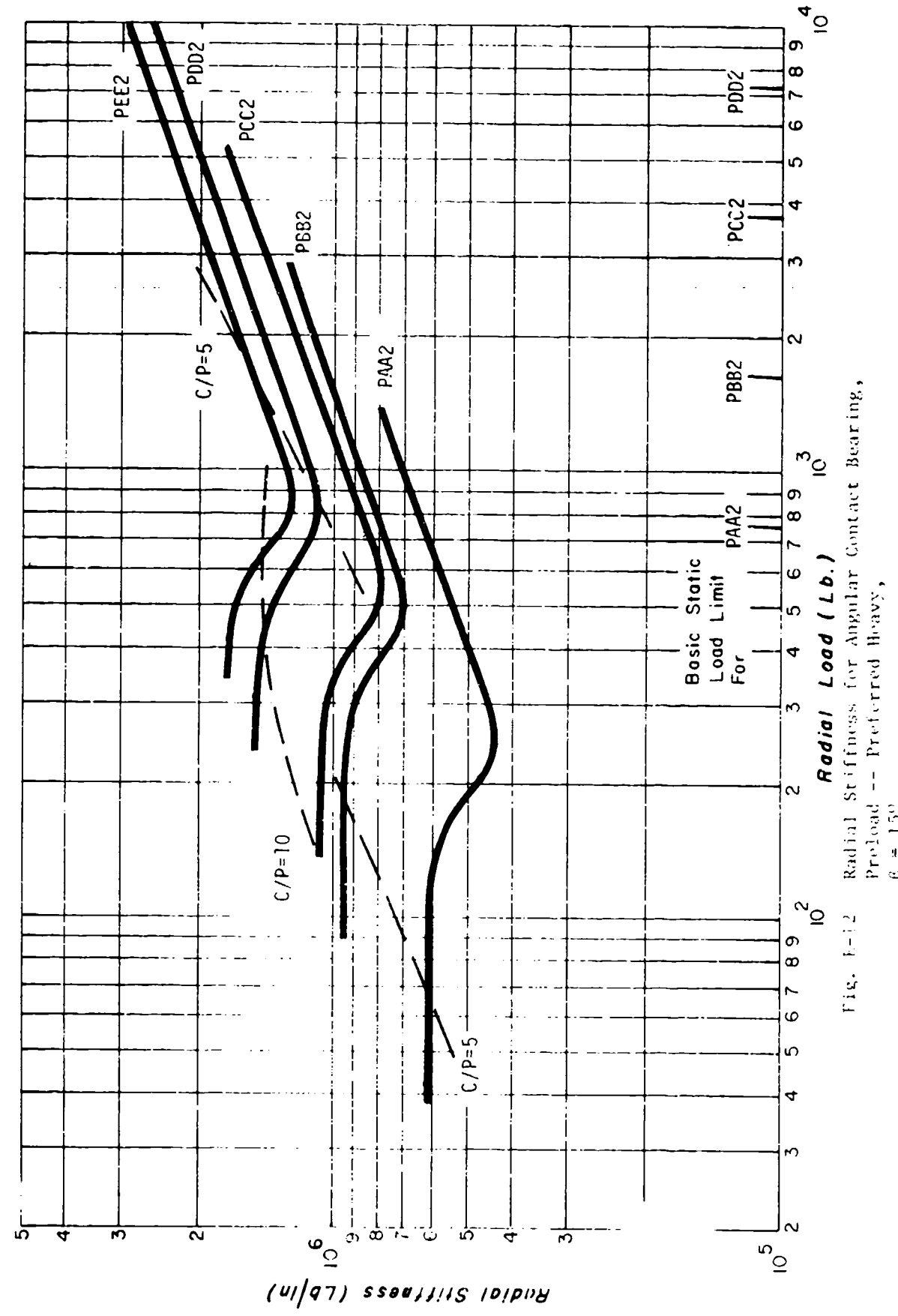


Fig. E-12 Radial Stiffness for Angular Contact Bearing,
Preload -- Preferred Heavy,
 $\beta = 15^\circ$

REFERENCES

1. Lewis, P. and Malanoski, S. B., Roller Bearing Dynamics Design Technology, Part IV: Ball Bearing Design Data Technical Report AFAPL-TR-65-45, Part IV.
2. Pan, C. H. T., Wu, E., and Krauter, A. I., Rotor Bearing Dynamics Technology Design Guides: Part I, Flexible Rotor Dynamics, AFAPL-TR-78-6, Part I, June 1978, Air Force Aero Propulsion Laboratory, Wright-Patterson Air Force Base, Ohio.
3. Mauriello, J. A., LaGasse and Jones, A. B., Rolling Element Bearing Retainer Analysis, DAAJ02-69-C-0080, TR105.7.10, USAAMRDL-TR-72-45.
4. Crecelius, W. T. and Pirvics, J., Computer Program Operation Manual on "SHABERTH" a Computer Program for the Analysis of the Steady State and Transient Thermal Performance of Shaft Bearing Systems, AFAPL-TR-76-90, Air Force Aero Propulsion Laboratory, Wright-Patterson Air Force Base, Ohio, October 1976.
5. Harris, T. A., Rolling Bearing Analysis, John Wiley & Sons, Inc., New York, 1966.
6. Palmgren, A., Ball and Roller Bearing Engineering, 3rd ed., Burbank, 1959, pp. 70-72.
7. Jones, A. B., Analysis of Stresses and Deflections, Vols. 1 and 2, New Departure Division, GMC, Bristol, Connecticut, 1946.